Title
Centromeric re-replication promotes aneuploidy

Author
Hanlon, Stacey L.

Publication Date
2014

Peer reviewed|Thesis/dissertation

CENTROMERIC RE-REPLICATION PROMOTES ANEUPLOIDY

by

STACEY L. HANLON

DISSERTATION

Submitted in partial satisfaction of the requirements for the degree of

DOCTOR OF PHILOSOPHY

in

Biochemistry and Molecular Biology

in the

GRADUATE DIVISION

of the

UNIVERSITY OF CALIFORNIA, SAN FRANCISCO

[redacted]

I DEDICATE THIS DISSERTATION

to the matriarchs of my family, past and present.

I WOULD LIKE TO ACKNOWLEDGE THE FOLLOWING

FOR THEIR IMPORTANT CONTRIBUTIONS TO MY SUCCESS:

Greg and Rhonda Hanlon • Shane and Lisa Hanlon • Arlene and Reinhart Oeltjen

Esther Hanlon • Joachim J. Li • David Toczyski • David O. Morgan

Patrick O'Farrell • Carol Gross • Christopher Richardson • Kenneth Finn

Michael A. Kienzler • Beth A. Cimini • Argenta R. Price

The 2007 incoming TETRAD graduate class • Francisco Castro • Danny Dam

Billy Luh • Rachel Mozesson • The Roland Bainton Lab • Joseph DeRisi

Tony Shermoen • Brenna Sinibaldi • Alex Orellana

The Ginger Carney Lab at Texas A&M • The Coca Cola Company • Folgers Coffee

Anchor Brewing Company • Subway Sandwiches • The State of Texas

The State of California

The work featured in Chapter 2 was under review at *eLife* at the time of dissertation submission:

Hanlon and Li. Re-replication of a centromere induces whole-chromosomal instability and aneuploidy.

Abstract

The cell relies on absolute symmetry to accurately segregate its genome into two daughter cells. The start of this symmetry is during DNA replication, where one chromosome is completely and precisely duplicated to produce two exact copies. These two copies are cohesed together and brought under tension by the mitotic spindle, which attaches microtubules to the kinetochore complexes assembled on centromeres. Lack of tension is sensed by the spindle assembly checkpoint (SAC), but when each chromatid pair is properly bioriented, the chromosomes are freed of their ties and are pulled to opposite spindle poles. Thus, bilateral symmetry is essential for proper chromosome segregation.

Despite the checkpoints and intrinsic nature of the system to biorient sister chromatids, chromosome missegregation does occur. The result is cellular progeny that is aneuploid, or having an abnormal number of chromosomes. Aneuploidy is a hallmark of cancer, so understanding how chromosome segregation could go awry has been intensely studied. Disrupting the spindle microtubules, the kinetochores, cohesin, or the SAC have proven to increase missegregation rates in model systems, however, this machinery is rarely inoperative in actual tumor samples, leaving scientists to search for other sources of aneuploidy.

Due to the essential role of bilateral symmetry in chromosome segregation, I investigated whether it could be disrupted outside of mitosis. The symmetry of the sister chromatids relies on a "once and only once" round of replication; if a re-replication event was to occur that encompassed a centromere, then the bilateral nature of the sister chromatid pair would be abolished. Using the Li Lab re-replication genetic system, I showed that centromeric re-replication can induce aneuploidy, either through the missegregation of the re-replicated chromosome or by the creation of an entire, whole chromosome. Microscopic analysis of

newly re-replicated cells demonstrates the extra centromere is able to attach to the mitotic spindle, indicating it may produce a merotelic attachment that could lead to the chromatid's missegregation or enhance the fragility of the re-replication bubble. Together, I have shown that centromeric re-replication is a potent inducer of aneuploidy, which may initiate investigation into the role re-replication may play in aneupoidy in cancer.

Table of Contents

List of Tables

List of Figures

Figures for Chapter One

Figures for Chapter Two

Figures for Appendices A-E

Chapter One: Introduction

The control of DNA replication

Whether it is responding to external signals, communicating with other cells, or just maintaining homeostasis, the cell relies on its DNA to provide the genetic instructions necessary to survive. In eukaryotic cells, the DNA is contained within the nucleus, which confers a second membrane for protection as well as providing spacial separation from other organelles and components of the cell. This DNA is organized into linear pieces called chromosomes, and the number of chromosomes varies from organism to organism. Humans have 23 pairs of chromosomes, and the budding yeast *Saccharomyces cerevisiae* has 16 pairs; this number is referred to as a cell's ploidy. When a cell has a single set of chromosomes, it is considered haploid, and when it has a pair of each chromosome, it is diploid.

Due to the importance of the information, great care is taken by the cell to ensure the faithful passage of its DNA to its progeny. Each daughter must receive a single, whole copy of every chromosome—nor more, no less. The first step in this process is the complete replication of the genome using hundreds of replication origins throughout the genome. There are so many origins that controlling each one individually would require absurd amounts of regulation, as well as increase the chance an origin will fire more or less than exactly once. Thus, the cell regulates all origins at once by temporally dividing the process of DNA replication into two parts: origin preparation (during G1 phase) and origin initiation (during S phase) (Costa *et al*. 2013; Siddiqui *et al*. 2013). While origins are being prepped, origin initiation cannot occur. Conversely, during the time the cell is able to initiate replication, origins cannot be prepped. Separating these processes means that each origin is sure to fire only once in a single cell cycle (Figure 1).

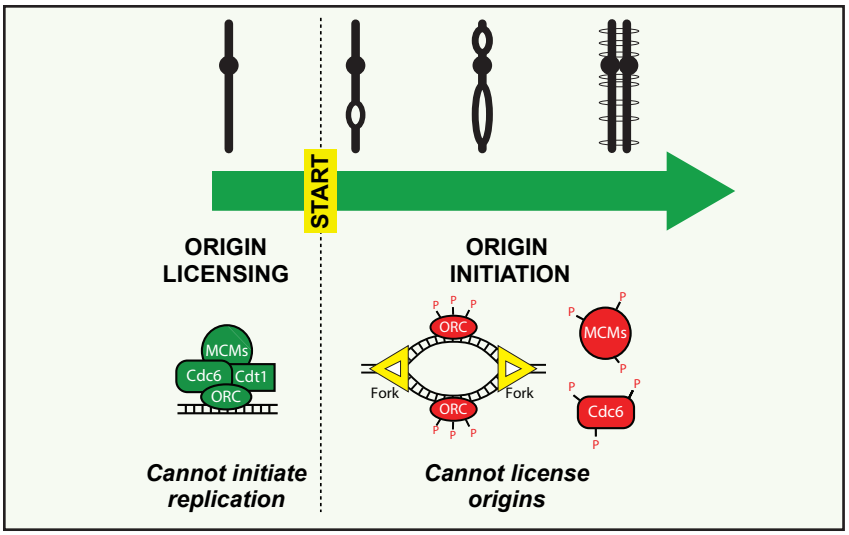

FIGURE 1: DNA REPLICATION CONTROL.

DNA replication is globally controlled by temporally separating origin licensing (pre-START) from origin initiation (post-START). This control prevents the re-licensing and re-initiation of origins within a single cell cycle.

During origin preparation, each replication origin is licensed, meaning it becomes decorated with proteins that will be used during replication. In *Saccharomyces cerevisiae*, origins of replication are sequence-defined and are called "autonomous replication sequences" or *ARS* elements (Dhar *et al*. 2012). These 80-120 bp sequences are able to confer replication activity on an extrachromosomal piece of DNA like a plasmid, and their strength is characterized by how well the plasmid is able to be maintained over several generations. In their endogenous chromosomal context, ARS elements vary in their timing and use during replication. Some origins are used in nearly cell cycle and fire early in S phase, while others are rarely used and only fire if necessary (McIntosh and Blow 2012). Despite their activity, all confirmed origins are subject to the same licensing factors so that each may have the potential to initiate replication in the upcoming S phase.

The main objective during origin licensing is to load the replicative helicase (Bell and Kaguni 2013). Six Mcm proteins (Mcm2-7) form a ring that will encircle a single strand of DNA that will serve to unzip the DNA ahead of the replication fork. To load this ring, several licensing proteins associate with an origin in a controlled, step-wise manner. First, the origin

recognition complex, or ORC, binds ATP and associates with the DNA (Klemm *et al*. 1997). Next comes Cdc6, which binds directly to the ORC complex. This association allows the Mcm2-7 ring bound to its escort protein, Cdt1, to be recruited to the origin (Kawasaki *et al*. 2006). The binding and hydrolysis of ATP by the Mcm2-7 complex is required for its loading and subsequence release of Cdt1 (Coster *et al* 2014; Kang *et al*. 2014). It is known that at least two copies are loaded onto double-stranded DNA, one for each fork (Evrin *et al*. 2009). This dimerization likely occurs before the helicases are stably associated with the origin (as indicated by their resistance to salt wash *in vitro*) and may be dependent on the presence of a second ORC and Cdc6 (Evrin *et al*. 2014). An origin that has successfully loaded stable Mcm2-7 rings has an established pre-replicative complex, or pre-RC.

During G1 phase, origin licensing is permitted and origin initiation is restricted. This temporal separation is made possible by regulating levels of cyclin-dependent kinase, or CDK, and Cdc7 kinase bound to Db4 (Dbf4-dependent kinase or DDK) (Labib 2010). CDK and DDK activity is low while origins are licensed, but at the start signal of S phase, the activity levels of these kinases rise exponentially. The phosphorylations they place have dual effects depending on the substrate.

For initiation proteins, the kinase phosphorylations are sequentially placed to enable components to associate with one another (Heller *et al* 2011). The CDK phosphorylation of replisome proteins Sld2 and Sld3 enable their binding to Dbp11, which may facilitate other interactions with Cdc45 and the GINS complex (Tanaka *et al*. 2007). The association of Cdc45 with GINS is likely also dependent upon CDK phosphorylation (Zegerman and Diffley 2007). DDK phosphorylation of Mcm 2, 4, and 6 help it associate with Cdc45 and GINS to form the CMG complex, which is essentially the activated form of the helicase (Ilves *et al*. 2010).

CDK phosphorylation of licensing proteins, however, leads to their inactivation by either targeting them for destruction or excluding them from the nucleus (Nguyen *et al*. 2001; Nishitani and Lygerou 2002). The CDK phosphorylation of ORC prevents its interaction with Cdt1, thereby preventing the loading (or reloading) of the Mcm2-7 helicase (Chen and Bell 2011). Cdc6 is phosphorylated and targeted for destruction in both S phase and mitosis (Perkins *et al*. 2001). Unbound Mcm2-7 complexes are also phosphorylated on Mcm3, which enables their export from the nucleus so they are unavailable for reloading (Liku *et al*. 2005).

The regulatory phosphorylations on licensing proteins by CDK enables global regulation of replication. These controls, however, are not redundant (Green *et al*. 2006). If they were, then the frequency of re-replication would not change whether one or all the regulations were in place, and the presence of the extra controls would simply exist for backup in case the primary regulation is lost. This redundancy model was widely accepted since re-replication was undetectable within a single cell cycle unless several CDK controls were disrupted at once. With the use of more sensitive assays that can detect lower amounts of re-replication, it is clear that removal of a single regulation enables mild re-replication, removal of two regulations produces more re-replication, and so on, indicating these controls are overlapping.

In the process of disrupting combinations of CDK controls, a particular pair of deregulations produced highly efficient re-replication originating from *ARS317* (Figure 2). This feature was turned into a tool by the Li Lab, which moved this origin to a region on Chromosome IV between Ty elements. These are naturally occurring transposable elements that provide short regions of homology and are scattered throughout the yeast genome. When re-replication is transiently initiated between these elements, the result is a high frequency of segmental amplifications that relies on homologous recombination (Green *et al*. 2010; Finn and Li 2013).

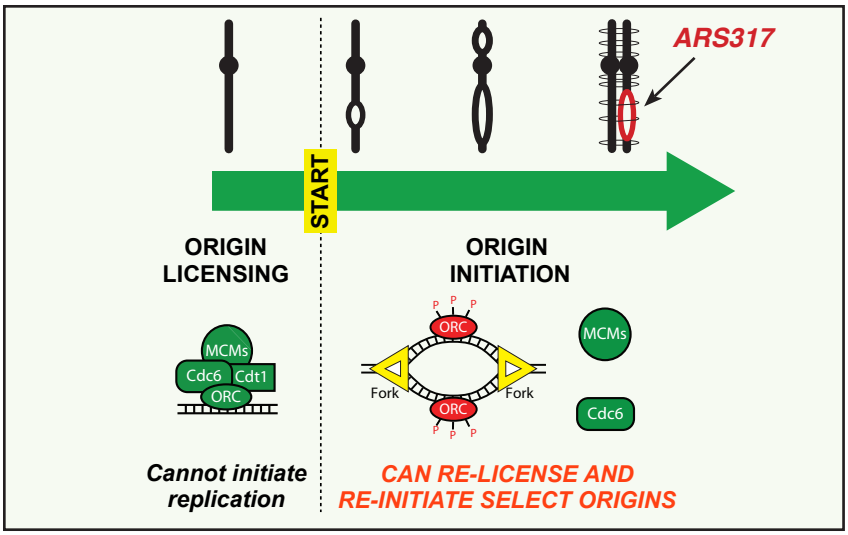

Figure 2: Overlapping DNA replication control leading to *ARS317* re-replication.

When two of the overlapping DNA replication controls are deregulated, the re-licensing and re-initiation of origins becomes more frequent. Shown here is the non-phosphorylated MCM2-7 and the non-phosphorylated Cdc6. When deregulated together, the origin *ARS317* efficiently refires.

If the regulation preventing re-replication was truly global, then one would expect its partial deregulation to increase the probably of re-replication evenly across all origins. This is not the case, however, as the re-initiation ability of *ARS317* was found to be due to a "re-initiation promoter" or RIP element. When placed in front of other replication origins, their replication efficiency and timing remained unchanged, however they were now able to re-replicate under permissive conditions (Richardson and Li 2014). This localized origin control suggests *ARS* elements may have more autonomy than previously thought: the global control may be a "federal" mode of regulation, whereas individual origins could have more local or "state" control to enable how and when the origin will fire. If an origin is more prone to re-replicate, it could have a variety of effects on genomic stability depending on its chromosomal context, as illustrated by the arm re-replication producing segmental duplications. The implication for the disruption of DNA replication control in creating more drastic genomic instability will be addressed in Chapter Two: Re-replication of a centromere causes whole-chromosomal instability and aneuploidy.

The control of chromosomal segregation

As DNA replication proceeds, the cell's strategy for accurate chromosome segregation is just beginning. The budding yeast *Saccharomyces cerevisiae* employs many mechanisms and layers of regulation to ensure each of its daughter cells receive a single, complete copy of the genome (Marston 2014). To physically segregate chromosomes, they must be pulled apart, but not until the cell is completely ready to do so. Thus, the newly-replicated strands of DNA (sister chromatids) must be held together until their segregation. To do this, the cell encircles the sister chromatids using rings of protein called cohesin that are established during the replication process (Uhlmann and Nasmyth 1998; Unal *et al*. 2008; Murayama *et al*. 2014). This ring ensures the chromatids to stay together until the cell is ready to split the genome in anaphase.

One of the earliest elements to be replicated on a chromosome is its centromere (McCarroll and Fangman 1988), which in budding yeast is a very simple sequence-defined element (Cottarel *et al*. 1989). The centromere is essential for the proper segregation of a chromosome (Verdaasdonk and Bloom 2011). Its main task is to provides the link between the DNA and the mitotic spindle by recruiting proteins that form a kinetochore (Biggins 2013). This elaborate structure binds to the DNA as wells as to an individual microtubule emanating from a spindle pole. The budding yeast centromere is always decorated with a kinetochore and therefore are always connected to one of the spindle poles (Collins *et al*. 2005). The exception is when the kinetochore is displaced from the DNA during replication, however as soon as the proteins reassemble onto the centromere, they are able to re-bind to a microtubule (Kitamura *et al*. 2007).

As replication finishes, each of the sister chromatids are bound to one another and are

likely attached to the spindle pole through one or both kinetochores. During this time, the poles where the spindle microtubules emanate from have duplicated and begin to move away from one another along the nuclear membrane (Winey and O'Toole 2001). If the sister centromeres of a chromatid pair are attached to different poles, then the chromatids will become bioriented with each centromere being pulled to opposite poles. However, if only one centromere is attached to a pole—or if both centromeres are attached to the same pole—the chromatid pair will not be bioriented. Lack of biorientation is a problem for the cell: if it was to divide without the biorientation of all its chromosomes, then it would not be able pull sisters chromatids away from one another into the daughter cells, which would result in aneuploidy.

To ensure each of the chromatid pairs are bioriented, the cell utilizes a spindle assembly checkpoint (SAC) (Lara-Gonzalez *et al*. 2012). This checkpoint can become activated if just a single chromatid pair is not properly oriented with the spindle since unopposed spindle forces on a single chromatid pair results in kinetochore complexes not held under tension. This lack of tension enables SAC components to bind at the kinetochore, ultimately leading to the formation of the mitotic checkpoint complex (MCC) comprised of BubR1/Mad2/Mad3/Bub3/Cdc20 (Foley and Kapoor 2013). The MCC physically interacts with the anaphase-promoting complex (APC) to prevent its activation, thus preventing the cell from entering anaphase. Additionally, errant microtubule-kinetochores connections are destabilized to retry for a correct attachment that generates tension. Once each kinetochore (and thus chromatid pair) is under tension, the microtubule-kinetochore connections are stabilized to produce proper chromosome biorientation (Dewar *et al*. 2004), and SAC components disappear from kinetochores. As the MCC is no longer produced, the inhibition of the APC is lifted to enable the initiation of anaphase: the rings of cohesin established in S phase are cut to allow the chromatids to separate (Uhlmann *et al*.

1999), and due to their biorientation, each is pulled to a different spindle pole.

Bilateral symmetry is essential for proper chromosome segregation: opposite spindle poles connecting sister chromatid centromeres produce a chromosomal structure that is easily bisected during anaphase. When the machinery meant to provide this symmetry goes awry, chromosome segregation is negatively affected to result in cellular aneuploidy (Figure 3). Since aneuploidy is a hallmark of cancer, much focus has been on if the failure of this machinery is responsible for the aneuploidy observed. The next section focuses on our current understanding of the causes and consequences of chromosomal instability in cancer.

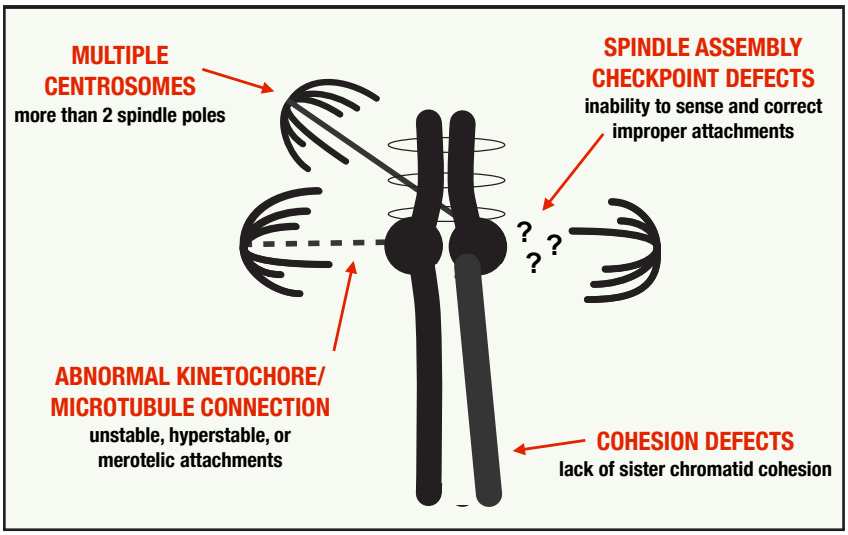

Figure 3: Errors in segregation machinery that have been found to produce chromosomal instability and aneuploidy.

The failure of mitotic components has long been the focus of how cells develop instability and produce aneuploidy. Shown is a visual summary of the errors that have been demonstrated to produce instability leading to aneuploidy.

Whole-chromosomal instability in cancer

The importance of bilateral symmetry during chromosome segregation has long been known. Beginning in 1902, Theodor Boveri's examined the effects of multipolar mitoses on chromosome distribution to daughter cells in sea urchin embryos. In his piece describing the work, Boveri first speculated how these abnormal mitoses may contribute to tumor formation (Boveri 1902). Not being an MD, Boveri was met with skepticism and was discouraged from continuing his project. He kept with it, and in his 1914 publication he expanded on his argument for abnormal mitoses driving tumor formation through the abnormal distribution of chromosomes (Figure 4A; Boveri 1914). Boveri hypothesizes how too many spindles during a multipolar mitosis could produce four aneuploid daughter cells, some missing chromosomes and others with too many.

Today, we know Boveri was right. Events that disrupt the bilateral symmetry of the mitotic apparatus have been shown to increase the rate of chromosome missegregation, a state known as whole-chromosomal instability or W-CIN (Holland and Cleveland 2009). This unstable state can lead to aneuploidy, which is a hallmark of cancer and can affect its progression (Figure 4B; Holland and Cleveland 2012; Zasadil *et al*. 2013). In fact, around 85% of solid tumor samples have been found to be aneuploid (Mitelman *et al*. 2012). Though it is still a matter of debate, it appears that this aneuploidy may not just be a consequence of W-CIN, but could provide its underlying cause (Weaver and Cleveland 2006; Sheltzer *et al*. 2011). Thus, finding potential sources of aneuploidy has been a large focus.

The most obvious source of aneuploidy starts with the disruption of segregation machinery to affect the bilateral symmetry of mitosis. Disruption of these mechanisms in

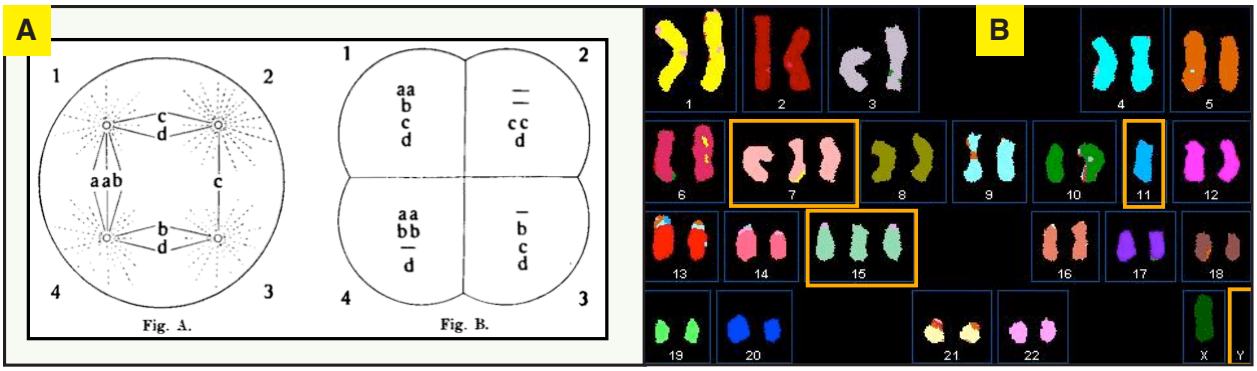

Figure 4: Aneuploidy: yesterday and today.
A) Boveri first proposed a source of aneuploidy in the early 1900s. This illustration is from his 1914 work, "*Concerning the origin of malignant tumors*."
B) A karyotype from the LS174T colon cancer cell line. As highlighted, Chromosomes 7 and 15 are trisomic, and Chromosomes 11 and the sex chromosome are monosomic (Abdel-Rahman *et al*. 2001).

model systems has proven to be a source of instability and aneuploidy (Schvartzman *et al*. 2010; Gordon *et al*. 2012). Results of cancer genome sequencing, however, has shown that mutations in these components are rare (Perez De Castro *et al*. 2006). Additionally, many cancers have a fully-functional mitotic checkpoint that is meant to protect against missegregation (Tighe *et al*. 2001). How does a cell with functional mitotic components become aneuploid?

In order to answer this question, strategy has shifted to connecting the known genetic abnormalities in cancer to aneuploidy generation (Hanahan and Weinberg 2011). Two of the most disrupted proteins are RB and p53, tumor-supressor genes that control cell cycle progression (Sherr and McCormick 2002). Though they have been consistently found to be disrupted in cancer, their connection to W-CIN has been unclear. Recently, it has been shown that their deregulation is crucial to promote W-CIN, indicating that the inactivation of these tumor-supressor pathways may be the first step taken by cancer cells to generate W-CIN (Schvartzman *et al*. 2011). Together, a new "oncogene-induced mitotic stress" model was produced to connect oncogenic inactivation and W-CIN (Malumbres 2011; Duijf and Benezra 2013). This model proposes that the timing of key cell cycle events such as replication and

mitotic checkpoint can become dysfunctional, leading to untimely replication and/or mitotic stress to promote W-CIN (Roschke and Rozenblum 2013)

The lack of genetic disruptions to mitotic components in combination with the fresh perspective the oncogenic-induced mitotic stress model provides is leading to a search for W-CIN sources that originate outside of mitosis. Since DNA replication timing is under the ultimate control of the pRb and p53 pathway, perhaps re-replication could contribute to W-CIN. Indeed, overexpression of replication factors has been documented in cancer (Bonds *et al*. 2002; Lionton *et al*. 2007; Murphy *et al*. 2005; Ren *et al*. 2006; Santarius *et al*. 2010; Carter *et al*. 2006) and have been found to be overexpressed in conjunction with p53 (Karakaidos *et al*. 2004). How would a lapse in replication control promoter W-CIN? If a centromere was to become re-replicated, the bilateral symmetry that is integral to the chromosomal segregation process would be disrupted since a single chromatid could become itself bioriented with the spindle. This effective merotely could promote the chromatid's missegregation during mitosis, despite all mitotic components and checkpoints being in tact. In the following chapter, I will report my findings regarding the generation of W-CIN after centromeric re-replication in the simple model system *Saccharomyces cerevisiae*.

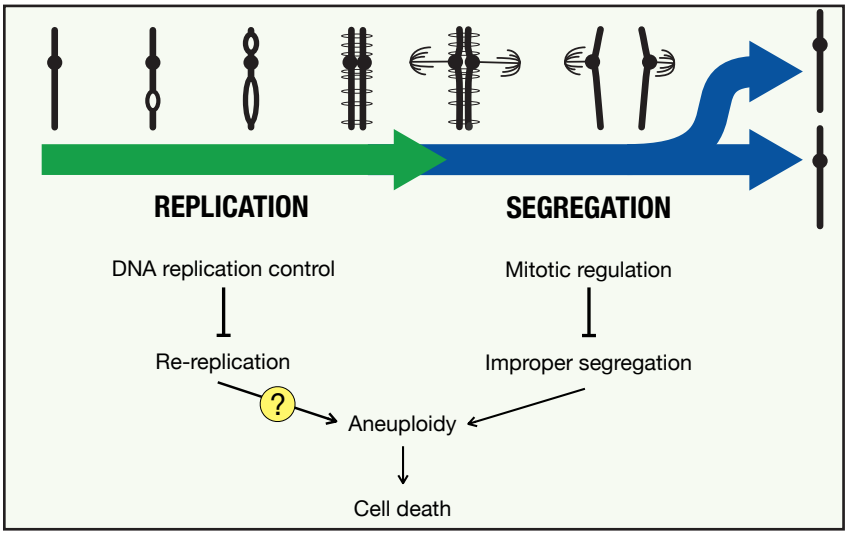

Figure 5: Visualization of hypothesis.

The search for sources of chromosomal instability and aneuploidy have focused mainly on errors occurring during segregation. During my graduate work, I asked if errors originating outside of segregation are able to promote aneuploidy. Chapter Two discusses the details and results of my findings.

References for Chapter One

Abdel-Rahman W. M., Katsura K., Rens W., Gorman P. A., Sheer D., Bicknell D., Bodmer W. F., Arends M. J., Wyllie A. H., Edwards P. A., 2001 Spectral karyotyping suggests additional subsets of colorectal cancers characterized by pattern of chromosome rearrangement. Proc Natl Acad Sci USA 98: 2538–2543.

Bell S. P., Kaguni J. M., 2013 Helicase Loading at Chromosomal Origins of Replication. Cold Spring Harb Perspect Biol 5: a010124–a010124.

Biggins S., 2013 The Composition, Functions, and Regulation of the Budding Yeast Kinetochore. Genetics 194: 817–846.

Bonds L., Baker P., Gup C., Shroyer K. R., 2002 Immunohistochemical localization of cdc6 in squamous and glandular neoplasia of the uterine cervix. Arch Pathol Lab Med 126: 1164–1168.

Boveri T., 1902 Ueber mehrpolige Mitosen als Mittel zur Analyse des Zellkerns . . Vehr Phys Med Ges Wurzburg NF: 67–90.

Boveri T., 2008 Concerning the origin of malignant tumours by Theodor Boveri. Translated and annotated by Henry Harris. J Cell Sci 121 Suppl 1: 1–84.

Carter S. L., Eklund A. C., Kohane I. S., Harris L. N., Szallasi Z., 2006 A signature of chromosomal instability inferred from gene expression profiles predicts clinical outcome in multiple human cancers. Nat Genet 38: 1043–1048.

Chen S., Bell S. P., 2011 CDK prevents Mcm2-7 helicase loading by inhibiting Cdt1 interaction with Orc6. Genes & Development 25: 363–372.

Collins K., Castillo A., Tatsutani S., Biggins S., 2005 De novo kinetochore assembly requires the centromeric histone H3 variant. Mol Biol Cell 16: 5649–5660.

Costa A., Hood I. V., Berger J. M., 2013 Mechanisms for initiating cellular DNA replication. Annu Rev Biochem 82: 25–54.

Coster G., Frigola J., Beuron F., Morris E. P., Diffley J. F. X., 2014 Origin Licensing Requires ATP Bindingand Hydrolysis by the MCM Replicative Helicase. Molecular Cell 55: 666–677.

Cottarel G., Shero J. H., Hieter P., Hegemann J. H., 1989 A 125-base-pair CEN6 DNA fragment is sufficient for complete meiotic and mitotic centromere functions in Saccharomyces cerevisiae. Mol Cell Biol 9: 3342–3349.

Dewar H., Tanaka K., Nasmyth K., Tanaka T., 2004 Tension between two kinetochores suffices for their bi-orientation on the mitotic spindle. Nature 428: 93–97.

Dhar M. K., Sehgal S., Kaul S., 2012 Structure, replication efficiency and fragility of yeast ARS elements. Research in Microbiologoy: 1–11.

Duijf P. H. G., Benezra R., 2013 The cancer biology of whole-chromosome instability. Oncogene.

Evrin C., Clarke P., Zech J., Lurz R., Sun J., Uhle S., Li H., Stillman B., Speck C., 2009 A double-hexameric MCM2-7 complex is loaded onto origin DNA during licensing of eukaryotic DNA replication. Proc Natl Acad Sci USA.

Evrin C., Fernandez-Cid A., Riera A., Zech J., Clarke P., Herrera M. C., Tognetti S., Lurz R., Speck C., 2014 The ORC/Cdc6/MCM2-7 complex facilitates MCM2-7 dimerization during prereplicative complex formation. Nucleic Acids Res 42: 2257–2269.

Finn K. J., Li J. J., 2013 Single-Stranded Annealing Induced by Re-Initiation of Replication Origins Provides a Novel and Efficient Mechanism for Generating Copy Number Expansion via Non-Allelic Homologous Recombination. PLoS Genet 9: e1003192.

Foley E. A., Kapoor T. M., 2013 Microtubule attachment and spindle assembly checkpoint signalling at the kinetochore. Nat Rev Mol Cell Biol 14: 25–37.

Gordon D. J., Resio B., Pellman D., 2012 Causes and consequences of aneuploidy in cancer. Nature Reviews Genetics: 1–15.

Green B. M., Finn K. J., Li J. J., 2010 Loss of DNA replication control is a potent inducer of gene amplification. Science 329: 943–946.

Green B. M., Morreale R. J., Ozaydin B., Derisi J. L., Li J. J., 2006 Genome-wide mapping of DNA synthesis in Saccharomyces cerevisiae reveals that mechanisms preventing reinitiation of DNA replication are not redundant. Mol Biol Cell 17: 2401–2414.

Hanahan D., Weinberg R. A., 2011 Hallmarks of cancer: the next generation. Cell 144: 646–674.

Heller R. C., Kang S., Lam W. M., Chen S., Chan C. S., Bell S. P., 2011 Eukaryotic Origin-Dependent DNA Replication In Vitro Reveals Sequential Action of DDK and S-CDK Kinases. Cell 146: 80–91.

Holland A. J., Cleveland D. W., 2009 Boveri revisited: chromosomal instability, aneuploidy and tumorigenesis. Nature Publishing Group 10: 478–487.

Holland A. J., Cleveland D. W., 2012 Losing balance: the origin and impact of aneuploidy in cancer. EMBO Rep 13: 501–514.

Ilves I., Petojevic T., Pesavento J. J., Botchan M. R., 2010 Activation of the MCM2-7 Helicase by Association with Cdc45 and GINS Proteins. Molecular Cell 37: 247–258.

Kang S., Warner M. D., Bell S. P., 2014 Multiple Functions for Mcm2–7 ATPase Motifs during Replication Initiation. Molecular Cell 55: 655–665.

Karakaidos P., Taraviras S., Vassiliou L. V., Zacharatos P., Kastrinakis N. G., Kougiou D., Kouloukoussa M., Nishitani H., Papavassiliou A. G., Lygerou Z., Gorgoulis V. G., 2004 Overexpression of the replication licensing regulators hCdt1 and hCdc6 characterizes a subset of non-small-cell lung carcinomas: synergistic effect with mutant p53 on tumor growth and chromosomal instability--evidence of E2F-1 transcriptional control over hCdt1. Am J Pathol 165: 1351–1365.

Kawasaki Y., Kim H.-D., Kojima A., Seki T., Sugino A., 2006 Reconstitution of Saccharomyces cerevisiae prereplicative complex assembly in vitro. Genes to Cells 11: 745-756.

Kitamura E., Tanaka K., Kitamura Y., Tanaka T. U., 2007 Kinetochore microtubule interaction during S phase in Saccharomyces cerevisiae. Genes & Development 21: 3319–3330.

Klemm R. D., Austin R. J., Bell S. P., 1997 Coordinate binding of ATP and origin DNA regulates the ATPase activity of the origin recognition complex. Cell 88: 493–502.

Labib K., 2010 How do Cdc7 and cyclin-dependent kinases trigger the initiation of chromosome replication in eukaryotic cells? Genes & Development 24: 1208–1219.

Lara-Gonzalez P., Westhorpe F. G., Taylor S. S., 2012 The Spindle Assembly Checkpoint. Current Biology 22: R966–R980.

Liku M. E., Nguyen V. Q., Rosales A. W., Irie K., Li J. J., 2005 CDK phosphorylation of a novel NLS-NES module distributed between two subunits of the Mcm2-7 complex prevents chromosomal rereplication. Mol Biol Cell 16: 5026–5039.

Liontos M., Koutsami M., Sideridou M., Evangelou K., Kletsas D., Levy B., Kotsinas A., Nahum O., Zoumpourlis V., Kouloukoussa M., Lygerou Z., Taraviras S., Kittas C., Bartkova J., Papavassiliou A. G., Bartek J., Halazonetis T. D., Gorgoulis V. G., 2007 Deregulated overexpression of hCdt1 and hCdc6 promotes malignant behavior. Cancer Res 67: 10899–10909.

Malumbres M., 2011 Oncogene-Induced Mitotic Stress: p53 and pRb Get Mad Too. Cancer Cell 19: 691–692.

Marston A. L., 2014 Chromosome Segregation in Budding Yeast: Sister Chromatid Cohesion and Related Mechanisms. Genetics 196: 31–63.

McCarroll R., Fangman W., 1988 Time of replication of yeast centromeres and telomeres. Cell(Cambridge) 54: 505–513.

McIntosh D., Blow J. J., 2012 Dormant origins, the licensing checkpoint, and the response to replicative stresses. Cold Spring Harb Perspect Biol 4.

Mitelman F., Johansson B., Mertens F. E., 2012 Mitelman Database of Chromosome Aberrations and Gene Fusions in Cancer. http://cgap.nci.nih.gov/Chromosomes/Mitelman

Murayama Y., Uhlmann F., 2014 Biochemical reconstitution of topological DNA binding by the cohesin ring. Nature 505: 367–371.

Murphy N., Ring M., Heffron C. C. B. B., Martin C. M., McGuinness E., Sheils O., O'Leary J. J., 2005 Quantitation of CDC6 and MCM5 mRNA in cervical intraepithelial neoplasia and invasive squamous cell carcinoma of the cervix. Mod Pathol 18: 844–849.

Nguyen V. Q., Co C., Li J. J., 2001 Cyclin-dependent kinases prevent DNA re-replication through multiple mechanisms. Nature 411: 1068–1073.

Nishitani H., Lygerou Z., 2002 Control of DNA replication licensing in a cell cycle. Genes Cells 7: 523–534.

Perez De Castro I., De Carcer G., Malumbres M., 2006 A census of mitotic cancer genes: new insights into tumor cell biology and cancer therapy. Carcinogenesis 28: 899–912.

Ren B., Yu G., Tseng G. C., Cieply K., Gavel T., Nelson J., Michalopoulos G., Yu Y. P., Luo J.-H., 2006 MCM7 amplification and overexpression are associated with prostate cancer progression. Oncogene 25: 1090–1098.

Richardson C. D., Li J. J., 2014 Regulatory Mechanisms That Prevent Re-initiation of DNA Replication Can Be Locally Modulated at Origins by Nearby Sequence Elements (S Gerbi, Ed.). PLoS Genet 10: e1004358.

Roschke A. V., Rozenblum E., 2013 Multi-Layered Cancer Chromosomal Instability Phenotype. Front. Oncol. 3: 302.

Santarius T., Shipley J., Brewer D., Stratton M. R., Cooper C. S., 2010 A census of amplified and overexpressed human cancer genes. Nat Rev Cancer 10: 59–64.

Schvartzman J.-M., Duijf P. H. G., Sotillo R., Coker C., Benezra R., 2011 Mad2 Is a Critical Mediator of the Chromosome Instability Observed upon Rb and p53 Pathway Inhibition. Cancer Cell 19: 701–714.

Schvartzman J.-M., Sotillo R., Benezra R., 2010 Mitotic chromosomal instability and cancer: mouse modelling of the human disease. Nat Rev Cancer 10: 102–115.

Sheltzer J. M., Blank H. M., Pfau S. J., Tange Y., George B. M., Humpton T. J., Brito I. L., Hiraoka Y., Niwa O., Amon A., 2011 Aneuploidy Drives Genomic Instability in Yeast. Science 333: 1026–1030.

Sherr C. J., McCormick F., 2002 The RB and p53 pathways in cancer. Cancer Cell 2: 103–112.

Siddiqui K., On K. F., Diffley J. F. X., 2013 Regulating DNA Replication in Eukarya. Cold Spring Harb Perspect Biol.

Tanaka S., Umemori T., Hirai K., Muramatsu S., Kamimura Y., Araki H., 2007 CDK-dependent phosphorylation of Sld2 and Sld3 initiates DNA replication in budding yeast. Nature 445: 328–332.

Tighe A., Johnson V. L., Albertella M., Taylor S. S., 2001 Aneuploid colon cancer cells have a robust spindle checkpoint. EMBO Rep 2: 609–614.

Uhlmann F., Lottspeich F., Nasmyth K., 1999 Sister-chromatid separation at anaphase onset is promoted by cleavage of the cohesin subunit Scc1. Nature 400: 37–42.

Uhlmann F., Nasmyth K., 1998 Cohesion between sister chromatids must be established during DNA replication. Current Biology 8: 1095–1101.

Unal E., Heidinger-Pauli J. M., Kim W., Guacci V., Onn I., Gygi S. P., Koshland D. E., 2008 A Molecular Determinant for the Establishment of Sister Chromatid Cohesion. Science 321: 566–569.

Verdaasdonk J. S., Bloom K., 2011 Centromeres: unique chromatin structures that drive chromosome segregation. Nature Publishing Group 12: 320–332.

Weaver B. A. A., Cleveland D. W., 2006 Does aneuploidy cause cancer? Curr Opin Cell Biol 18: 658–667.

Winey M., O'Toole E. T., 2001 The spindle cycle in budding yeast. Nat Cell Biol 3: E23–7.

Zasadil L. M., Britigan E. M. C., Weaver B. A., 2013 2n or not 2n: Aneuploidy, polyploidy and chromosomal instability in primary and tumor cells. Semin Cell Dev Biol: 1–10.

Zegerman P., Diffley J. F. X., 2007 Phosphorylation of Sld2 and Sld3 by cyclin-dependent kinases promotes DNA replication in budding yeast. Nature 445: 281–285.

Chapter Two: Re-replication of a centromere causes whole-chromosomal instability and aneuploidy

Re-replication of a Centromere Induces Whole-Chromosomal Instability and Aneuploidy

Authors: Stacey L. Hanlon[1] and Joachim J. Li[2]*

Affiliations:

[1] Department of Biochemistry and Biophysics, University of California, San Francisco, CA 94158.

[2] Department of Microbiology and Immunology, University of California, San Francisco, CA 94158.

*Correspondence to: joachim.li@ucsf.edu, 415-476-8782.

At the time of dissertation, this manuscript was submitted and under review at eLife.

Abstract

Aneuploidy, a hallmark of cancer, often arises from whole-chromosomal instability (W-CIN). Many cancers exhibiting W-CIN, however, show no direct insult to the mitotic proteins that ensure proper segregation of chromosomes, stimulating interest in non-mitotic defects that can disrupt chromosome segregation. Here we show in *Saccharomyces cerevisiae* that transient re-replication of centromeric DNA, due to deregulation of replication initiation proteins, greatly induces aneuploidy of the rereplicated chromosome. Some of this aneuploidy arises from missegregation of sister chromatids, indicating that centromeric re-replication can disrupt proper chromosome behavior during mitosis. Aneuploidy also arises from the generation of an extra sister chromatid via homologous recombination, suggesting that centromeric re-replication can trigger breakage and repair events that expand chromosome numbers without causing chromosomal rearrangements. Given the emerging connections between the deregulation of replication initiation proteins and oncogenesis, our findings offer the possibility of a new non-mitotic source of aneuploidy that may be relevant to cancer.

Introduction

During their life cycle, cells must duplicate their genome exactly once and then precisely segregate the two copies into the daughter cells. In eukaryotes, elaborate regulatory controls ensure that each of these processes occur with great fidelity. Because DNA replication and chromosome segregation are such distinct processes occurring at opposite stages of the cell cycle, these controls are usually studied independently of each other.

The initiation of DNA replication is regulated at thousands of replication origins scattered throughout eukaryotic genomes This initiation is restricted to one round per cell cycle by multiple mechanisms that inhibit early initiation proteins—the origin recognition complex (ORC), Cdc6, Cdt1, and replicative helicase Mcm2-7—after they have executed their initiation function: the loading of Mcm2-7 at origins to license them for initiation (1-3). Once these origins initiate in S phase, the inactivation of these licensing proteins prevents re-licensing and hence re-initiation for the remainder of the cell cycle. Much of this inactivation is mediated by cyclin-dependent kinases (CDKs) through phosphorylation and/or direct binding. In addition, Cdt1 is inhibited in metazoans by replication-coupled proteolysis or by binding to inhibitory proteins called geminins. Each of these many mechanisms contributes to minimizing the probability of re-initiation, as deregulation of these mechanisms leads to progressively more re-initiation as more mechanisms are compromised.

After chromosomal replication, faithful segregation of the resulting sister chromatids requires the correct bi-polar attachment of sister centromeres to microtubules emanating from opposite poles of the mitotic spindle (4, 5). This biorientation of sister chromatids is established in mitosis at kinetochore complexes that are assembled onto centromeres and serve as an

attachment site for microtubules. Rings of cohesin complexes are thought to embrace both sister chromatids especially around their centromeres, preventing their premature separation and allowing for the detection of tension across sisters when they become bioriented. The absence of this tension is sensed by the spindle assembly checkpoint (SAC), which prevents anaphase until all sister chromatid pairs become bioriented (6). When anaphase proceeds, the cohesin rings are cleaved, releasing each chromatid to be pulled to the spindle pole to which they are attached. Importantly, this precise segregation of sister chromatids depends on the premise of bilateral symmetry for both the spindle and the sister kinetochores.

In cancer cells, the fidelity of chromosome segregation is frequently compromised, resulting in increased missegregation rates (i.e., whole-chromosomal instability, or W-CIN) and aneuploidy (7). Approximately 90% of solid tumors and 50% of hematopoetic cancers are aneuploid, with many exhibiting W-CIN (8, 9). Moreover, there are increasing hints that aneuploidy may contribute to tumorigenesis and is not simply an associated consequence (10). Thus there is much interest in understanding how in cancer cells aquire W-CIN..

Despite their essential roles in chromosome segregation, genes directly involved in kinetochore function, spindle function, cohesion, or the SAC are rarely mutated in sequenced cancer genomes (11). Instead, investigators are now focused on other perturbations that can facilitate merotelic kinetochore attachments, where one sister chromatid is attached to microtubules from opposing centrosomes at the poles of mitotic spindles (11, 12). These merotelic attachments are frequently observed in cancer cells with W-CIN and can lead to a tug-of-war on the affected chromatid, increasing its chance of missegregating. One perturbation that has received considerable support is the amplification of centrosomes, which is thought to facilitate merotelic attachments by disrupting the precise bilateral symmetry of the

spindle. Despite its prevalence in many cancers, however, centrosome amplification is not observed in all cancers displaying W-CIN (13), raising the question of what other perturbations can contribute to W-CIN.

Given that replication initiation proteins are often deregulated in cancer cells (14), one appealing potential source of W-CIN is the re-replication of centromeres, as it has the potential to disrupt segregation in multiple ways. The most obvious way is by eliminating the bilateral symmetry of sister centromeres and making the re-replicated chromatid susceptible to a pseudo-merotelic attachment, but re-replication through a centromere could also conceivably compromise its kinetochore or its cohesion. To explore this possibility, we asked whether transient and localized re-replication of a centromere could disrupt the segregation of a chromosome in the budding yeast *Saccharomyces cerevisiae*. We find that centromeric re-replication is a potent way of inducing missegregation of both sister chromatids to one daughter cell. Surprisingly, we also discover that centromeric re-replication can induce aneuploidy by formation of an extra sister chromatid. This formation is dependent on homologous recombination (HR), suggesting that centromeric re-replication can lead to chromosomal breaks that then undergo homologous recombination to reconstitute intact chromatids. Finally, microscopic examination of re-replicated centromeres suggests that they have the ability to reassemble functional kinetochores and be placed under tension. In summary, the deregulation of DNA replication initiation can have a significant impact on the mitotic mechanisms that ensure faithful chromosome segregation and provides a potential new source of W-CIN and aneuploidy in cancer cells.

Results

We previously demonstrated that the cell cycle controls preventing reinitiation of replication are critical for genome stability by showing that compromising these controls leads to intrachromosomal amplifications (15). In those studies we developed a system in which conditional deregulation of replication initiation proteins can induce transient and localized re-replication of any chromosome segment of interest. This system provided an opportunity to explore how the regulation of DNA replication influences the execution of mitosis by allowing us to induce the re-replication of a centromere and break a fundamental premise of mitosis: the bilateral symmetry of centromeres in sister-chromatid pairs.

To examine if re-replication could affect chromosomal stability, we designed an assay to quantify the segregation fidelity of a budding yeast chromosome following the transient, localized re-replication of its centromere. We had previously shown that conditional deregulation of a specific subset of DNA replication controls makes origins susceptible to re-initiation, with the most prominent and detectable re-initiation occurring at the origin *ARS317* (15, 16). To induce overt re-replication of a centromere, we inserted a cassette containing *ARS317* 8 kb from the Chromosome V centromere (*CEN5*) on one of the two homologs in a diploid re-replicating strain. To monitor the copy number of the re-replicating chromosome, the cassette also carried the copy-number reporter *ade3-2p*, which makes cells containing zero, one, or more copies white, pink, or red, respectively (17).

In our assay (Fig. 1A), exponentially growing cells were allowed to proceed through a normal S phase before being arrested in metaphase using the spindle inhibitor nocodazole. At the arrest, re-replication was transiently induced until half of the *ARS317* in the population had

re-initiated, as measured by array comparative genomic hybridization (aCGH) (Fig. 1B). Cells were released from the arrest either before or after the induction of re-replication by plating for individual colonies. These colonies were screened for colored sectors that suggested the *ade3-2p* marked Chromosome V homolog missegregated in the mitosis following the induced re-replication. Normal segregation of one sister chromatid to each daughter cell (1:1 segregation) produces a uniformly pink colony. However, missegregation of both sister chromatids to one daughter (2:0 segregation) would leave it cell with both copies of the *ade3-2p* reporter and the other daughter with none, generating colonies divided into large red and white sectors (Fig. 1C).

The frequency of red/white sectored colonies observed after centromeric re-replication was 7.8×10^{-3}, nearly 20 times the frequency observed in colonies plated before the induction of re-replication (Fig. 2A). In contrast, this induction did not significantly stimulate the frequency of red/white colonies in a congenic strain lacking *ARS317* or a strain where *ARS317* was relocated near the right end of Chromosome V (Fig. 2A). In the latter strain, re-initiation from *ARS317* was too far away to cause measurable *CEN5* re-replication (Fig. 1B, bottom panel), demonstrating that it was specifically centromeric re-replication that induced the high frequency of red/white colony formation.

To determine if the red/white sectored colonies induced by *CEN5* re-replication are genotypically consistent with a 2:0 missegregation of the re-replicated Chromosome V homolog, we used aCGH to assess genomic copy number in each sector. Assuming that the unmarked nonrereplicating homolog segregates normally 1:1, we would expect the red sector to contain a total of three copies of Chromosome V and the white sector to contain one copy. Nine out of 11 red/white sectored colonies showed such a distribution of Chromosome V (Fig. 2B, Table S2),

suggesting that a large proportion of the red/white sectored colonies scored likely arose from a 2:0 missegregation event. Of the much fewer red/white colonies derived from the re-replicating strain completely lacking *ARS317*, a similar proportion (3/4) also corresponded to colonies that had undergone 2:0 missegregation of the *ade3-2p* marked Chromosome V homolog (Table S2).

This aCGH analysis allowed us to estimate the frequency of apparent 2:0 missegregation events from the frequency of red/white colonies (Fig. 2C, Table S7). Centromeric re-replication induced by *ARS317* caused a missegregation frequency of 6.4×10^{-3} in the following mitosis, approximately 12-fold higher than the missegregation frequency observed in the absence of *ARS317*. We suspect that the latter frequency is itself elevated both because of the prolonged nocodazole arrest (18, 19) and because of cryptic re-replication occurring throughout the genome independent of *ARS317* (and possibly involving *CEN5*) (16, 20). Hence, we were most interested in comparing the re-replication-induced frequency of Chromosome V 2:0 missegregation events to the spontaneous frequency of these events. Although the latter has not been directly measured for Chromosome V in wild-type diploid cells, upper limits can be estimated by the spontaneous rate of Chromosome V loss ($2\text{-}8 \times 10^{-6}$ per cell division (21, 22)) and gain (3×10^{-7} per cell division (23)), respectively. Thus, the frequency of 2:0 missegregation events induced by transient centromeric re-replication in a single cell cycle is at least a 10^3 - 10^4 higher than the expected spontaneous frequency of these events. We conclude that centromeric re-replication can be a potent inducer of W-CIN and aneuploidy.

Surprisingly, we also discovered a second source of aneuploidy induced by centromeric re-replication from *ARS317*. Colonies divided into large red and pink sectors were observed following centromeric re-replication at a frequency of 2.4×10^{-2}, ten-fold higher than the frequency of red/pink colonies observed in a strain lacking *ARS317* (Fig. 3A). The color of the

sectors suggested the presence of one copy of the *ade3-2p* marked Chromosome V homolog in the pink sector and at least two copies in the red sector, consistent with there being three copies of the re-replicating homolog segregating in a 2:1 manner. For most of these red/pink colonies, this 2:1 segregation was confirmed by aCGH data showing a total of three copies of Chromosome V in the red sector and two copies in the pink sector (Table S3). Using the aCGH data to convert red/pink colony frequencies to 2:1 segregation frequencies (Table S7), we observed that strains with *ARS317* driving centromeric re-replication induced these events at a frequency of 2.0×10^{-2}, 22-fold higher than strains without *ARS317* (Fig. 3B). This induction of 2:1 segregation suggests that centromeric re-replication can induce chromosome gain by forming a whole additional copy of the chromosome. Upper limits on the frequency of these 2:1 events is provided by the spontaneous rate of chromosome gain, 3×10^{-7} per cell division (23). Thus, the frequency of 2:1 missegregation events induced by transient centromeric re-replication in a single cell cycle is approximately 10^4 to 10^5 higher than the expected spontaneous frequency of these events.

A trivial explanation for chromosome gain is that, despite the predominantly localized nature of the re-replication induced by *ARS317* on Chromosome V (Fig. 1B), a small fraction of these chromosomes somehow manage to re-replicate to completion. If that were the case, however, we would expect the red-pink colony frequency to be independent of the chromosomal location of *ARS317*. Using the strain with *ARS317* relocated near the right end of Chromosome V to minimize centromeric re-replication (Fig. 1B), we found that the red/pink colony frequency was similar to that of the strain completely lacking *ARS317* (Fig. 3A). We thus conclude that the extra copy of Chromosome V detected in the red/pink colonies is dependent on centromeric re-replication and unlikely to be due to re-replication of the entire chromosome.

An alternative route for generating these extra chromosomes is suggested by our previous observation that re-replication forks are highly susceptible to breakage (24). Hence, we wondered whether the extra chromosomes in our red/pink colonies could have been the product of double-strand break (DSB) repair. Eukaryotes rely primarily on two pathways to repair DSBs (25-27). One is homologous recombination (HR), which in budding yeast is dependent of Rad52, a protein that can facilitate complementary strand annealing and single-strand exchange (28, 29). The other is nonhomologous endjoining (NHEJ), which depends on Dnl4, the ortholog of DNA Ligase IV in budding yeast (30). To test if DSB repair plays a role in the induction of 2:1 segregation events, we performed centromeric re-replication experiments in *rad52*Δ, *dnl4*Δ, and *rad52*Δ*dnl4*Δ backgrounds.

Deletion of *RAD52* reduced the induced frequency of red/pink colonies (Fig. 3C) and 2:1 segregation events (as determined by aCGH) (Fig. 3D and Tables S3, S7) by approximately half. Thus a significant proportion of 2:1 segregation events induced by centromeric re-replication depend on HR. Curiously, the induced frequency of red/pink colonies and 2:1 segregation events nearly tripled when *DNL4* was deleted (Fig. 3C, 3D and Tales S3, S7). Moreover, the vast majority of these additional colonies and segregation events were dependent on *RAD52*, as demonstrated by the drop to *rad52*Δ levels in the *rad52*Δ*dnl4*Δ double deletion strain (Fig. 3C & 3D). Importantly, none of the changes in frequencies observed with any of the deletions could be attributed to changes in re-replication efficiency because the re-replication profiles of the deletion mutants were comparable to that of the wild-type strain (Fig. S2). In addition, the effect of the deletions was specific to the 2:1 segregation events because the red-white colony frequencies associated with 2:0 missegregation events were not affected by the deletions (Fig. S3). Together these results suggest that DNA damage induced by centromeric re-replication can

be efficiently repaired by HR in a manner that generates an extra whole sister chromatid. This route to aneuploidy appears to be partially inhibited by NHEJ, possibly by competition for the damage substrate (25, 26).

By temporally isolating the centromeric re-replication of a chromosome from its normal replication and segregation, the experimental strategy used above provided the cleanest demonstration that re-replication induces 2:0 and 2:1 segregation events. This strategy, however, left open the possibility that the spindle disruption and/or metaphase arrest caused by nocodazole was also required for the induction of these events (18, 19). Hence, we asked if centromeric re-replication induced in unarrested, asynchronously-dividing cells was sufficient to induce 2:0 and 2:1 events. We activated re-replication for three hours in these cells, which induced equivalent amounts of centromeric re-replication as that induced by three hours of re-replication in nocodazole-arrested cells (Fig. S4). The state of the cells plated after the re-replication was also comparable in that they had undergone re-replication for approximately one cell cycle before the DNA damage caused by re-replication (31-34) triggered their transient arrest in mitosis (Fig. S5). In the absence of nocodazole, we still observed strong induction of red/white and red/pink colonies relative to a strain lacking *ARS317* (Fig. 4A, 4C). Analysis of chromosomal copy number using aCGH confirmed that this colony induction reflected increases in the frequencies of 2:0 and 2:1 segregation events (Fig. 4B, 4D and Tables S4, S5, S7). Thus, centromeric re-replication induced in cycling cells is sufficient to generate these events.

As a first step toward exploring the molecular events that lead from centromeric re-replication to chromosome missegregation or breakage we examined the mitotic behavior of re-replicated centromeres by fluorescence microscopy. The re-replicating *CEN5* was fluorescently marked with *TET* operator arrays placed 2 kb to the left of the centromere in haploid cells

expressing TdTomato-tagged Tet repressors. At this distance, bipolar spindle tension placed on normal bioriented sister centromeres in metaphase can be detected by the separation of sister arrays into two resolvable fluorescent spots (35-37). To monitor the position of the marked centromeres relative to the mitotic spindle, the microtubule subunit Tub1 was tagged with GFP.

Cycling cells induced to re-replicate trigger a DNA damage response that casuses them to arrest in metaphase (Figure S5, (32)). At this point, we can observe the opposing action of bipolar spindle tension and pericentromeric cohesion on centromeres. When *ARS317* was not present to re-initiate replication near *CEN5*, all metaphase arrested cells displayed two resolvable fluorescent spots during periodic imaging over a 20 min period. This was consistent with the "centromere breathing" expected of bioriented sister centromeres. In contrast, when *ARS317* was positioned near *CEN5* so that 40-50% of these centromeres re-replicated, cells displaying three or four spots were observed (Fig. 5A and 5B). The total number of additional spots observed was 33-40% above that expected for bioriented sister centromeres in the absence of centromeric re-replication. This implies that a large proportion of the re-replicated centromeres of a sister chromatid can be pulled apart from each other as well as from the centromere (or possibly re-replicated centromeres) of the other sister chromatid. During the periodic imaging, both unrereplicated and re-replicated centromeres could be seen moving back and forth along the length of the metaphase spindle. The highly dynamic nature of these oscillations was captured with time-lapse imaging of re-replicated cells containing three spots (Fig. 5C, Movie S3). These results are consistent with re-replicated centromeres in each cell undergoing separation and oscillations due to bipolar spindle tension.

To determine if the separation and motion of centromeres was indeed dependent on spindle tension, the cells we scored for spot numbers were continuously imaged after treatment

with nocodazole, which inhibits microtubule polymerization. For the cells without *ARS317* near *CEN5*, approximately 85% of the sister centromere pairs collapsed to a single spot as the mitotic spindle disappeared, similar to a previously published quantification of the effects of nocodazole on centromere breathing (38). This collapse is due to pericentromeric cohesion, which resists the spindle tension placed on bioriented sister centromeres. For cells with *ARS317* near *CEN5*, most of those with two or three spots end up with one spot displaying little directed motion (Fig. 5A and 5B, Movies S1 and S2). The collapse of three spots to one indicates that many of these re-replicated centromeres separated and oscillated because of spindle tension. It further implies that these re-replicated centromeres reassembled functional kinetochores, maintained pericentromeric cohesion, and underwent pseudo-merotelic attachments.

We note that, although many cells with four resolvable spots showed a reduction in the number and motion of spots upon nocodazole addition, most did not collapse down to a single spot. There were also a few cells with three spots that retained all three after nocodazole treatment. These observations suggests that in some cases pericentromeric cohesion of re-replicated centromeres may be compromised, particularly if more than one centromere is re-replicated.

Discussion

We have shown that centromeric re-replication can provide a highly potent way to induce W-CIN and aneuploidy in cells where the mitotic segregation machinery is intrinsically intact. This aneuploidy is generated in part through missegregation of both sister chromatids to one daughter cell. Such a re-replication induced missegregation may be relevant to cancers associated with W-CIN that have no obvious molecular insult to their mitotic proteins or structural defect in their mitotic spindle. Exactly how centromeric re-replication promotes missegregation remains to be determined, but it has the potential to perturb the segregation machinery in multiple ways. Three of the most obvious possibilities are disruption of kinetochores, disruption of centromeric cohesion, and pseudo-merotelic attachment to a sister chromatid with duplicated kinetochores.

In budding yeast, replication forks disrupt kinetochores inherited from the previous cell cycle, but these kinetochores are rapidly reassembled onto replicated centromeres after the fork passes through (39). Hence, although re-replication forks are also likely to disrupt kinetochores, this only poses a problem if kinetochores cannot reassemble back onto the re-replicated centromeres. In principle, we might not expect a major problem, as budding yeast kinetochores can assemble and become functional throughout the cell cycle (40). Moreover, our observation that more than two centromeres in a re-replicating strain can be microscopically resolved in a microtubule dependent manner is consistent with the assembly of functional kinetochores on many re-replicated centromeres. Nonetheless, we cannot rule out that failure to reassemble kinetochores onto re-replicated centromeres in a minority of cells was responsible for some of the missegregation we detected in our sectored colony assay.

The microtubule-dependent separation of re-replicated centromeres also suggests that pericentromeric cohesion is often preserved following centromeric re-replication. Such cohesion is presumably responsible for the collapse of re-replicated and separated *CEN5* spots to a single spot following the disruption of microtubules. However, this complete collapse is less likely when more than three spots are present in a cell, suggesting that in some instances, particularly when more than one centromere re-replicates, pericentromeric cohesion may be compromised.

Once centromeres re-replicate and reassemble kinetochores, microtubules from opposite spindle poles can form bipolar attachments to the duplicated kinetochores in the re-replication bubble, making a pseudo-merotelic attachment to the sister chromatid (Figure 6). Our observation of three or four resolvable centromeres oscillating back and forth along the spindle in a microtubule dependent manner is consistent with such pseudo-merotely. During anaphase such attachments can cause the re-replicated sister chromatid to be pulled by both poles of a mitotic spindle, increasing the chances of its missegregation. Importantly, the re-replication bubble at the center of this pseudo-merotely is a transient chromosomal structure. It can be readily eliminated during DNA replication in subsequent S phases, leaving a simple chromosomal aneuploidy to be propagated in both daughter cells following the missegregation. Thus, re-replication can induce aneuploidy in a hit-and-run fashion, in contrast to dicentric chromosomes, whose equivalent bipolar attachment inevitably leads to chromosome breakage and rearrangement (41-43).

In addition to inducing aneuploidy by missegregating sister chromatids, centromeric re-replication can also induce aneuploidy by the formation of extra sister chromatids, as manifest by the appearance of 2:1 segregation events. The dependence of at least half of these events on *RAD52*, a gene essential for the main forms of homologous recombination in budding yeast,

implies that many of these extra chromatids are generated by chromosome breakage and recombinational repair. The breakage is not surprising: we have previously shown that re-replication forks are susceptible to breakage (24), and their fragility may be exacerbated by mechanical stress when a centromeric re-replication bubble is placed under bipolar tension by pseudo-merotelic attachment. What is striking, however, is the apparent efficiency with which the repair of these breaks can be channeled into the formation of extra sister chromatids, in sharp contrast to the chromosomal rearrangements that almost always result from dicentric chromosome breaks. Whether similar generation of aneuploidy by extra sister chromatid formation can occur in mammalian cells with their much larger chromosomes remains to be seen. Nonetheless, centromeric re-replication in budding yeast has identified a novel way in which aneuploidy can be generated.

It is possible that centromeric re-replication can also lead to other chromosomal consequences that we did not observe either because they are lethal or because we did not score them. For example, the large rise in *RAD52*-dependent 2:1 segregation events in a *dnl4* mutant background provides a hint that there may be other competing fates for chromosome breakage events that involve nonhomologous end-joining. In our primary colony screen, we focused on colonies that were obviously induced by centromeric re-replication and that we anticipated would be most straightforward to interpret, namely red-white and red-pink sectored colonies. Analysis of some of the other colonies with different or more complex shapes and color patterns may uncover other types of chromosomal loss, gain or rearrangements induced by centromeric re-replication.

There is accumulating evidence suggesting that re-replication occurs in cancers and is relevant to oncogenesis. First, deregulation of the replication initiation proteins Cdc6 and Cdt1,

which can promote re-replication in cell culture and model organisms (33, 44-49), has been observed in multiple types of cancers (50-55). Second, experimental overexpression of replication initiation proteins can promote carcinogenesis in mouse models (52, 56, 57). Re-replication in either natural or experimentally derived cancer cells, however, has been difficult to detect by standard replication assays (44, 52, 56, 57). This is likely due to the insensitivity of these assays and the extensive DNA damage induced by re-replication, which makes re-replication at levels detectable by current assays highly lethal (31-34, 44, 45, 58-61). In our experiments, we could minimize this lethality by conditionally and transiently inducing re-replication. However, any re-replication occurring natively without such experimental manipulation would likely be limited to low cryptic levels that are compatible with cell viability. Fortunately, the development of more sensitive re-replication assays shows promise in detecting such low levels in cancer cells (62).

The striking efficiency with which centromeric re-replication induces aneuploidy in our experiments makes it conceivable for much lower levels of re-replication to still induce substantial W-CIN. Indeed, this efficiency may account for why W-CIN could be detected in cell lines overexpressing Cdt1 despite the inability to detect re-replication (63). Our study thus raises the possibility that centromeric re-replication can provide a new source of W-CIN and aneuploidy in cancer.

Materials and Methods

Oligonucleotides

Oligonucleotides used for disrupting *RAD52*, *DNL4*, or *HMRa,* inserting the *URA3* marker, or inserting the targeting marker *TRP1* for the tetO array insertion are listed in Table S10.

Plasmids

The plasmids pSH006 and pSH005 were constructed for integrating the copy number reporter *ade3-2p (17)* with or without *ARS317*, respectively, at ChrV_160kb near *CEN5*. The plasmid pSH006 contains the *kanMX-ade3-2p-ARS317* cassette cut from pBJL2890 (15) with XbaI and StuI, and pSH005 contains the *kanMX-ade3-2p* cassette from pBJL2889 (15) with XbaI and StuI, but both cassettes are flanked by homology sequences from ChrV_160 as listed in Table S9. To make pSH008, pSH006 was cut with BsaBI and XbaI, filled in, and ligated to remove a secondary NotI site.

The plasmids pSH020 and pSH019 were constructed for integrating *ade3-2w* with or without *ARS317*, respectively, at ChrV_548kb near the right end of Chromosome V. The plasmid pSH020 contains a *natMX-ade3-2w-ARS317* cassette based on the cassette in pSH008 but with *natMX* replacing *kanMX* and *ade3-2w* replacing *ade3-2p*. The allele *ade3-2w* is a derivative of *ade3-2p* where a frameshift mutation has been engineered at the beginning (+46) of the open reading frame by inserting a single nucleotide. The cassette in pSH020 is flanked by homology

sequences from ChrV_548 that are listed in Table S9. The plasmid pSH019 is equivalent to pSH005 but has no *ARS317* in the cassette.

The plasmid pSH013 was constructed to introduce *bar1*Δ by two-step gene replacement. It contains genomic sequences upstream and downstream of the *BAR1* open reading frame (separated by a SpeI restriction site) cloned into pRS306 (64).

The plasmid pSR14 was obtained from the Dave Morgan Lab (UCSF) with permission from its original source, the Susan Gasser Lab (Friedrich Miescher Institute). This plasmid contains 128 tandem copies of the *tet TET* operator, the *LEU2* marker, and target sequence for its integration into the genome (65).

The plasmid pCUP1-TetR-tdTomato-ADE2 was obtained from Dan Liu in the Dave Morgan Lab (UCSF) to produce a *tet TET* repressor linked to the fluorescent protein tdTomato (red). To construct it, the *tet TET* repressor linked to the tdTomato sequence was placed after the pCUP1 promoter. This fragment was integrated into the middle of *ADE2*, and the entire fragment inserted into pRS406. The tdTomato lacks a nuclear localization sequence.

The plasmid pBJL2667 contains the tubulin subunit *Tub1* linked to the fluorescent marker GFP (green) in pRS304. This plasmid was derived from Aaron Straight's (Stanford) plasmid pAFS91 by Brian Green, a former student in the lab.

Sequences files for all plasmids are available upon request.

Strain construction

All haploid and diploid strains used in our experiments are in a genetic background that can conditionally induce re-initiation of DNA replication, most prominently from the origin *ARS317*. They also have one homolog of Chromosome V marked with the *ade3-2p* copy number reporter to the right its centromere *CEN5* (ChrV_160kb). This *ade3-2p* marked homolog also contains *ARS317* close to the centromere *CEN5* (ChrV_160kb), *ARS317* near the right end of the chromosome (ChrV_548kb), or no *ARS317* at all. The basic strategy for generating these diploids was to mate a *MATa* haploid strain containing the *ade3-2p* marked Chromosome V with a congenic *MATα* strain containing a *URA3* marked Chromosome V.

All haploid strains used in these matings were derived from the haploid strain YL3155 (15) (*MATa ORC2-(NotI, SgrAI) orc6(S116A) leu2 ura3-52 trp1-289 ade2 ade3 MCM7-2NLS bar1::LEU2 CAN1 HMRa*). YJL3155 is primed to re-initiate DNA replication because the *MCM7-2NLS* allele makes the Mcm2-7 complex constitutively nuclear (66), and the *orc6(S116A)* partially prevents CDK inhibition of the origin recognition complex (ORC) by mutating one of the 11 CDK consensus phosphorylation sites in ORC (67). To generate the haploid strains used in the matings, various combinations of changes to the following loci were made:

MATα - *MATα* haploids were obtained by switching from *MATa* using *pGAL-HO* in pSB283 (68).

*hmra*Δ*::hphMX* – for both haploids, the endogenous *ARS317* was removed by deleting the entire *HMRa* locus. This was done by integrating an *hmra*Δ*::hphMX* disruption fragment that was generated by two-step PCR amplification from pAG26 (69) using primers described in Table S10.

*bar1*Δ - for both haploids, *bar1::LEU2* was converted to *bar1*Δ by loop-in/loop-out gene replacement using BsrG1 linearized pSH013.

*ura3*Δ*::{ACT1term-pGAL1/10-delntCDC6,cdk2A-CDC6term}* – for both haploids, a galactose-inducible, stabilized version of *CDC6* was integrated in place of the *uras3-52* allele by loop-in/loop-out gene replacement with SmaI linearized pKJF019 (24).

ChrV_160::{kanMX, ade3-2p, ±ARS317} – for the *MATa* haploids, *CEN5* was marked with the copy number reporter *ade3-2p* by integration of a cassette containing *kanMX* and *ade3-2p* at ChrV_160kb (right of the centromere). When *ARS317* was to be positioned near *CEN5*, we used a {*kanMX, ade3-2p, ARS317}* cassette excised from pSH008 with SacI and NotI. When *ARS317* was not to be on the chromosome or to be located on the right arm (at ChrV_548kb), we used a *{kanMX, ade3-2p}* cassette excised from pSH005 with SacI and NotI.

ChrV_160::URA3 – for the *MAT*α haploids *URA3* was integrated near *CEN5* by one step gene insertion with a *URA3* integration fragment generated by two step PCR amplification from pRS316 using the primers described in Table S10.

ChrV_548::{natMX, ade3-2w, ±ARS317} – for the *MATa* haploids, a cassette containing *natMX* and *ade3-2w* (an inactive color reporter) was integrated near the right end at ChrV_568kb. When *ARS317* was to be positioned at this location we used a {*natMX, ade3-2w, ARS317*} cassette excised from pSH020 excised with SacI and NotI. When *ARS317* was not to be on the chromosome or to be located near *CEN5*, we used a {*NatMX, ade3-2w*} cassette excised from pSH019 with SacI and NotI.

*dnl4*Δ - to make diploid strains homozygous for the *dnl4* deletion, *DNL4* in both *MATa* and *MATα* haploids was deleted by integrating a *dnl4*Δ*::LEU2* disruption fragment that was generated by two step PCR amplification from pRS315 (64) using the primers described in Table S10.

*rad52*Δ - to make diploid strains homozygous for the *rad52* deletion but wild-type for *DNL4*, *RAD52* in both *MATa* and *MATα* haploids was deleted by integrating a *rad52*Δ*::LEU2* disruption fragment that was generated by two step PCR amplification from pRS315 using the primers described in Table S10. To make diploid stains homozygous for both *rad52* and *dnl4*, *MATa* and *MATα* haploids that already contained the *dnl4*Δ*::LEU2* allele had their *RAD52* genes deleted using a different marker. A *rad52*Δ*::URA3* disruption fragment that was generated by two step PCR amplification from pAG36 (69) was used for the *MATa* haploids, and a *rad52*Δ*::natMX* disruption fragment that was generated by two step PCR amplification from pAG36 was used for the *MATα* haploids. Primers used for the PCR are listed in Table S10.

trp1-289::{GFP-TUB1, TRP1} – the plasmid pBJL2667 was linearized with Bsu36I and integrated via loop-in at the endogenous *trp1-289* locus.

ade2::{pCUP1-tetR-tdTomato, URA3, ADE2} – the plasmid pCUP1-TetR-tdTomato-ADE2 was linearized with BglII and looped-in at the endogenous *ade2* locus. Due to the inability of a functional *ADE2* to confer complete adenine prototrophy without a fully-functional *ADE3*, cells were selected for the *URA3* marker in the backbone of the plasmid. However, the presence of a fully-functional *ADE2* prevents accumulation of the red pigment produced in an *ade3-2p ade2* background, meaning colonies were now without color (white).

Chr5_151::{LEU2, tetOx128} – The plasmid pSR14 was linearized with AscI and stability integrated into ChrV at 151 kb, which is to the left of *CEN5* (the re-replication cassette is to the right of the centromere). To integrate this construct at the proper location, targeting homology was generated and integrated first. A fragment containing *TRP1* and specific targeting sequence was generated by PCR amplification from pRS314 using primers described in Table S10. This construct was placed at ChrV_151, which provided the targeting homology for the sequences at the end of the linearized pSR14. Cells were visually inspected for bright red spots prior to strain archiving.

Media and Cell Growth

Cells were grown in or on YEP medium (70) supplemented with 2% wt/vol dextrose (YEPD), 8% wt/vol dextrose (YEP8D), or 3% wt/vol raffinose + 0.05% wt/vol dextrose (to form YEPRd).

The color development plates were synthetic base with 2% wt/vol dextrose (SD), with the final amino acid concentrations as follows: adenine [10 μg/mL], uracil [20 μg/mL], tryptophan [20 μg/mL], histidine [20 μg/mL], arginine [20 μg/mL], methionine [20 μg/mL], tyrosine [30 μg/mL], leucine [60 μg/mL], isoleucine [30 μg/mL], lysine [30 μg/mL], phenyalanine [50 μg/mL], glutamate [100 μg/mL], aspartate [100 μg/mL], valine [150 μg/mL], threonine [200 μg/mL], serine [200 μg/mL]. These plates contain low adenine and are referred to as SDClowA plates. All cell growth was performed at 30°C except where otherwise noted.

The color from the ade3-2p reporter was most consistent when SDClowA plates were poured in a precise manner three days prior to use. For a 2 L batch, the following was added together in a 4 L flask: 13.4g Yeast Nitrogen base without amino acids, 40g Bacto-agar, 1 stir bar, and 1850mL MQH_2O. The opening of the flask was covered with foil, and the mix was stirred for 5 minutes. Media was autoclaved on a liquid cycle (30 minutes at 121°C with slow exhaust) in a dry autoclavable plastic tray. To prevent excessive heating the flask was removed as soon as the jacket pressure allowed the door to open, and the media was stirred for 10 minutes to mix and cool. At this point powdered amino acid mix and 100mL 40% Dextrose were added. The media then stirred for an additional 10 minutes to further mix and cool. Plates were poured using a PourBoy 4 plate pouring machine to dispense 33 mL of media per plate. These SDClowA plates were stacked unwrapped to allow them to dry but shielded from light until use in the assay.

For microscopy, cells were imaged in SDC-Trp media to maintain selective pressure on the integrated GFP-Tub1 construct. Prior to imaging, cells were grown and induced in S media supplemented with 3% wt/vol raffinose + 0.05% wt/vol dextrose (to form SRd). Amino acid

concentrations for both medias are as follows: adenine [40 μg/mL], uracil [40 μg/mL], tryptophan [0 μg/mL], histidine [40 μg/mL], arginine [40 μg/mL], methionine [40 μg/mL], tyrosine [60 μg/mL], leucine [120 μg/mL], isoleucine [60 μg/mL], lysine [60 μg/mL], phenyalanine [100 μg/mL], glutamate [200 μg/mL], aspartate [200 μg/mL], valine [300 μg/mL], threonine [400 μg/mL], serine [400 μg/mL].

Re-replication induction and sectoring assay

Colony color development and sectoring frequencies were most reproducible when freshly thawed cells were used and the re-replication induction and plating were performed in a precise manner. Yeast were thawed from frozen glycerol stocks onto YEPD plates and grown at 30°C. The following day, this patch was used to inoculate 25 mL of YEPD and was grown to an OD_{600} between 0.4 and 0.5 over the course of 4-5 hours at 30°C in a shaking (250 rpm) waterbath. From this culture, we inoculated the experimental culture grown at 30°C in non-repressive rich media containing 3% raffinose and 0.05% dextrose (YEPRd) so that after 13-15 hours, the culture would be growing exponentially at an OD_{600} between 0.4 and 0.5.

To arrest cells, nocodazole (US Biological, Salem, MA; Cat. no. N3000) was added to the culture at a final concentration of 15 μg/mL. After two hours of incubation, effective mitotic arrest was confirmed microscopically (>90% large budded cells) and 40% galactose was added to the arrested culture to a final concentration of 2.7%. Galactose induction was allowed to proceed for three hours before cells were washed and plated. A modification of this assay was used for YJL9631 and YJL9633, which have *ARS317* integrated at the right end of Chromosome

V. Total re-initiation from the right end of Chromosome V in these strains was higher after 3 hours of induction than the centromeric re-initiation from strains with *ARS317* integrated near *CEN5*, possibly from the low-level endogenous re-replication occurring on the end of the arm. Thus, to compare the consequences of equivalent amounts of re-initiation at the two locations, we reduced the galatose induction time for YJL9631 and YJL9633 to two hours. This was done by delaying the galatose induction until 3 hours after addition of nocodazole so that all strains were exposed to nocodazole for the same amount of time (5 hr). Cell cycle arrest and maintenance of arrest during the induction of re-replication were confirmed by flow cytometry.

After the induction, cells were diluted into YEPD to an approximate concentration of 1000 CFU/ml concentration, as estimated from the OD_{600} and the expected viability drop due to prolonged nocodazole arrest (~6x after 5 hr in nocodazole). From this dilution, 200µL (~200 CFU) were promptly spread onto SDClowA plates using 6-8 sterile glass beads per plate. The plates were incubated face-up at 30°C in the middle of an air incubator for 5-7 days, after which the plates were placed into a dark drawer at room temperature (18-22°C) for further color development. After 2-3 days there was optimal distinction between red and pink colors, and the plates were scored for color-sectored colonies.

The total number of colonies was hand-counted, then plates were manually screened using a Leica Modular Stereomicroscope MZ6 and a Leica KL1500 LCD 150-watt halogen cold light source and ring-light fixture. Lamp was set to 3200 K with the aperture 80% open. To be scored, sectored colonies were required to be at least 1 mm in diameter and have a red portion that was less than 75% but more than 25% of the total colony. This range of sector sizes was

chosen to accommodate differences in the time the two daughter cells might take to recover from the cell cycle arrest or possible differences in doubling times for the two daughter lineages. We were, however, stringent about sector color. The pink portion of each red/pink colony had to have the same tint as the surrounding pink colonies (indicative of the color a single copy of *ade3-2p* produced), and the red portion had to be of an unmistakably darker tint than the pink portion. The white portion had to be completely white and without colored tint. Colonies containing more than two colors were not scored. All sectors had to originate from the center of the colony, indicating they had been formed in an early cell division immediately following centromeric re-replication. Colonies with colored sectors originating from outside the center were not scored.

After all plates were screened and sectors tallied, colonies were picked from their original plate and struck onto a new SDClowA plate, then grown as described above to develop color. This colony purification process allowed us to obtain clonal isolates from each sector of the colony. From the streak, individual colonies were picked (one of each color) and patched onto rich media with 2% dextrose. These patches provided the material for glycerol freezer stocks, kept in 96-well plates at –80°C.

Monitoring re-replication via aCGH

The remainder of the cells not used in the platings described above were harvested after the induction of re-replication and their DNA extracted as previously described (referred to as "method 2") (24). We have referred to this protocol as the "Clean Genomic Prep" on the GEO

microarray database. This DNA was hybridized against reference DNA from YJL8590 (collected from a nocodazole-arrested culture that did not undergo re-replication) in the manner described previously (16). Briefly, reference DNA was labeled with Cy5 fluorescent dye and DNA from the re-replicating strain was labeled with Cy3 fluorescent dye. Equal quantities were combined and applied to an in-house printed microarray (GEO platform number GPL3412) and hybridized at 63°C for at least 20 hours. Arrays were then scanned using an Axon Scanner 4B and analyzed as described previously (16). All microarray data is deposited in the Gene Expression Omnibus (http://www.ncbi.nlm.nih.gov/geo/) with accession number GSE55641.

Copy-number determination via aCGH

Sectored colonies were chosen at random for analysis of copy number across the genome. For such colonies, both purified sectors were thawed from the glycerol freezer plate stock onto YEPD plates and grown at 30°C overnight. A part of each patch was then used to inoculate 5 mL liquid YEP8D, which was grown to saturation over 2-3 days at 30°C with most cells arrested in G0 phase.

To obtain the DNA, the extraction method used in the re-replication DNA extraction was simplified to handle numerous small cultures at once. This DNA protocol is referred to as the "Small DNA Prep" on the GEO microarray database. 1 mL from a saturation culture was moved to a 2 mL screw-capped tube and spun down in a Eppendorf 5417C microfuge at 14,000 rpm for 3 minutes. Cell pellets were washed twice with 1 mL water and spun down at 14,000 rpm for 3 minutes for each wash. Cell pellets were then flash-frozen in liquid nitrogen and either

processed immediately or stored at –80°C for future extraction. To the frozen cell pellets, 200 µL lysis buffer (2% Triton X-100, 1% SDS, 100 mM NaCl, 10 mM TrisCl pH 8, 20 mM EDTA) was added and tubes were allowed to rock gently at 4°C for 10 minutes to mix in the buffer as well as thaw the pellet. Then, 400 µL small glass beads and 200 µL phenol:chloroform:isoamyl alcohol (25:24:1) were added to the tube and vortexed immediately to mix. Tubes were vortexed on high for 10 minutes in a Vortex genie, after which 400 µL 1x TE pH 7.5 and 400 µL phenol:chloroform:isoamyl alcohol (25:24:1) were added the tubes were vortexed to mix. Tubes were spun down at 13300 rpm for 10 minutes in the microfuge on soft. 500 µL of the clear, top aqueous phase was transferred to new screw-capped tubes, along with 500 µL chloroform:isoamyl alcohol (24:1), which were vortexed well to mix. Tubes were spun at 5100 rpm for 10 minutes in the microfuge, and 450 µL of the top phase was moved to a new microfuge tubes. Volumes were brought up to 500µL with 50µL 1x TE pH 7.5, and 400 µL isopropanol and 5 µL 5 M NaCl were added followed by vortexing. Tubes were spun at 10600 rpm for 10 minutes in the microfuge. The supernatant was carefully aspirated out of microfuge tubes, and the pellet was washed with 750 µL 70% ethanol by vortexing well. Tubes were spun at 10600 rpm for 5 minutes in the microfuge and the supernatant was carefully aspirated out. DNA pellets were dried for 10 minutes with gentle heat in a speedvac. Pellets were resuspended in 175 µL 1x TE pH 7.5 by heating in a 37°C waterbath with vortexing for 15 minutes. 1 µL RNase (Qiagen, Cat. no. 19101, DNase free, 100mg/mL) was added to each tube, which were inverted to mix and incubated in the 37°C waterbath for 1 hour. After the incubation, 100 µg Proteinase K (Roche, Cat. no. 03115852001) was added to each tube and inverted to mix, then placed in a 55°C waterbath to incubate for 30 minutes. Then, 400 µL chloroform:isoamyl alcohol (24:1) was added to each tube followed by vortexing and a spin at 7500 rpm for 10

minutes in the microfuge. The top 150 µL was removed and added to new microfuge tubes, followed by 120 µL isopropanol and 1.5 µL 5 M NaCl. Tubes were vortexed and spun at 9600rpm for 10 minutes in the microfuge. The supernatant was carefully aspirated out of microfuge tubes, and the pellet was washed with 750 µL 70% ethanol by vortexing well. Tubes were spun at 9600 rpm for 5 minutes in the microfuge and the wash was carefully aspirated out. DNA pellets were dried for 10 minutes with gentle heat in a speedvac. Pellets were dissolved in 50 µL 2 mM Tris pH 7.8 and placed in the 37°C waterbath for 15 minutes to ensure complete resuspension. DNA was then kept at –20°C until used for aCGH.

DNA from the sector isolates was hybridized against reference DNA from YJL8590 (collected from a nocodazole-arrested culture that did not undergo re-replication) in the manner described previously (16). Briefly, reference DNA was labeled with Cy5 fluorescent dye and DNA from the color sector was labeled with Cy3 fluorescent dye. Equal quantities were combined and applied to an in-house printed microarray (GEO platform number GPL3412) and hybridized at 63°C for at least 20 hours. Arrays were then scanned using an Axon Scanner 4B and analyzed as described previously to generate copy number information across the genome (16). All microarray data is deposited in the Gene Expression Omnibus (http://www.ncbi.nlm.nih.gov/geo/) with accession number GSE55641.

To interpret the copy number of Chromosome V in the red or white sectors, we had to take into account the fact Chromosome V monosomy and trisomy are not stable in the long term. Populations of diploid cells containing these aneuploidies are eventually taken over by cells that have become disomic for Chromosome V. Hence, during the growth, freezing, and thawing of

these aneuploidy cells, the population average of Chromosome V copy number gradually declines from 3C to 2C (for trisomy) or increases from 1C to 2C (for monosomy). In constrast, the populations of cells that start off euploid with a 2C copy number of Chromosome V never show any significant difference from 2.00 C during continued growth. Hence, we scored red sectors with Chromosome V copy number > 2.2C as trisomic for Chromosome V and white sectors with Chromosome V copy number < 1.8C as monosomic for Chromosome V. Both criteria had to hold in order for a red/white colony to be scored as a 2:0 segregation event. For red/pink colonies to be scored as a 2:1 segregation event, Chromosome V copy number in the red sectors had to be > 2.2C and in the pink sector at 2.00 C.

During our copy number analysis we discovered several sectored colonies, in which the Chromosome V copy number in the red and/or white sectors was significantly different than 2.00 C, but not different enough to satisfy the threshholds of > 2.2C and < 1.8C respectively. Because we suspected that the stress of freeze-thawing placed selective pressure on the outgrowth of euploid cells, we isolated DNA directly from the frozen cells to perform aCGH. Cells from the frozen stock were placed directly in a screw-cap tube with 1 ml water, then processed the same as described for saturation cultures. In almost all of these cases, the new copy number analysis established that the red sectors had a much greater than 2 C copy number for Chromosome V, while the white sectors had a much less than 1.8 C copy number for Chromosome V.

Live-cell microscopy: cell growth and re-replication induction

Cell growth and re-replication induction were performed in a similar manner as the re-replication assays described above. Yeast were thawed from frozen glycerol stocks onto SDC-Trp plates and grown at 30°C. The following day, this patch was used to inoculate 25 mL of SDC-Trp and was grown to an OD_{600} between 0.2 and 0.4 over the course of 6 hours at 30°C in a shaking (250 rpm) waterbath. From this culture, we inoculated the experimental culture grown at 30°C in non-repressive rich media containing 3% raffinose and 0.05% dextrose (SRd) so that after 13.5 hours, the culture would be growing exponentially at an OD_{600} between 0.3 and 0.5.

Since re-replication can be efficiently induced in exponentially-growing cells, and we wanted to maintain the spindle to place tension on the chromosomes, an prior arrest with nocodazole was not performed. Instead, 40% galactose was added to the log-phase culture to a final concentration of 2.7%. Galactose induction was allowed to proceed for 2.75 hours, after which a small sample (500 µL) was removed and imaged live to produce a time-lapse movie of the dynamics of a re-replicated cell (Figure 5C); this sample was taken early so the imaging would occur after a full three hours of induction. The remainder of the culture was washed by vacuum filtration using 10 volumes of pre-warmed sterile water, then resuspended in 25 mL pre-warmed SDC-Trp media. From this new resuspension, a small sample (500 µL) was taken for imaging before and after nocodazole treatment (Figures 5A and B).

Live-cell microscopy: imaging

All live imaging was conducted in a temperature-controlled chamber maintained at 30°C with yeast immobilized to the bottom of a chambered coverslip (Lab-Tek/Thermo Fisher, Cat.

no.12565401). Briefly, the bottom of the chamber was coated using 100 µL of 0.5 µg/mL Concanavalin A Type IV (Sigma-Aldrich, Cat. no. C2010-25MG) and allowed to air dry in the dark at 30°C for 1 hour. Roughly 3.5E+06 cells in 500 µL was pipetted into the chamber and allowed to sit for 15 minutes at 30°C, after which the chamber was gently washed twice to remove excess cells. Chambers were then imaged on the Deltavision deconvolution microscope (Applied Precision) using SoftWorx image acquisition software.

Imaging re-replicated cells to observe spot-spindle dynamics – Re-replicating cell spindle and spot dynamics (Figure 5A an Movie S1) were visualized with a 100× 1.40 UPLS Apo objective (Olympus) and a CoolSNAP_HQ / ICX285 camera. To visualize DNA, Hoechst 33342 stain was added at a final concentration of 10 µg/mL to the cells prior to imaging. A set of three images (one for each channel) was taken every 6 seconds for 10 minutes; the Z plane remained unchanged and was prevented from drifting using the UltimateFocus feature. The settings for each excitation wavelength are as follows: RD-TR-PE (red channel; ex: 555 nm, em: 617 nm; 32% power; 0.6 s exposure), FITC (green channel; ex: 490 nm, em: 528 nm; 50% power, 1 s exposure), and DAPI (blue channel; ex: 360 nm, em: 457 nm; 32% power; 0.2 s exposure).

Time-lapse imaging of re-replicated cells to examine spots before nocodazole treatment – Spot and spindle visualization before and after nocodazole (Figure 5B, C) was imaged with a 60× 1.42 NA Plan Apo objective (Olympus**)** and a CoolSNAP_HQ / ICX285 camera. No Hoechst stain was added to these samples. X, Y, and Z coordinates were recorded for 25 locations on the chambered coverslip, 10 for the no *ARS317* strain and 15 for the *ARS317* at *CEN5* strain. For each of these points, a Z-stack was taken ±1 µm from the recorded Z coordinate in steps of 0.5

μm for both the red and green channels. This recorded Z coordinate was prevented from drifting using the UltimateFocus technology. Four stacks were acquired for each marked position as quickly as possible, resulting in images taken every 7 minutes for nearly 20 minutes. The settings for each excitation wavelength are as follows: RD-TR-PE (red channel; ex: 555 nm, em: 617 nm; 32% power; 0.8 s exposure), and FITC (green channel; ex: 490 nm, em: 528 nm; 50% power, 1 s exposure).

Addition of nocodazole and time-lapse imaging after treatment – Nocodazole was added with extreme care to the chambers without their removal from the rig using a curved Pasteur pipette. Immediately before addition, nocodazole was added to 500 μL fresh SDC-Trp media and then dripped into each chamber for a final nocodazole concentration of 75 μg/mL. Nocodazole was kept separate from the media until the last minute to keep as much in solution as possible as it will precipitate in aqueous solutions. Using the same 25 points as the pre-nocodazole imaging, a Z-stack was taken ±1 μm from the recorded Z coordinate in steps of 0.5 μm for both the red and green channels. This recorded Z coordinate was prevented from drifting using the UltimateFocus technology. Four stacks were acquired for each marked position every 10 minutes for 2 hours. The settings for each excitation wavelength are as follows: RD-TR-PE (red channel; ex: 555 nm, em: 617 nm; 32% power; 0.8 s exposure), and FITC (green channel; ex: 490 nm, em: 528 nm; 50% power, 1 s exposure).

Analysis of spot number before and after nocodazole addition

Analysis re-replicated cells to examine spot number before nocodazole treatment – All images were assigned with a random numerical prefix using the free demo version of Renamerox (Branox Technologies) so that they may be scored blindly. Using the free imaging software Fiji (71), a single Z-stack was opened and cells meeting specific criteria were annotated with a letter. The criteria is as follows: the cell must be large-budded, but not actively budding (as can be determined by observing the cell through time), and the cell's spindle must also be in short (≤ 2 μm) as to indicate it is not undergoing anaphase. Using the Z- and time-dimension, the number of centromeric spots for each cell was determined and recorded. Due to the dynamic nature of the spindle and spots, as well as centromeric breathing, it was necessary to look beyond a single plane or time frame for each cell to assess the correct number of spots. Additionally, it was unknown how many spots may arise from centromeric re-replication, therefore using the time- and Z-dimensions enabled us to record an accurate number of spots pre-nocodazole treatment.

Analysis re-replicated cells to examine spot number after nocodazole treatment – All images were assigned with a random numerical prefix using the free demo version of Renamerox (Branox Technologies) so that they may be scored blindly. Using the free imaging software Fiji (71), single Z-stacks were opened until the file matching the pre-nocodazole treatment was found. Then, using the annotated pre-nocodazole image as a guide, each cell was revisited after 2 hours of nocodazole treatment. At this specific timepoint, the Z-planes were examined to determine how many spots were present. Several spots that were originally scored in the pre-nocodazole treatment were thrown out due to one of the following reasons: the cell underwent anaphase before the nocodazole treatment had an effect; the cell's spots separated into opposite lobes after spindle disappearance, indicating they were mid-anaphase; the spindle was not broken

down; the centromeric spot was not visible at the final 2 hour timepoint, either because it lost signal or it became out of focus; or the cell died. Thus, only large-budded cells in metaphase prior to nocodazole with spindle breakdown and visible spot(s) 2 hours after nocodazole were scored. For each strain in each trial, ≥ 100 cells were scored. Values were recorded and can be seen graphically in Figure 5B or in Table S11.

It should be noted that all images were scored with only moderate changes to brightness and contrast as needed.

Image creation for Figure 5

Images viewed in Figure 5A – images were adjusted for brightness and contrast only.

Images viewed in Figure 5C – the red channel of this montage was subjected to Fiji's bleach correction using an exponential line fit. The resulting image fit a curve with R^2 > 0.99. To remove background, it was subtracted using Fiji's background subtraction, using a rolling ball radius of 200 pixels. The green channel was altered only in brightness and contrast. The blue channel underwent a simple ratio (0.5) bleach correction.

Acknowledgements

We thank David Morgan, David Toczyski, Pat O'Farrell, Chris Richardson, and Ken Finn for helpful discussions and reading the manuscript. We thank Roland Bainton for use of his Leica stereoscope. We are also grateful to Elizabeth Blackburn for the use of her Deltavision microscope, as well as her lab member Beth Cimini for the microscopy expertise and guidance. The microarray (aCGH) data in this publication has been deposited in NCBI's Gene Expression Omnibus (Edgar *et al*., 2002) and are accessible through GEO Series accession number GSE55641 (http://www.ncbi.nlm.nih.gov/geo/query/acc.cgi?acc=GSE55641)."

Competing interests

The authors claim no competing interests.

References

1. Arias EE, Walter JC. Strength in numbers: preventing rereplication via multiple mechanisms in eukaryotic cells. Genes Dev. 2007;21(5):497-518.

2. Hook SS, Lin JJ, Dutta A. Mechanisms to control rereplication and implications for cancer. Curr Opin Cell Biol. 2007;19(6):663-71.

3. Siddiqui K, On KF, Diffley JFX. Regulating DNA Replication in Eukarya. Cold Spring Harb Perspect Biol. 2013.

4. Biggins S. The composition, functions, and regulation of the budding yeast kinetochore. Genetics. 2013;194(4):817-46.

5. Tanaka TU. Kinetochore-microtubule interactions: steps towards bi-orientation. EMBO J. 2010;29(24):4070-82.

6. Lara-Gonzalez P, Westhorpe FG, Taylor SS. The spindle assembly checkpoint. Curr Biol. 2012;22(22):R966-80.

7. Roschke AV, Rozenblum E. Multi-layered cancer chromosomal instability phenotype. Front Oncol. 2013;3:302.

8. Mitelman F, Johansson B, Mertens FE. Mitelman Database of Chromosome Aberrations and Gene Fusions in Cancer. http://cgapncinihgov/Chromosomes/Mitelman. 2012.

9. Zasadil LM, Britigan EM, Weaver BA. 2n or not 2n: Aneuploidy, polyploidy and chromosomal instability in primary and tumor cells. Semin Cell Dev Biol. 2013;24(4):370-9.

10. Weaver BA, Cleveland DW. Does aneuploidy cause cancer? Curr Opin Cell Biol. 2006;18(6):658-67.

11. Orr B, Compton DA. A double-edged sword: how oncogenes and tumor suppressor genes can contribute to chromosomal instability. Front Oncol. 2013;3:164.

12. Gordon DJ, Resio B, Pellman D. Causes and consequences of aneuploidy in cancer. Nat Rev Genet. 2012;13(3):189-203.

13. Chan JY. A clinical overview of centrosome amplification in human cancers. Int J Biol Sci. 2011;7(8):1122-44.

14. Carter SL, Eklund AC, Kohane IS, Harris LN, Szallasi Z. A signature of chromosomal instability inferred from gene expression profiles predicts clinical outcome in multiple human cancers. Nat Genet. 2006;38(9):1043-8.

15. Green BM, Finn KJ, Li JJ. Loss of DNA replication control is a potent inducer of gene amplification. Science. 2010;329(5994):943-6.

16. Green BM, Morreale RJ, Ozaydin B, Derisi JL, Li JJ. Genome-wide mapping of DNA synthesis in Saccharomyces cerevisiae reveals that mechanisms preventing reinitiation of DNA replication are not redundant. Mol Biol Cell. 2006;17(5):2401-14.

17. Koshland D, Kent JC, Hartwell LH. Genetic analysis of the mitotic transmission of minichromosomes. Cell. 1985;40(2):393-403.

18. Wood JS. Genetic effects of methyl benzimidazole-2-yl-carbamate on Saccharomyces cerevisiae. Mol Cell Biol. 1982;2(9):1064-79.

19. Zimmermann FK, Mayer VW, Scheel I. Induction of aneuploidy by oncodazole (nocodazole), an anti-tubulin agent, and acetone. Mutat Res. 1984;141(1):15-8.

20. Richardson CD, Li JJ. Regulatory mechanisms that prevent re-initiation of DNA replication can be locally modulated at origins by nearby sequence elements. PLoS Genet. 2014;10(6):e1004358.

21. Hartwell LH, Smith D. Altered fidelity of mitotic chromosome transmission in cell cycle mutants of S. cerevisiae. Genetics. 1985;110(3):381-95.

22. Klein HL. Spontaneous chromosome loss in Saccharomyces cerevisiae is suppressed by DNA damage checkpoint functions. Genetics. 2001;159(4):1501-9.

23. Covo S, Puccia CM, Argueso JL, Gordenin DA, Resnick MA. The sister chromatid cohesion pathway suppresses multiple chromosome gain and chromosome amplification. Genetics. 2014;196(2):373-84.

24. Finn KJ, Li JJ. Single-Stranded Annealing Induced by Re-Initiation of Replication Origins Provides a Novel and Efficient Mechanism for Generating Copy Number Expansion via Non-Allelic Homologous Recombination. PLoS Genet. 2013;9(1):e1003192.

25. Kass EM, Jasin M. Collaboration and competition between DNA double-strand break repair pathways. FEBS Lett. 2010;584(17):3703-8.

26. Symington LS, Gautier J. Double-strand break end resection and repair pathway choice. Annu Rev Genet. 2011;45:247-71.

27. Grabarz A, Barascu A, Guirouilh-Barbat J, Lopez BS. Initiation of DNA double strand break repair: signaling and single-stranded resection dictate the choice between homologous recombination, non-homologous end-joining and alternative end-joining. Am J Cancer Res. 2012;2(3):249-68.

28. Mortensen UH, Lisby M, Rothstein R. Rad52. Curr Biol. 2009;19(16):R676-7.

29. San Filippo J, Sung P, Klein H. Mechanism of eukaryotic homologous recombination. Annu Rev Biochem. 2008;77:229-57.

30. Lieber MR. The mechanism of double-strand DNA break repair by the nonhomologous DNA end-joining pathway. Annu Rev Biochem. 2010;79:181-211.

31. Archambault V, Ikui AE, Drapkin BJ, Cross FR. Disruption of mechanisms that prevent rereplication triggers a DNA damage response. Mol Cell Biol. 2005;25(15):6707-21.

32. Green BM, Li JJ. Loss of rereplication control in Saccharomyces cerevisiae results in extensive DNA damage. Mol Biol Cell. 2005;16(1):421-32.

33. Melixetian M, Ballabeni A, Masiero L, Gasparini P, Zamponi R, Bartek J, et al. Loss of Geminin induces rereplication in the presence of functional p53. The Journal of Cell Biology. 2004;165(4):473-82.

34. Zhu W, Dutta A. An ATR- and BRCA1-mediated Fanconi anemia pathway is required for activating the G2/M checkpoint and DNA damage repair upon rereplication. Mol Cell Biol. 2006;26(12):4601-11.

35. Pearson CG, Maddox PS, Salmon ED, Bloom K. Budding yeast chromosome structure and dynamics during mitosis. J Cell Biol. 2001;152(6):1255-66.

36. He X, Asthana S, Sorger PK. Transient sister chromatid separation and elastic deformation of chromosomes during mitosis in budding yeast. Cell. 2000;101(7):763-75.

37. Goshima G, Yanagida M. Time course analysis of precocious separation of sister centromeres in budding yeast: continuously separated or frequently reassociated? Genes Cells. 2001;6(9):765-73.

38. Ocampo-Hafalla MT, Katou Y, Shirahige K, Uhlmann F. Displacement and re-accumulation of centromeric cohesin during transient pre-anaphase centromere splitting. Chromosoma. 2007;116(6):531-44.

39. Kitamura E, Tanaka K, Kitamura Y, Tanaka TU. Kinetochore microtubule interaction during S phase in Saccharomyces cerevisiae. Genes Dev. 2007;21(24):3319-30.

40. Collins KA, Castillo AR, Tatsutani SY, Biggins S. De novo kinetochore assembly requires the centromeric histone H3 variant. Mol Biol Cell. 2005;16(12):5649-60.

41. Gascoigne KE, Cheeseman IM. Induced dicentric chromosome formation promotes genomic rearrangements and tumorigenesis. Chromosome Res. 2013;21(4):407-18.

42. Stimpson KM, Matheny JE, Sullivan BA. Dicentric chromosomes: unique models to study centromere function and inactivation. Chromosome Res. 2012;20(5):595-605.

43. Hill A, Bloom K. Acquisition and processing of a conditional dicentric chromosome in Saccharomyces cerevisiae. Mol Cell Biol. 1989;9(3):1368-70.

44. Vaziri C, Saxena S, Jeon Y, Lee C, Murata K, Machida Y, et al. A p53-dependent checkpoint pathway prevents rereplication. Mol Cell. 2003;11(4):997-1008.

45. Zhu W, Chen Y, Dutta A. Rereplication by depletion of geminin is seen regardless of p53 status and activates a G2/M checkpoint. Mol Cell Biol. 2004;24(16):7140-50.

46. Mihaylov IS, Kondo T, Jones L, Ryzhikov S, Tanaka J, Zheng J, et al. Control of DNA replication and chromosome ploidy by geminin and cyclin A. Mol Cell Biol. 2002;22(6):1868-80.

47. Kim J, Feng H, Kipreos ET. C. elegans CUL-4 prevents rereplication by promoting the nuclear export of CDC-6 via a CKI-1-dependent pathway. Curr Biol. 2007;17(11):966-72.

48. Nishitani H, Nurse P. p65cdc18 plays a major role controlling the initiation of DNA replication in fission yeast. Cell. 1995;83(3):397-405.

49. Thomer M, May NR, Aggarwal BD, Kwok G, Calvi BR. Drosophila double-parked is sufficient to induce re-replication during development and is regulated by cyclin E/CDK2. Development. 2004;131(19):4807-18.

50. Bonds L, Baker P, Gup C, Shroyer KR. Immunohistochemical localization of cdc6 in squamous and glandular neoplasia of the uterine cervix. Arch Pathol Lab Med. 2002;126(10):1164-8.

51. Karakaidos P, Taraviras S, Vassiliou LV, Zacharatos P, Kastrinakis NG, Kougiou D, et al. Overexpression of the replication licensing regulators hCdt1 and hCdc6 characterizes a subset of non-small-cell lung carcinomas: synergistic effect with mutant p53 on tumor growth and chromosomal instability--evidence of E2F-1 transcriptional control over hCdt1. Am J Pathol. 2004;165(4):1351-65.

52. Liontos M, Koutsami M, Sideridou M, Evangelou K, Kletsas D, Levy B, et al. Deregulated overexpression of hCdt1 and hCdc6 promotes malignant behavior. Cancer Res. 2007;67(22):10899-909.

53. Murphy N, Ring M, Heffron CCBB, Martin CM, McGuinness E, Sheils O, et al. Quantitation of CDC6 and MCM5 mRNA in cervical intraepithelial neoplasia and invasive squamous cell carcinoma of the cervix. Mod Pathol. 2005;18(6):844-9.

54. Ren B, Yu G, Tseng GC, Cieply K, Gavel T, Nelson J, et al. MCM7 amplification and overexpression are associated with prostate cancer progression. Oncogene. 2006;25(7):1090-8.

55. Santarius T, Shipley J, Brewer D, Stratton MR, Cooper CS. A census of amplified and overexpressed human cancer genes. Nat Rev Cancer. 2010;10(1):59-64.

56. Arentson E, Faloon P, Seo J, Moon E, Studts JM, Fremont DH, et al. Oncogenic potential of the DNA replication licensing protein CDT1. Oncogene. 2002;21(8):1150-8.

57. Seo J, Chung YS, Sharma GG, Moon E, Burack WR, Pandita TK, et al. Cdt1 transgenic mice develop lymphoblastic lymphoma in the absence of p53. Oncogene. 2005;24(55):8176-86.

58. Lin JJ, Milhollen MA, Smith PG, Narayanan U, Dutta A. NEDD8-targeting drug MLN4924 elicits DNA rereplication by stabilizing Cdt1 in S phase, triggering checkpoint activation, apoptosis, and senescence in cancer cells. Cancer Res. 2010;70(24):10310-20.

59. Wilmes GM, Archambault V, Austin RJ, Jacobson MD, Bell SP, Cross FR. Interaction of the S-phase cyclin Clb5 with an "RXL" docking sequence in the initiator protein Orc6 provides an origin-localized replication control switch. Genes Dev. 2004;18(9):981-91.

60. Lovejoy CA, Lock K, Yenamandra A, Cortez D. DDB1 maintains genome integrity through regulation of Cdt1. Mol Cell Biol. 2006;26(21):7977-90.

61. Jin J, Arias EE, Chen J, Harper JW, Walter JC. A family of diverse Cul4-Ddb1-interacting proteins includes Cdt2, which is required for S phase destruction of the replication factor Cdt1. Mol Cell. 2006;23(5):709-21.

62. Dorn ES, Chastain PD, 2nd, Hall JR, Cook JG. Analysis of re-replication from deregulated origin licensing by DNA fiber spreading. Nucleic Acids Res. 2009;37(1):60-9.

63. Tatsumi Y, Sugimoto N, Yugawa T, Narisawa-Saito M, Kiyono T, Fujita M. Deregulation of Cdt1 induces chromosomal damage without rereplication and leads to chromosomal instability. J Cell Sci. 2006;119(Pt 15):3128-40.

64. Sikorski RS, Hieter P. A system of shuttle vectors and yeast host strains designed for efficient manipulation of DNA in Saccharomyces cerevisiae. Genetics. 1989;122(1):19-27.

65. Rohner S, Gasser SM, Meister P. Modules for cloning-free chromatin tagging in Saccharomyces cerevisae. Yeast. 2008;25(3):235-9.

66. Nguyen VQ, Co C, Irie K, Li JJ. Clb/Cdc28 kinases promote nuclear export of the replication initiator proteins Mcm2-7. Curr Biol. 2000;10(4):195-205.

67. Nguyen VQ, Co C, Li JJ. Cyclin-dependent kinases prevent DNA re-replication through multiple mechanisms. Nature. 2001;411(6841):1068-73.

68. Berlin V, Brill JA, Trueheart J, Boeke JD, Fink GR. Genetic screens and selections for cell and nuclear fusion mutants. Methods Enzymol. 1991;194:774-92.

69. Goldstein AL, McCusker JH. Three new dominant drug resistance cassettes for gene disruption in Saccharomyces cerevisiae. Yeast. 1999;15(14):1541-53.

70. Sherman F. Getting started with yeast. Methods Enzymol. 2002;350:3-41.

71. Schindelin J, Arganda-Carreras I, Frise E, Kaynig V, Longair M, Pietzsch T, et al. Fiji: an open-source platform for biological-image analysis. Nat Methods. 2012;9(7):676-82.

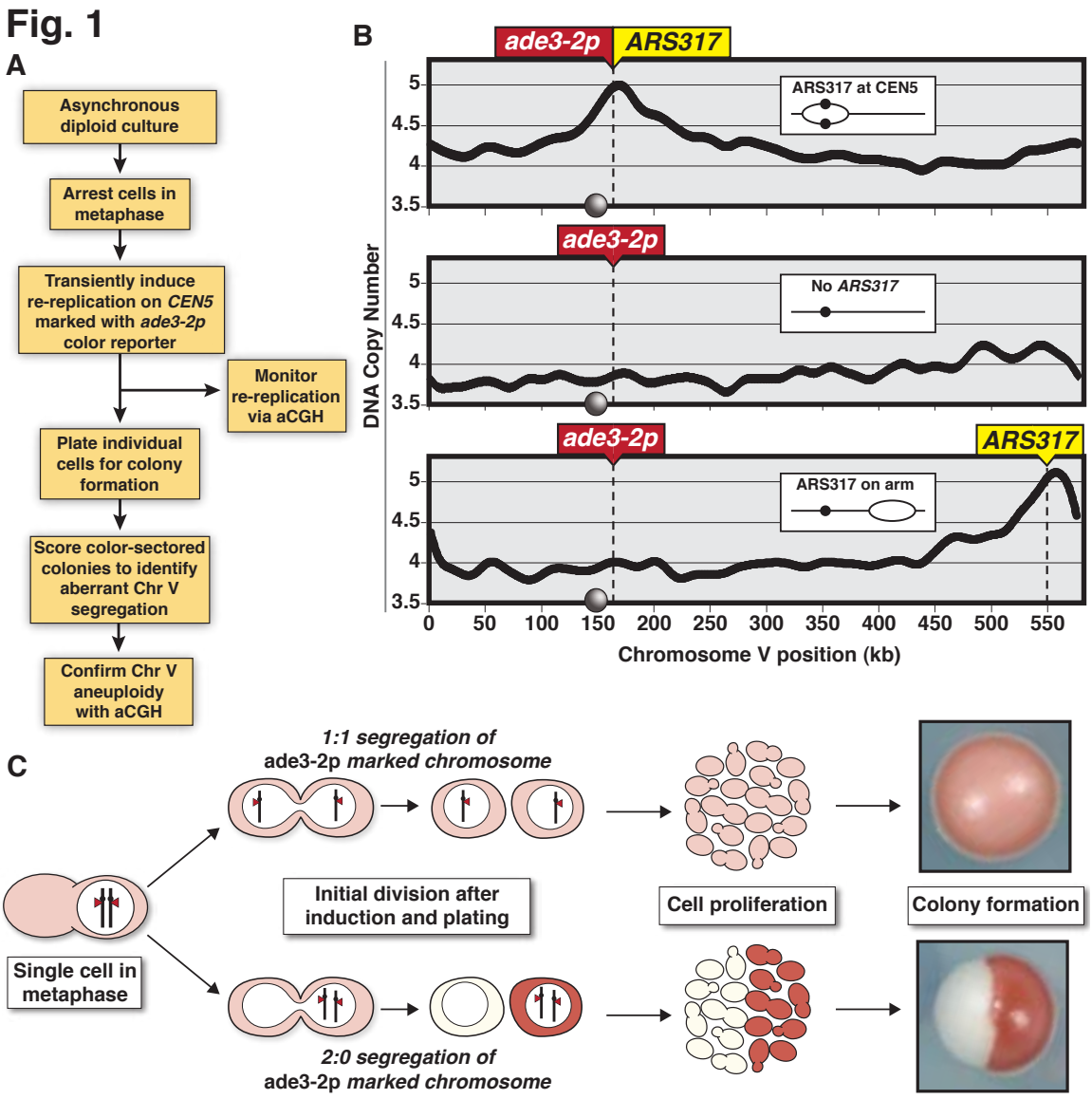

Fig. 1: Monitoring chromosome segregation fidelity after centromeric re-replication. (**A**) Experimental flowchart starting with diploid re-replicating cells containing one Chromosome V homolog marked with the *ade3-2p* copy number reporter. (**B**) Re-replication profile of Chromosome V for diploid cells arrested in metaphase (with baseline copy number of 4C) and induced to re-replicate (see Table S1). *ARS317* and *ade3-2p* mark integration sites of the re-initiating origin and the copy number reporter, respectively. Inset shows schematic of re-replication bubbles inferred from profiles. Circles on X-axis and in schematic represent centromere *CEN5*. (**C**) Schematic showing how first division 1:1 segregation of *ade3-2p* marked homolog leads to pink colonies and 2:0 missegregation leads to red/white sectored colonies.

Fig. 2

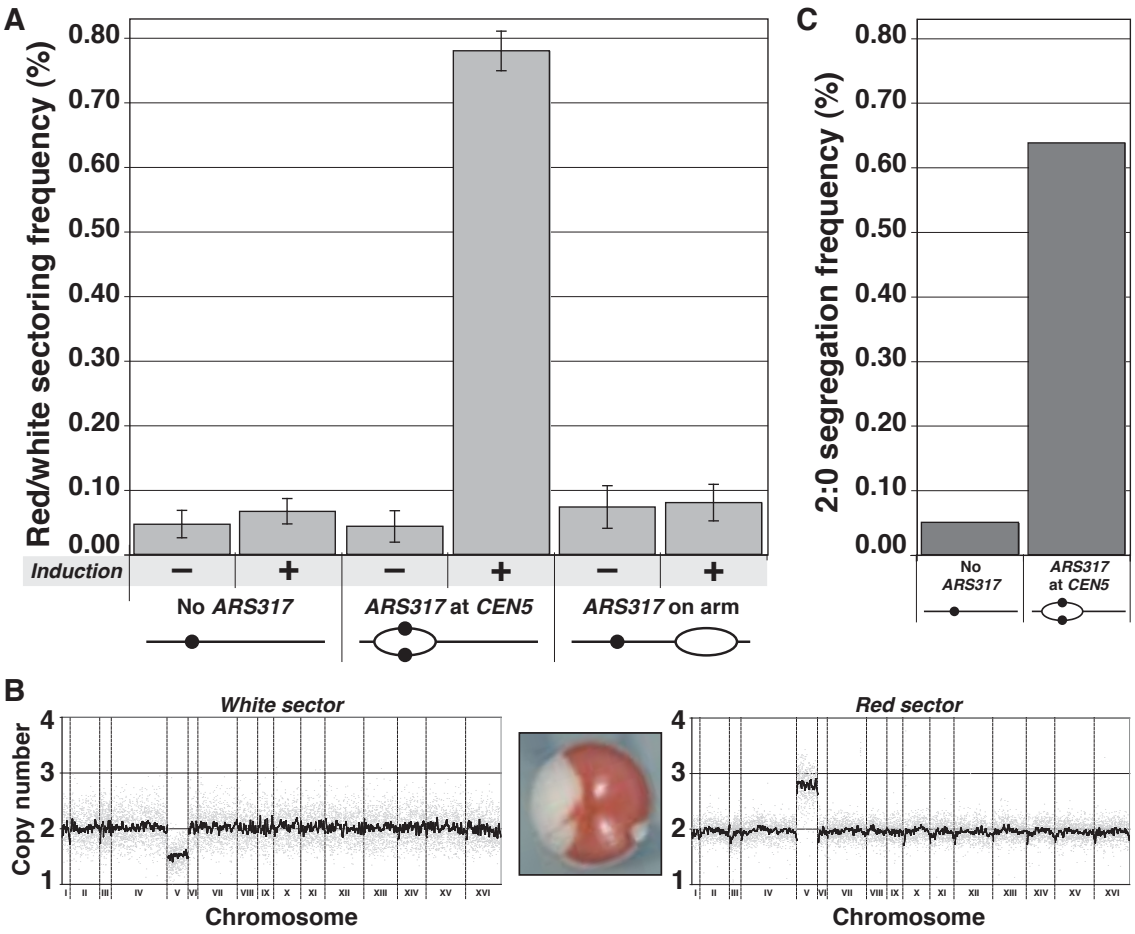

Fig. 2: Centromeric re-replication causes 2:0 missegregation of chromosomes. (**A**) Centromeric re-replication induces red/white sectored colonies. Diploid re-replicating strains (characterized in Fig. 1B and induced to re-replicate as described in Fig. 1A) were scored for the frequency of red/white sectored colonies either before (-) or after (+) induction of re-replication (see Table S6). Data is presented as the average ± SEM for $n \geq 3$ trials. (**B**) aCGH copy number analysis of a representative red/white colony that was scored as a 2:0 segregation event (see Materials and Methods). (**C**) Estimated frequency of 2:0 segregation events after 3 hr of re-replication. The average sectoring frequency for each strain shown in (A) was multiplied by the fraction of aCGH-analyzed isolates that showed 2:0 segregation of the *ade2-3p* marked Chromosome V homolog (see Tables S2 and S7).

Fig. 3

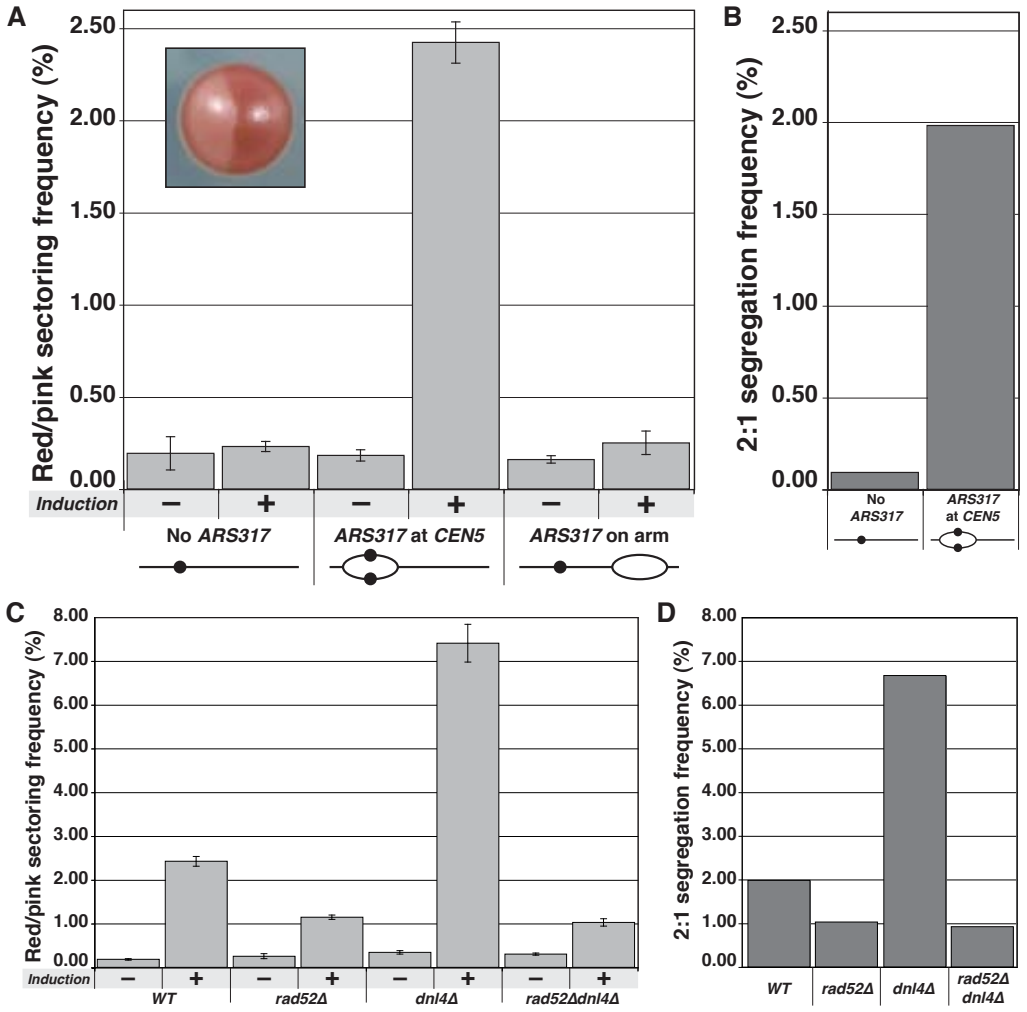

Fig. 3: Centromeric re-replication causes 2:1 segregation through chromosome gain. (**A**) Centromeric re-replication induces red/pink sectored colonies. Diploid re-replicating strains characterized in Fig. 1B and induced to re-replicate as described in Fig. 1A, were scored for the frequency of red/pink sectored colonies (see inset) either before (-) or after (+) induction of re-replication (see Table S6). Data is presented as the average ± SEM for n ≥ 3 trials. (**B**) Estimated frequency of 2:1 segregation events after 3 hr of re-replication. The average sectoring frequency for each strain shown in (A) was multiplied by the fraction of aCGH-analyzed isolates that showed 2:1 segregation of the *ade2-3p* marked Chromosome V homolog (see Tables S3 and S7). (**C**) Dependence of red/pink colony frequencies induced by centromeric re-replication on homologous recombination. Diploid re-replicating strains with re-initiating origin *ARS317* at *CEN5* and homozygous deletions of the indicated genes were scored for the frequency of red/pink sectored colonies as described and presented in (A) (see Table S6). (**D**) Dependence on homologous recombination of 2:1 segregation events induced by centromeric re-replication. Segregation events were estimated as described in (B) using the frequencies reported in (C) (see Tables S3 and S7).

Fig. 4

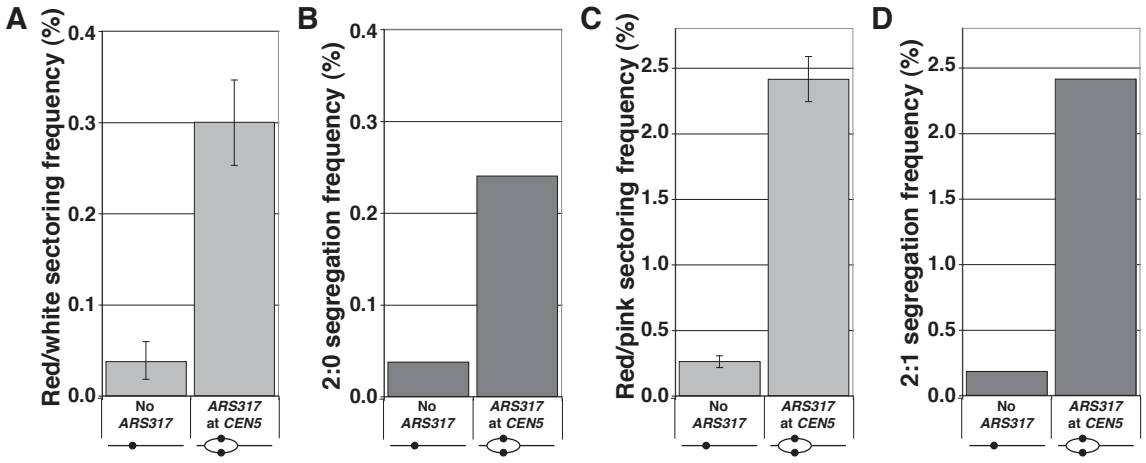

Fig. 4: Centromeric re-replication induced in cycling cells causes 2:0 and 2:1 segregation.

Re-replication and quantification of 2:0 and 2:1 segregation events was as described in Fig. 1A, except the arrest prior to the induction of re-replication was omitted. The re-replication profiles of diploid strains used are shown in Fig. S4. (**A** and **C**) Frequencies of red/white and red/pink sectored colonies are presented as the average ± SEM for n ≥ 3 trials (see Table S6). (**B** and **D**) Estimates of 2:0 and 2:1 segregation frequencies were calculated as previously described in Fig. 2C and 3B (see Tables S4, S5, and S7).

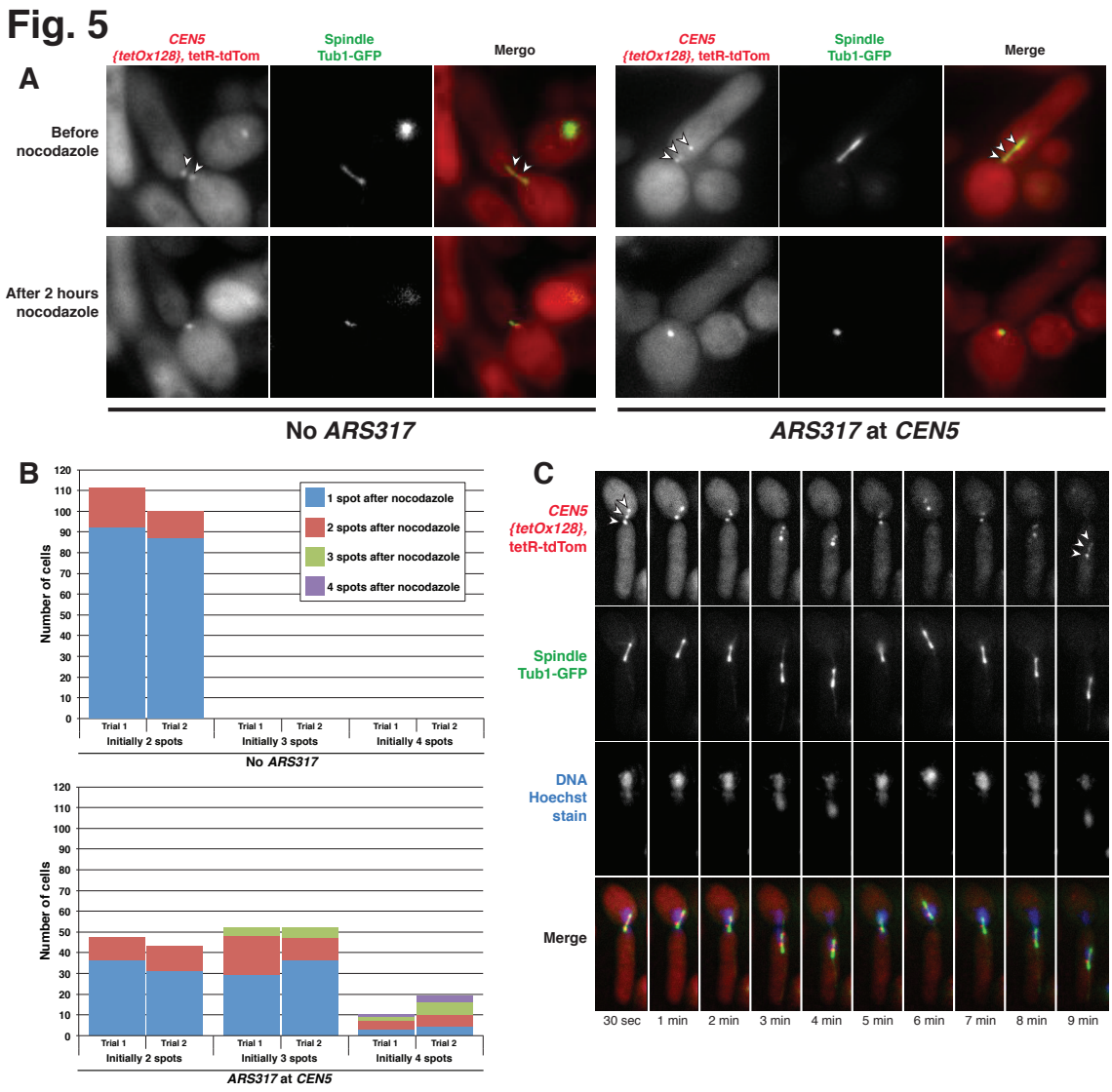

Fig. 5: Dynamic spot movement and separation are dependent on an intact spindle. (**A**) Exponentially-growing cells with the re-replicating origin *ARS317* near *CEN5* or without *ARS317* were induced to re-replicate for three hours. Cells were then washed and the induction stopped with the addition of dextrose, followed by live imaging of cells in the absence of nocodazole in open microscopy imaging chambers. Nocodazole was added to each chamber, and the same cells were imaged live after two hours when the spindles had completely disappeared. Spots corresponding to the *TET* operator arrays bound to tdTomato-tagged *TET* repressors to the left of *CEN5* are indicated by arrowheads. (**B**) Quantification of the number of spots observed before and after nocodazole addition in cells with *ARS317* near *CEN5* or without *ARS317*. The number of cells scored pre-nocodazole is charted based on initial spot number, with each bar divided into the number of cells having one, two, three, or four spots observed post-nocodazole treatment (see Table S11). Each strain in both trials was scored for ≥ 100 cells. (**C**) Time-lapse imaging of a live cell at a single Z-plane that has undergone centromeric re-replication. The three spots corresponding to *TET* operator arrays bound to tdTomato-tagged *TET* repressors (on the left of *CEN5*) are indicated by arrowheads in the first and last panels.

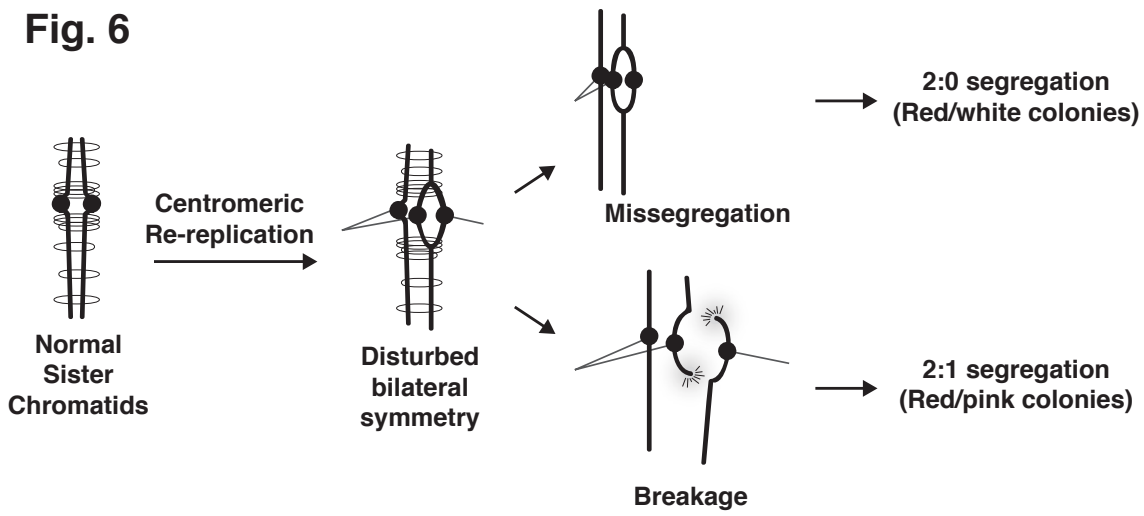

Fig. 6: Model of how centromeric replication may affect chromosome segregation. Normal sister chromatids are held together via cohesin to ensure their bi-orientation with the mitotic spindle. When a centromere is re-replicated, this bilateral symmetry is disturbed, possibly disrupting the pericentromeric cohesin and/or allowing the merotelic attachment of a single chromatid to both spindle poles. During anaphase, this chromatid could missegregate to produce the 2:0 segregation pattern (consistent with red/white colony formation), or break and repair in a *RAD52*-dependent manner to produce a 2:1 segregation pattern (consistent with red/pink colony formation).

Fig. S1

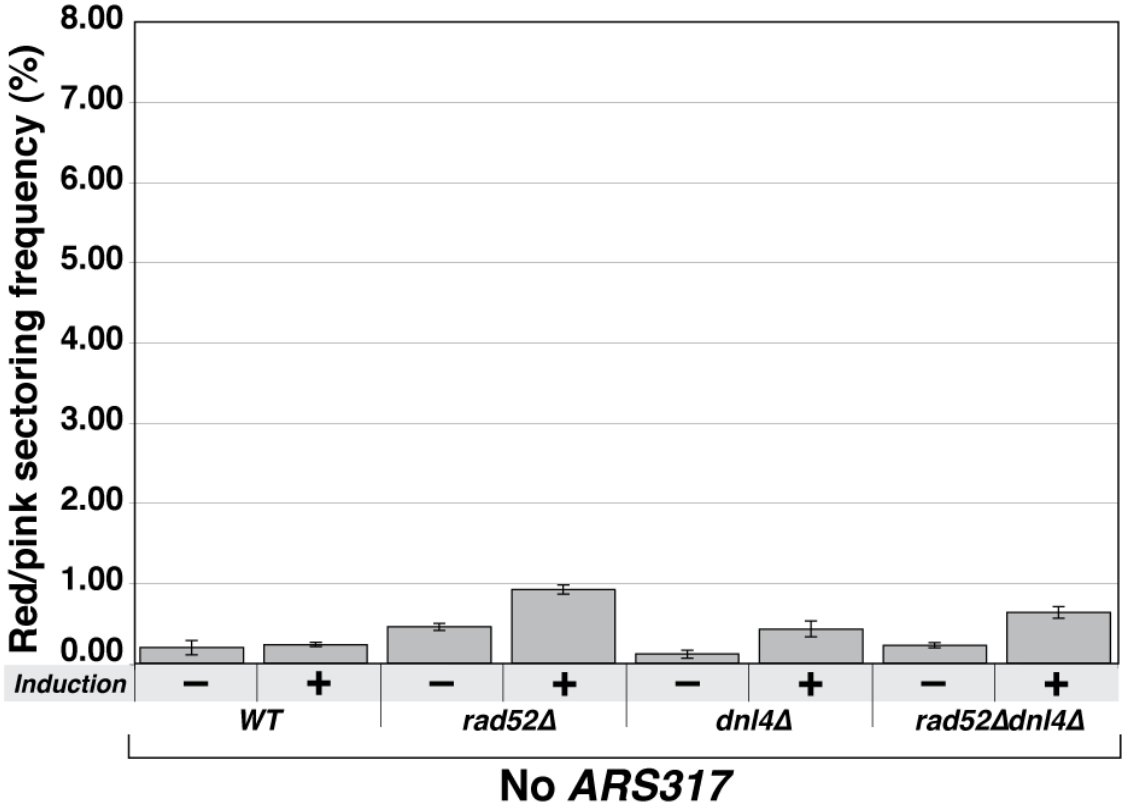

Fig. S1: Red/pink colony frequencies induced by re-replication in strains lacking the re-initiating origin *ARS317* and deficient in recombinational repair.
Diploid re-replicating strains with no *ARS317* on the *ade3-2p* marked Chromosome V homolog and containing homozygous deletions of the indicated genes were scored for the frequency of red/pink sectored colonies both before (–) and after (+) re-replication as described in Fig. 3 (see Table S6). Frequencies are presented as the average ± SEM for n ≥ 3 trials.

Fig. S2

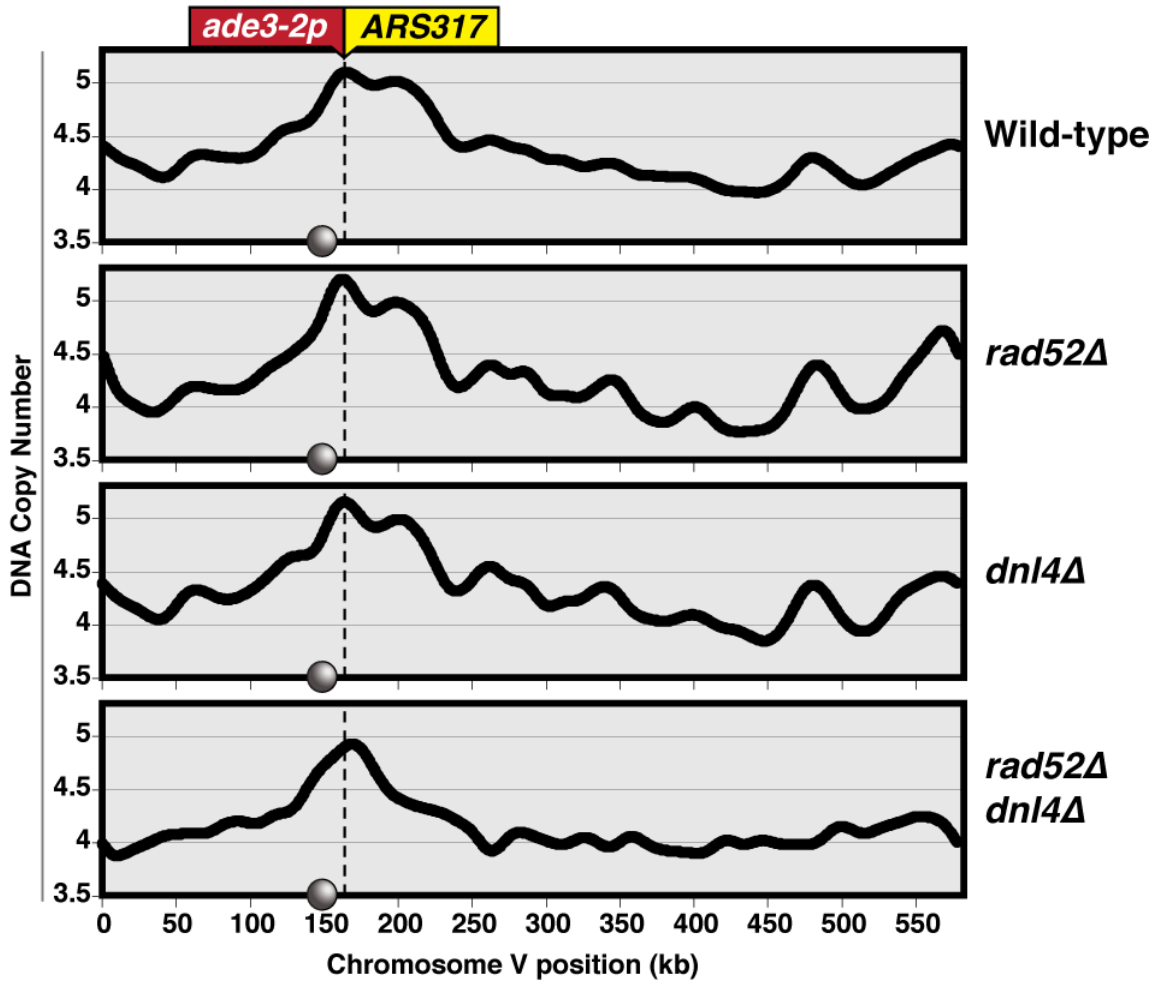

Fig. S2: Re-replication profile of Chromosome V for diploid strains deficient in recombinational repair.
Diploid re-replicating strains with homozygous deletions of indicated genes and both re-initiating origin *ARS317* and *ade3-2p* integrated at *CEN5* (circle) were arrested in metaphase and induced to re-replicate for 3 hr as described in Fig. 1A (see Table S1). DNA copy number was analyzed by array CGH with baseline normalized to 4C.

Fig. S3

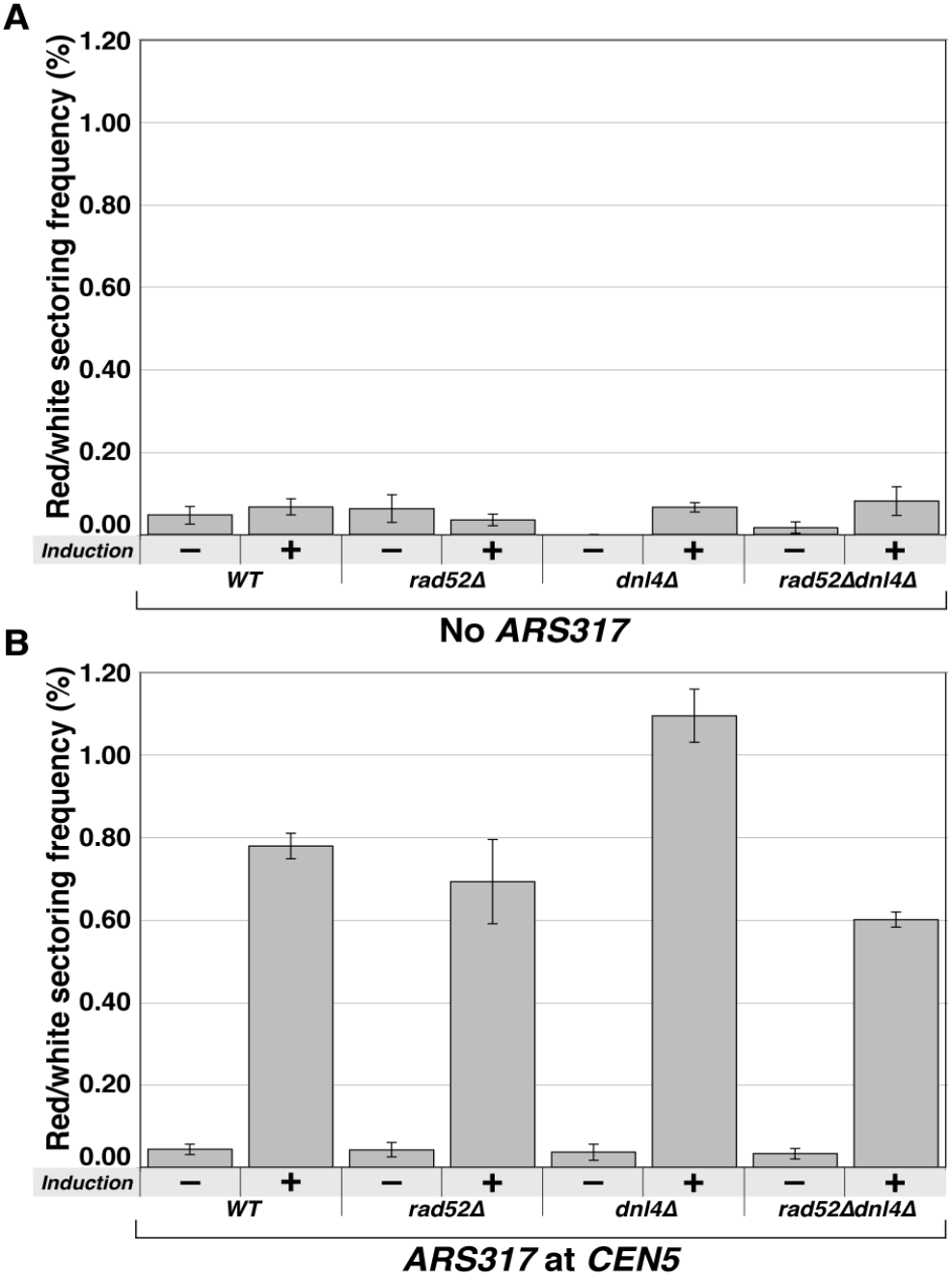

Fig. S3: Red/white sectoring frequencies for strains deficient in recombinational repair. Diploid re-replicating strains with homozygous deletions of indicate genes and *ade3-2p* integrated at *CEN5* were induced to re-replicate as described in Fig. 1A were scored for the frequency of red/white sectored colonies either before (-) or after (+) a 3 hr induction of re-replication (see Table S6). Data is presented as the average ± SEM for n ≥ 3 trials. (**A**) Strains containing no *ARS317*. (**B**) Strains containing *ARS317* integrated at *CEN5*.

Fig. S4

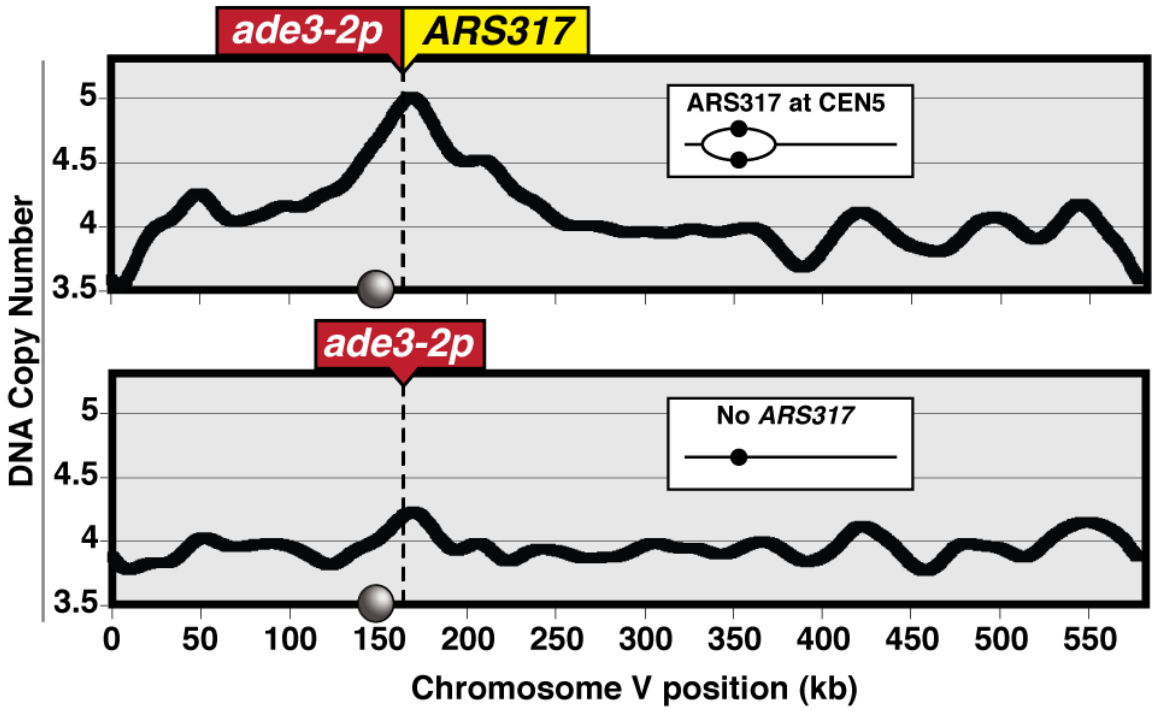

Fig. S4: Re-replication profiles of Chromosome V for diploid strains induced to re-replicate for 3 hr without prior metaphase arrest (see Table S1).
ARS317 and *ade3-2p* mark integration sites of the re-initiating origin and the copy number reporter, respectively. Inset shows schematic of re-replication bubbles inferred from profiles. Circles on X-axis and in schematic represent centromere *CEN5*.

Fig. S5

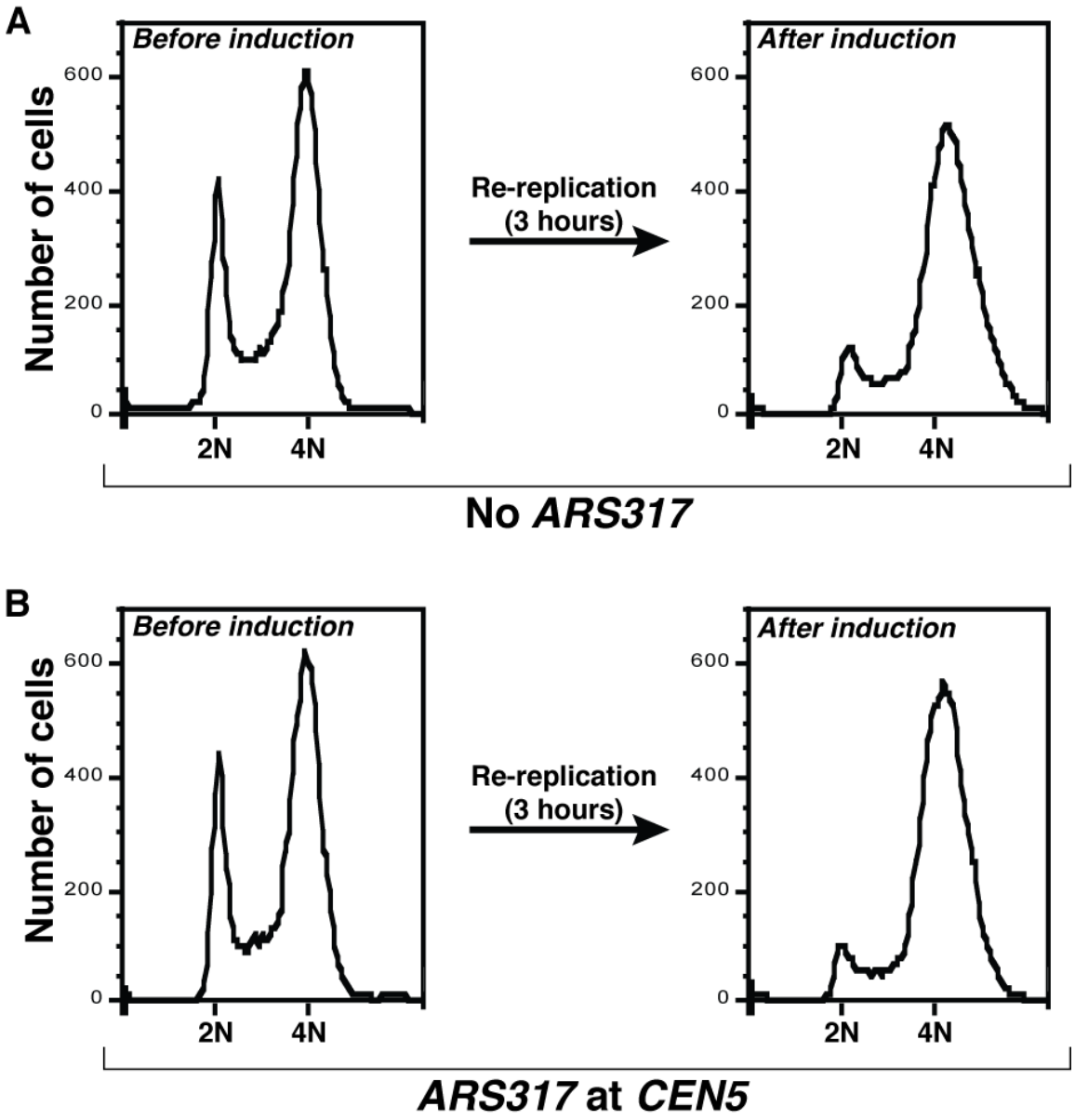

Fig. S5: Cycling cells induced to re-replicate transiently arrest in M phase.
Flow cytometry of strains analyzed in Fig. S4 before and after the induction of re-replication. (**A**) Strain containing no *ARS317*. (**B**) Strain containing *ARS317* integrated at *CEN5*.

Table S1: Array CGH for the re-replication profiles presented in this work.

Strain	Relevant genotype	Figure	Sample no. in GEO
YJL9637	ARS317 at CEN5	1B, top	GSM1340735
YJL9629	No ARS317	1B, middle	GSM1340736
YJL9631	ARS317 moved to Chr5_548	1B, bottom	GSM1340737
YJL9637	ARS317 at CEN5	S2, top	GSM1346228
YJL10171	ARS317 at CEN5, *rad52*Δ	S2, top middle	GSM1340738
YJL10176	ARS317 at CEN5, *dnl4*Δ	S2, bottom middle	GSM1340739
YJL10238	ARS317 at CEN5, *rad52*Δ*dnl4*Δ	S2, bottom	GSM1340740
YJL9637	ARS317 at CEN5 (no arrest)	S4, top	GSM1340741
YJL9627	No ARS317 (no arrest)	S4, bottom	GSM1340742

Table S2: Array CGH corresponding to Fig. 2. Chromosomes other than Chr5 are at a copy number of 2.0 unless listed in "Other genomic changes" with copy number reported in parentheses. For chromosomal segments with a copy number other than 2.0, the boundaries of the segments are indicated by chromosomal coordinates within brackets. We inferred that the ade3-2p marked Chr5 homolog had undergone a 2:0 segregation event if the total Chr5 copy number was > 2.2 in the red sector and < 1.8 in the white sector (see Materials and Methods). LT = left telomere; RT = right telomere.

Parental Strain	Relevant genotype	Colony number	Sector	Chr5 Copy No.	Other genomic changes	2:0 Chr5 segregation	Sample no. in GEO
YJL9627	No ARS317	SHE4-14-29R	Red	2.6	Chr10(2.7)	+	GSM1340743
YJL9627	No ARS317	SHE4-14-29W	White	1.5	Chr10(1.5)		GSM1340744
YJL9627	No ARS317	SHE4-14-30R	Red	2.8	–	+	GSM1340745
YJL9627	No ARS317	SHE4-14-30W	White	1.5	Chr8(1.5)		GSM1340746
YJL9627	No ARS317	SHE4-14-31R	Red	2.8	–	+	GSM1340747
YJL9627	No ARS317	SHE4-14-31W	White	1.2	–		GSM1340748
YJL9629	No ARS317	SHE5-29-9R	Red	2.0	Chr1(1)	–	GSM1340749
YJL9629	No ARS317	SHE5-29-9W	White	1.8	Chr1(1.0); Chr9(2.2); Chr12{660kb-690kb(1.7)}		GSM1340750
YJL9637	ARS317 at CEN5	SHE5-23-16R	Red	2.7	Chr12(2.3)	+	GSM1340751
YJL9637	ARS317 at CEN5	SHE5-23-16W	White	1.7	Chr3{LT-5kb(2.5),6kb-90kb(3.6)}; Chr6{LT-140kb(1),140kb-RT(2.8)}		GSM1340752
YJL9637	ARS317 at CEN5	SHE5-23-21R	Red	2.0	Chr8(1.2); Chr14(1.2)	–	GSM1340753
YJL9637	ARS317 at CEN5	SHE5-23-21W	White	1.5	Chr8(1.2); Chr14(1.5)		GSM1340754
YJL9637	ARS317 at CEN5	SHE5-23-22R	Red	2.7	–	+	GSM1340755
YJL9637	ARS317 at CEN5	SHE5-23-22W	White	1.3	–		GSM1340756
YJL9637	ARS317 at CEN5	SHE5-23-23R	Red	2.6	Chr16(2.7)	+	GSM1340757
YJL9637	ARS317 at CEN5	SHE5-23-23W	White	1.2	–		GSM1340758
YJL9637	ARS317 at CEN5	SHE4-14-65R	Red	2.7	–	+	GSM1340759
YJL9637	ARS317 at CEN5	SHE4-14-65W	White	1.5	–		GSM1340760
YJL9637	ARS317 at CEN5	SHE5-23-24R	Red	2.8	Chr10(2.75)	+	GSM1340761
YJL9637	ARS317 at CEN5	SHE5-23-24W	White	1.1	Chr10(1.1)		GSM1340762
YJL9639	ARS317 at CEN5	SHE5-25-16R	Red	2.7	Chr7{575kb-800kb(3)}; Chr12{950kb-975kb(3)}	+	GSM1340763
YJL9639	ARS317 at CEN5	SHE5-25-16W	White	1.3	–		GSM1340764
YJL9639	ARS317 at CEN5	SHE5-25-17R	Red	2.0	Chr3(2.7)	–	GSM1340765
YJL9639	ARS317 at CEN5	SHE5-25-17W	White	1.3	–		GSM1340766
YJL9639	ARS317 at CEN5	SHE5-25-19R	Red	2.7	–	+	GSM1340767
YJL9639	ARS317 at CEN5	SHE5-25-19W	White	1.6	Chr16(2.7)		GSM1340768
YJL9639	ARS317 at CEN5	SHE5-25-20R	Red	2.7	–	+	GSM1340769
YJL9639	ARS317 at CEN5	SHE5-25-20W	White	1.3	–		GSM1340770
YJL9639	ARS317 at CEN5	SHE5-25-23R	Red	2.7	Chr1(2.7)	+	GSM1340771
YJL9639	ARS317 at CEN5	SHE5-25-23W	White	1.4	–		GSM1340772

Table S3: Array CGH corresponding to Fig. 3. Chromosomes other than Chr5 are at a copy number of 2.0 unless listed in "Other genomic changes" with copy number reported in parentheses. For chromosomal segments with a copy number other than 2.0, the boundaries of the segments are indicated by chromosomal coordinates within brackets. We inferred that the ade3-2p marked Chr5 homolog had undergone a 2:1 segregation event if the total Chr5 copy number was > 2.2 in the red sector and = 2.0 in the pink sector (see Materials and Methods). LT = left telomere; RT = right telomere; Mix = whole copy number of Chr5 cannot be reported due to segmental gains or losses.

Parental Strain	Relevant genotype	Colony number	Sector	Chr5 Copy No.	Other genomic changes	2:1 Chr5 segregation	Sample no. in GEO
YJL9627	No ARS317	SHE4-14-27R	Red	2.0	Chr7(2.7); Chr16(2.7)	–	GSM1340773
YJL9627	No ARS317	SHE4-14-27P	Pink	2.0	Chr16(2.7)		GSM1340774
YJL9627	No ARS317	SHE4-14-32R	Red	2.0	Chr2(2.7); Chr11{LT-370kb(1)}; Chr12{690kb-RT(2.8)}	–	GSM1340775
YJL9627	No ARS317	SHE4-14-32P	Pink	2.0	Chr11(1.7)		GSM1340776
YJL9627	No ARS317	SHE4-14-35R	Red	2.7	Chr13(2.7)	+	GSM1340777
YJL9627	No ARS317	SHE4-14-35P	Pink	2.0	–		GSM1340778
YJL9627	No ARS317	SHE4-14-36R	Red	Mix	Chr5{LT-160kb(2.9)}; Chr7{910kb-RT(2.9)}	– *	GSM1340779
YJL9627	No ARS317	SHE4-14-36P	Pink	2.0	–		GSM1340780
YJL9627	No ARS317	SHE4-14-38R	Red	2.0	Chr3(2.8)	–	GSM1340781
YJL9627	No ARS317	SHE4-14-38P	Pink	2.0	Chr10(2.7)		GSM1340782
YJL9627	No ARS317	SHE4-14-39R	Red	2.7	Chr3(2.5); Chr7{820kb-870kb(2.7)}; Chr11(2.7)	+	GSM1340783
YJL9627	No ARS317	SHE4-14-39P	Pink	2.0	–		GSM1340784
YJL9627	No ARS317	SHE4-14-40R	Red	2.8	Chr3{LT-170kb(2.6)}; Chr4{1200kb-RT(2.7)}	+	GSM1340785
YJL9627	No ARS317	SHE4-14-40P	Pink	2.0	–		GSM1340786
YJL9627	No ARS317	SHE4-14-41R	Red	Mix	Chr3(2.8); Chr5{450kb-RT(1)}; Chr15{LT-100kb(2.8)}	–	GSM1340787
YJL9627	No ARS317	SHE4-14-41P	Pink	2.0	–		GSM1340788
YJL9629	No ARS317	SHE5-29-8R	Red	2.8	Chr13(2.7)	+	GSM1340789
YJL9629	No ARS317	SHE5-29-8P	Pink	2.0	–		GSM1340790
YJL9629	No ARS317	SHE5-29-11R	Red	2.0	–	–	GSM1340791
YJL9629	No ARS317	SHE5-29-11P	Pink	2.0	–		GSM1340792
YJL9637	ARS317 at CEN5	SHE5-23-41R	Red	2.7	–	+	GSM1340793
YJL9637	ARS317 at CEN5	SHE5-23-41P	Pink	2.0	Chr4{900kb-100kb(3)}		GSM1340794
YJL9637	ARS317 at CEN5	SHE5-23-43R	Red	2.8	–	+	GSM1340795
YJL9637	ARS317 at CEN5	SHE5-23-43P	Pink	2.0	–		GSM1340796
YJL9637	ARS317 at CEN5	SHE4-14-88R	Red	2.7	–	+	GSM1340797
YJL9637	ARS317 at CEN5	SHE4-14-88P	Pink	2.0	–		GSM1340798
YJL9637	ARS317 at CEN5	SHE5-23-59R	Red	2.7	–	+	GSM1340799
YJL9637	ARS317 at CEN5	SHE5-23-59P	Pink	2.0	–		GSM1340800
YJL9637	ARS317 at CEN5	SHE5-23-64R	Red	2.7	Chr3{150kb-160kb(3)}	+	GSM1340801
YJL9637	ARS317 at CEN5	SHE5-23-64P	Pink	2.0	Chr15(2.6)		GSM1340802
YJL9637	ARS317 at CEN5	SHE5-23-53R	Red	Mix	Chr5{135kb-450kb(3), 450kb-RT(3.5)}	– *	GSM1340803
YJL9637	ARS317 at CEN5	SHE5-23-53P	Pink	2.0	–		GSM1340804
YJL9639	ARS317 at CEN5	SHE5-25-56R	Red	2.7	–	+	GSM1340805
YJL9639	ARS317 at CEN5	SHE5-25-56P	Pink	2.0	–		GSM1340806
YJL9639	ARS317 at CEN5	SHE5-25-58R	Red	2.7	Chr5{425kb-475kb(2)}	+ **	GSM1340807
YJL9639	ARS317 at CEN5	SHE5-25-58P	Pink	2.0	Chr5{425kb-475kb(1)}		GSM1340808
YJL9639	ARS317 at CEN5	SHE5-25-72R	Red	2.6	Chr12{650kb-700kb(1.1)}	+	GSM1340809
YJL9639	ARS317 at CEN5	SHE5-25-72P	Pink	2.0	–		GSM1340810

Table S3 (continued)

Parental Strain	Relevant genotype	Colony number	Sector	Chr5 Copy No.	Other genomic changes	2:1 Chr5 segregation	Sample no. in GEO
YJL9639	ARS317 at CEN5	SHE5-25-80R	Red	2.5	–	+	GSM1340811
YJL9639	ARS317 at CEN5	SHE5-25-80P	Pink	2.0	–		GSM1340812
YJL9639	ARS317 at CEN5	SHE5-25-86R	Red	2.7	–	− *	GSM1340813
YJL9639	ARS317 at CEN5	SHE5-25-86P	Pink	Mix	Chr5{LT-160kb(2.7), 540kb-RT(2.7)}		GSM1340814
YJL10171	ARS317 at CEN5, *rad52*Δ	SHE5-01-93R	Red	2.0	Chr9(1.3); Chr14(1.9)	−	GSM1340815
YJL10171	ARS317 at CEN5, *rad52*Δ	SHE5-01-93P	Pink	2.0	Chr1(1.2)		GSM1340816
YJL10171	ARS317 at CEN5, *rad52*Δ	SHE5-01-99R	Red	2.4	–	+	GSM1340817
YJL10171	ARS317 at CEN5, *rad52*Δ	SHE5-01-99P	Pink	2.0	–		GSM1340818
YJL10171	ARS317 at CEN5, *rad52*Δ	SHE5-01-105R	Red	2.7	Chr1(1)	+	GSM1340819
YJL10171	ARS317 at CEN5, *rad52*Δ	SHE5-01-105P	Pink	2.0	Chr1(1.2)		GSM1340820
YJL10171	ARS317 at CEN5, *rad52*Δ	SHE5-01-109R	Red	2.5	–	+	GSM1340821
YJL10171	ARS317 at CEN5, *rad52*Δ	SHE5-01-109P	Pink	2.0	–		GSM1340822
YJL10171	ARS317 at CEN5, *rad52*Δ	SHE5-01-114R	Red	2.5	–	+	GSM1340823
YJL10171	ARS317 at CEN5, *rad52*Δ	SHE5-01-114P	Pink	2.0	–		GSM1340824
YJL10171	ARS317 at CEN5, *rad52*Δ	SHE5-01-118R	Red	2.5	Chr3(2.6)	+	GSM1340825
YJL10171	ARS317 at CEN5, *rad52*Δ	SHE5-01-118P	Pink	2.0	Chr3(2.7)		GSM1340826
YJL10171	ARS317 at CEN5, *rad52*Δ	SHE5-01-123R	Red	2.9	Chr14(1.1)	+	GSM1340827
YJL10171	ARS317 at CEN5, *rad52*Δ	SHE5-01-123P	Pink	2.0	–		GSM1340828
YJL10171	ARS317 at CEN5, *rad52*Δ	SHE5-01-129R	Red	2.5	Chr1(1); Chr16(2.5)	+	GSM1340829
YJL10171	ARS317 at CEN5, *rad52*Δ	SHE5-01-129P	Pink	2.0	Chr1(1.1); Chr16(2.4)		GSM1340830
YJL10171	ARS317 at CEN5, *rad52*Δ	SHE5-01-136R	Red	2.5	–	+	GSM1340831
YJL10171	ARS317 at CEN5, *rad52*Δ	SHE5-01-136P	Pink	2.0	–		GSM1340832
YJL10171	ARS317 at CEN5, *rad52*Δ	SHE5-01-141R	Red	2.5	Chr1(1.1)	+	GSM1340833
YJL10171	ARS317 at CEN5, *rad52*Δ	SHE5-01-141P	Pink	2.0	–		GSM1340834
YJL10176	ARS317 at CEN5, *dnl4*Δ	SHE5-01-149R	Red	2.7	–	+	GSM1340835
YJL10176	ARS317 at CEN5, *dnl4*Δ	SHE5-01-149P	Pink	2.0	–		GSM1340836
YJL10176	ARS317 at CEN5, *dnl4*Δ	SHE5-01-151R	Red	Mix	Chr5{160kb-540kb(2.6), 540kb-RT(2.7)}	− *	GSM1340837
YJL10176	ARS317 at CEN5, *dnl4*Δ	SHE5-01-151P	Pink	2.0	–		GSM1340838
YJL10176	ARS317 at CEN5, *dnl4*Δ	SHE5-01-155R	Red	2.9	–	+	GSM1340839
YJL10176	ARS317 at CEN5, *dnl4*Δ	SHE5-01-155P	Pink	2.0	–		GSM1340840
YJL10176	ARS317 at CEN5, *dnl4*Δ	SHE5-01-157R	Red	2.8	–	+	GSM1340841
YJL10176	ARS317 at CEN5, *dnl4*Δ	SHE5-01-157P	Pink	2.0	Chr8(2.7); Chr9(2.7)		GSM1340842
YJL10176	ARS317 at CEN5, *dnl4*Δ	SHE5-01-165R	Red	2.8	–	+	GSM1340843
YJL10176	ARS317 at CEN5, *dnl4*Δ	SHE5-01-165P	Pink	2.0	–		GSM1340844
YJL10176	ARS317 at CEN5, *dnl4*Δ	SHE5-01-171R	Red	3.3	Chr3(2.5); Chr9(2.5); Chr11(2.5); Chr16(2.5)	+ ***	GSM1340845
YJL10176	ARS317 at CEN5, *dnl4*Δ	SHE5-01-171P	Pink	2.5	Chr3(2.5); Chr9(2.5); Chr11(3.3); Chr16(2.5)		GSM1340846
YJL10176	ARS317 at CEN5, *dnl4*Δ	SHE5-01-173R	Red	2.8	–	+	GSM1340847
YJL10176	ARS317 at CEN5, *dnl4*Δ	SHE5-01-173P	Pink	2.0	–		GSM1340848
YJL10176	ARS317 at CEN5, *dnl4*Δ	SHE5-01-177R	Red	2.9	–	+	GSM1340849
YJL10176	ARS317 at CEN5, *dnl4*Δ	SHE5-01-177P	Pink	2.0	–		GSM1340850

Table S3 (continued)

Parental Strain	Relevant genotype	Colony number	Sector	Chr5 Copy No.	Other genomic changes	2:1 Chr5 segregation	Sample no. in GEO
YJL10176	ARS317 at CEN5, *dnl4Δ*	SHE5-01-192R	Red	2.7	–	+	GSM1340851
YJL10176	ARS317 at CEN5, *dnl4Δ*	SHE5-01-192P	Pink	2.0	–		GSM1340852
YJL10176	ARS317 at CEN5, *dnl4Δ*	SHE5-01-194R	Red	2.8	–	+	GSM1340853
YJL10176	ARS317 at CEN5, *dnl4Δ*	SHE5-01-194P	Pink	2.0	–		GSM1340854
YJL10238	ARS317 at CEN5, *rad52Δdnl4Δ*	SHE5-23-85R	Red	2.0	Chr14(1.2)	−	GSM1340855
YJL10238	ARS317 at CEN5, *rad52Δdnl4Δ*	SHE5-23-85P	Pink	2.0	–		GSM1340856
YJL10238	ARS317 at CEN5, *rad52Δdnl4Δ*	SHE5-23-87R	Red	2.5	Chr1(1)	+	GSM1340857
YJL10238	ARS317 at CEN5, *rad52Δdnl4Δ*	SHE5-23-87P	Pink	2.0	–		GSM1340858
YJL10238	ARS317 at CEN5, *rad52Δdnl4Δ*	SHE5-23-89R	Red	2.2	–	+	GSM1340859
YJL10238	ARS317 at CEN5, *rad52Δdnl4Δ*	SHE5-23-89P	Pink	2.0	–		GSM1340860
YJL10238	ARS317 at CEN5, *rad52Δdnl4Δ*	SHE5-23-91R	Red	2.3	–	+	GSM1340861
YJL10238	ARS317 at CEN5, *rad52Δdnl4Δ*	SHE5-23-91P	Pink	2.0	–		GSM1340862
YJL10238	ARS317 at CEN5, *rad52Δdnl4Δ*	SHE5-23-93R	Red	2.4	Chr2(2.4)	+	GSM1340863
YJL10238	ARS317 at CEN5, *rad52Δdnl4Δ*	SHE5-23-93P	Pink	2.0	Chr1(1.6)		GSM1340864
YJL10240	ARS317 at CEN5, *rad52Δdnl4Δ*	SHE5-25-119R	Red	2.2	–	+	GSM1340865
YJL10240	ARS317 at CEN5, *rad52Δdnl4Δ*	SHE5-25-119P	Pink	2.0	–		GSM1340866
YJL10240	ARS317 at CEN5, *rad52Δdnl4Δ*	SHE5-25-129R	Red	2.2	–	+	GSM1340867
YJL10240	ARS317 at CEN5, *rad52Δdnl4Δ*	SHE5-25-129P	Pink	2.0	Chr1(2.4)		GSM1340868
YJL10240	ARS317 at CEN5, *rad52Δdnl4Δ*	SHE5-25-130R	Red	2.2	–	+	GSM1340869
YJL10240	ARS317 at CEN5, *rad52Δdnl4Δ*	SHE5-25-130P	Pink	2.0	–		GSM1340870
YJL10240	ARS317 at CEN5, *rad52Δdnl4Δ*	SHE5-25-134R	Red	2.4	–	+	GSM1340871
YJL10240	ARS317 at CEN5, *rad52Δdnl4Δ*	SHE5-25-134P	Pink	2.0	–		GSM1340872
YJL10240	ARS317 at CEN5, *rad52Δdnl4Δ*	SHE5-25-135R	Red	2.4	–	+	GSM1340873
YJL10240	ARS317 at CEN5, *rad52Δdnl4Δ*	SHE5-25-135P	Pink	2.0	–		GSM1340874

* Segment of Chr5 containing ade3-2p was at higher copy number than 2.0, accounting for red color of sector. However, the entire chromosome was not affected, so these isolates were not scored as 2:1 segregation events.

** Small segemental copy number loss in Chr5 in both sectors was consistent with a pre-exisiting deletion in one of the Chr5 homologs. Remaining copy number data was consistent with a 2:1 segregation event and colony was scored as such.

*** Copy number of Chr5 in both sectors and sector color was consistent with a pre-existing extra copy of the non-rereplicating Chr5 homolog. Remaining copy number data was consistent with a 2:1 segregation event and colony was scored as such.

Table S4: Array CGH corresponding to Fig. 4 (red/white colonies). Chromosomes other than Chr5 are at a copy number of 2.0 unless listed in "Other genomic changes" with copy number reported in parentheses. For chromosomal segments with a copy number other than 2.0, the boundaries of the segments are indicated by chromosomal coordinates within brackets. We inferred that the ade3-2p marked Chr5 homolog had undergone a 2:0 segregation event if the total Chr5 copy number was > 2.2 in the red sector and < 1.8 in the white sector (see Materials and Methods). LT = left telomere; RT = right telomere; Mix = whole copy number of Chr5 cannot be reported due to segmental gains or losses.

Parental Strain	Relevant genotype	Colony number	Sector	Chr5 Copy No.	Other genomic changes	2:0 Chr5 segregation	Sample no. in GEO
YJL9627	No ARS317 (no arrest)	SHE5-24-20R	Red	2.8	–	+	GSM1340875
YJL9627	No ARS317 (no arrest)	SHE5-24-20W	White	1.8	–		GSM1340876
YJL9637	ARS317 at CEN5 (no arrest)	SHE5-24-12R	Red	2.7	–	+	GSM1340877
YJL9637	ARS317 at CEN5 (no arrest)	SHE5-24-12W	White	1.7	–		GSM1340878
YJL9637	ARS317 at CEN5 (no arrest)	SHE5-24-14R	Red	2.6	Chr3(2.7); Chr12(2.6)	+	GSM1340879
YJL9637	ARS317 at CEN5 (no arrest)	SHE5-24-14W	White	1.3	Chr3(2.9)		GSM1340880
YJL9637	ARS317 at CEN5 (no arrest)	SHE5-24-15-R	Red	2.8	–	+	GSM1340881
YJL9637	ARS317 at CEN5 (no arrest)	SHE5-24-15W	White	1.7	Chr1(2.7)		GSM1340882
YJL9637	ARS317 at CEN5 (no arrest)	SHE5-24-16R	Red	2.7	–	+	GSM1340883
YJL9637	ARS317 at CEN5 (no arrest)	SHE5-24-16W	White	1.2	Chr7{810kb-880kb(3)}; Chr12{970kb-RT(1.1)}; Chr15{RT-120kb(3)}		GSM1340884
YJL9637	ARS317 at CEN5 (no arrest)	SHE5-24-18R	Red	2.8	–	+	GSM1340885
YJL9637	ARS317 at CEN5 (no arrest)	SHE5-24-18W	White	1.2	Chr1(1.1)		GSM1340886
YJL9637	ARS317 at CEN5 (no arrest)	SHE5-24-19R	Red	Mix	Chr5{LT-140kb(4), 140kb-290kb(3.2), 290kb-RT(2.5)}; Chr7 (2.5); Chr11(2.5); Chr16(2.5)	– *	GSM1340887
YJL9637	ARS317 at CEN5 (no arrest)	SHE5-24-19W	White	1.3	–		GSM1340888
YJL9639	ARS317 at CEN5 (no arrest)	SHE5-24-21R	Red	Mix	Chr2{260kb-RT(2.7)}; Chr3{LT-5kb(2.5), 10kb-90kb(3.3), 90kb-290kb(2.5)}; Chr5{LT-150kb(3), 150kb-RT(2.7)}	– *	GSM1340889
YJL9639	ARS317 at CEN5 (no arrest)	SHE5-24-21W	White	1.5	–		GSM1340890
YJL9639	ARS317 at CEN5 (no arrest)	SHE5-24-25R	Red	2.7	Chr8(2.7)	+	GSM1340891
YJL9639	ARS317 at CEN5 (no arrest)	SHE5-24-25W	White	1.2	Chr12{660kb-690kb(1.2)}		GSM1340892
YJL9639	ARS317 at CEN5 (no arrest)	SHE5-24-28R	Red	2.8	–	+	GSM1340893
YJL9639	ARS317 at CEN5 (no arrest)	SHE5-24-28W	White	1.3	–		GSM1340894
YJL9639	ARS317 at CEN5 (no arrest)	SHE5-24-29R	Red	2.8	–	+	GSM1340895
YJL9639	ARS317 at CEN5 (no arrest)	SHE5-24-29W	White	1.2	–		GSM1340896

* Copy number of Chr5 in both sectors was consistent with 2:0 segregation of Chr5. However, because of additional segmental copy number increases affecting Chr5 in the red sector, other explanations besides whole-chromosome missegregation were possible, hence these colonies were not scored as 2:0 segregation events.

Table S5: Array CGH corresponding to Fig. 4 (red/pink colonies). Chromosomes other than Chr5 are at a copy number of 2.0 unless listed in "Other genomic changes" with copy number reported in parentheses. For chromosomal segments with a copy number other than 2.0, the boundaries of the segments are indicated by chromosomal coordinates within brackets. We inferred that the ade3-2p marked Chr5 homolog had undergone a 2:1 segregation event if the total Chr5 copy number was > 2.2 in the red sector and = 2.0 in the pink sector (see Materials and Methods). LT = left telomere; RT = right telomere; Mix = whole copy number of Chr5 cannot be reported due to segmental gains or losses.

Parental Strain	Relevant genotype	Colony number	Sector	Chr5 Copy No.	Other genomic changes	2:1 Chr5 segregation	Sample no. in GEO
YJL9627	No ARS317 (no arrest)	SHE5-24-1R	Red	2.0	Chr3{LT-5kb(2.7), 6kb-90kb(3.5), 90kb-RT(2.7)}; Chr12{975kb-RT(1.1)}; Chr13(2.7)	–	GSM1340897
YJL9627	No ARS317 (no arrest)	SHE5-24-1P	Pink	2.0	–		GSM1340898
YJL9627	No ARS317 (no arrest)	SHE5-24-2R	Red	2.7	–	+	GSM1340899
YJL9627	No ARS317 (no arrest)	SHE5-24-2P	Pink	2.0	Chr4{900kb-980kb(3)}		GSM1340900
YJL9627	No ARS317 (no arrest)	SHE5-24-3R	Red	2.0	Chr3(2.7)	–	GSM1340901
YJL9627	No ARS317 (no arrest)	SHE5-24-3P	Pink	2.0	Chr1(2.7)		GSM1340902
YJL9627	No ARS317 (no arrest)	SHE5-24-4R	Red	2.7	–	+	GSM1340903
YJL9627	No ARS317 (no arrest)	SHE5-24-4P	Pink	2.0	–		GSM1340904
YJL9627	No ARS317 (no arrest)	SHE5-24-5R	Red	Mix	Chr4{1000kb-RT(2.7)}; Chr5{LT-440kb(2.7)}	– *	GSM1340905
YJL9627	No ARS317 (no arrest)	SHE5-24-5P	Pink	2.0	–		GSM1340906
YJL9627	No ARS317 (no arrest)	SHE5-24-6R	Red	2.7	Chr1(2.6)	+	GSM1340907
YJL9627	No ARS317 (no arrest)	SHE5-24-6P	Pink	2.0	Chr1(2.6)		GSM1340908
YJL9627	No ARS317 (no arrest)	SHE5-24-7R	Red	2.7	Chr3{150kb-170kb(2.6)}	+	GSM1340909
YJL9627	No ARS317 (no arrest)	SHE5-24-7P	Pink	2.0	Chr3{150kb-170kb(2.6)}; Chr8{LT-200kb(2.7)}; Chr15{140kb-RT(2.7)}		GSM1340910
YJL9627	No ARS317 (no arrest)	SHE5-24-8R	Red	2.7	–	+	GSM1340911
YJL9627	No ARS317 (no arrest)	SHE5-24-8P	Pink	2.0	–		GSM1340912
YJL9627	No ARS317 (no arrest)	SHE5-24-9R	Red	2.7	–	+	GSM1340913
YJL9627	No ARS317 (no arrest)	SHE5-24-9P	Pink	2.0	–		GSM1340914
YJL9627	No ARS317 (no arrest)	SHE5-24-10R	Red	2.6	Chr6(2.6); Chr8(2.6)	+	GSM1340915
YJL9627	No ARS317 (no arrest)	SHE5-24-10P	Pink	2.0	Chr1(3.5); Chr3(2.6); Chr13(2.6)		GSM1340916
YJL9637	ARS317 at CEN5 (no arrest)	SHE5-24-32R	Red	2.7	Chr1(2.7)	+	GSM1340917
YJL9637	ARS317 at CEN5 (no arrest)	SHE5-24-32P	Pink	2.0	Chr10(2.7)		GSM1340918
YJL9637	ARS317 at CEN5 (no arrest)	SHE5-24-35R	Red	2.7	–	+	GSM1340919
YJL9637	ARS317 at CEN5 (no arrest)	SHE5-24-35P	Pink	2.0	–		GSM1340920
YJL9637	ARS317 at CEN5 (no arrest)	SHE5-24-39R	Red	3.4	Chr3(2.5); Chr10(2.7)	+	GSM1340921
YJL9637	ARS317 at CEN5 (no arrest)	SHE5-24-39P	Pink	2.0	Chr2(2.7)		GSM1340922
YJL9637	ARS317 at CEN5 (no arrest)	SHE5-24-44R	Red	2.8	–	+	GSM1340923
YJL9637	ARS317 at CEN5 (no arrest)	SHE5-24-44P	Pink	2.0	–		GSM1340924
YJL9637	ARS317 at CEN5 (no arrest)	SHE5-24-47R	Red	2.7	Chr4{880kb-980kb(3)}; Chr7{575kb-RT(3)}; Chr16{LT-70kb(1)}	+	GSM1340925
YJL9637	ARS317 at CEN5 (no arrest)	SHE5-24-47P	Pink	2.0	Chr4{880kb-980kb(3)}; Chr7{575kb-RT(3)}; Chr16{LT-70kb(1)}		GSM1340926
YJL9637	ARS317 at CEN5 (no arrest)	SHE5-24-52R	Red	2.7	–	+	GSM1340927
YJL9637	ARS317 at CEN5 (no arrest)	SHE5-24-52P	Pink	2.0	–		GSM1340928
YJL9639	ARS317 at CEN5 (no arrest)	SHE5-24-63R	Red	2.7	–	+	GSM1340929
YJL9639	ARS317 at CEN5 (no arrest)	SHE5-24-63P	Pink	2.0	–		GSM1340930
YJL9639	ARS317 at CEN5 (no arrest)	SHE5-24-68R	Red	2.7	–	+	GSM1340931
YJL9639	ARS317 at CEN5 (no arrest)	SHE5-24-68P	Pink	2.0	–		GSM1340932

Table S5 (continued)

Parental Strain	Relevant genotype	Colony number	Sector	Chr5 Copy No.	Other genomic changes	2:1 Chr5 segregation	Sample no. in GEO
YJL9639	ARS317 at CEN5 (no arrest)	SHE5-24-74R	Red	2.8	–	+	GSM1340933
YJL9639	ARS317 at CEN5 (no arrest)	SHE5-24-74P	Pink	2.0	Chr3{155kb-170kb(2.7)}		GSM1340934
YJL9639	ARS317 at CEN5 (no arrest)	SHE5-24-76R	Red	2.8	–	+	GSM1340935
YJL9639	ARS317 at CEN5 (no arrest)	SHE5-24-76P	Pink	2.0	–		GSM1340936

* Segment of Chr5 containing ade3-2p was at higher copy number than 2.0, accounting for red color of sector. However, the entire chromosome was not affected, so these isolates were not scored as 2:1 segregation events.

Table S6: Results of all re-replication assays reported in this work. Both the measured frequencies (as depicted in figure graphs) and actual colony counts are listed. Mean of trials is not weighted.

Relevant genotype	Strain	Trial No.	Sectoring Frequencies					Actual Colony Counts					
			Before induction		After Induction			Before Induction			After Induction		
			Red/White	Red/Pink	Red/White	Red/Pink		Red/White	Red/Pink	All colonies	Red/White	Red/Pink	All colonies
ARS317 at CEN5	9637	1	0.00%	0.24%	0.85%	2.32%		0	4	1655	34	93	4014
	9637	2	0.06%	0.25%	0.88%	2.22%		2	8	3141	40	101	4545
	9639	3	0.07%	0.22%	0.80%	2.57%		2	6	2767	29	93	3620
	9637	4	0.10%	0.10%	0.78%	2.57%		2	2	2044	14	46	1787
	9637	5	0.00%	0.14%	0.83%	2.99%		0	3	2083	16	58	1938
	9639	6	0.05%	0.16%	0.79%	2.06%		1	3	1918	16	42	2035
	9637	7	0.10%	0.25%	0.71%	2.07%		2	5	2000	11	32	1545
	9639	8	0.00%	0.15%	0.93%	2.94%		0	3	1991	17	54	1837
	9637	9	0.00%	0.21%	0.67%	2.06%		0	4	1923	12	37	1798
	9637	10	0.10%	0.10%	0.54%	1.94%		2	2	2082	10	36	1853
	9639	11	0.00%	0.19%	0.81%	2.89%		0	3	1592	17	61	2110
	Mean of trials		0.04%	0.18%	0.78%	2.42%	*Totals*	11	43	23196	216	653	27082
	SEM		0.01%	0.02%	0.03%	0.11%							
No ARS317	9627	1	0.05%	0.38%	0.10%	0.27%		1	7	1819	4	11	4083
	9627	2	0.00%	0.20%	0.08%	0.25%		0	6	3061	4	12	4756
	9629	3	0.09%	0.00%	0.02%	0.16%		1	0	1155	1	8	4893
	Mean of trials		0.05%	0.19%	0.07%	0.23%	*Totals*	2	13	6035	9	31	13732
	SEM		0.03%	0.11%	0.02%	0.03%							
ARS317 moved to Chr5_520	9631	1	0.14%	0.14%	0.08%	0.21%		2	2	1451	3	8	3878
	9631	2	0.08%	0.21%	0.02%	0.40%		2	5	2399	1	19	4794
	9633	3	0.00%	0.13%	0.14%	0.14%		0	3	2274	5	5	3461
	Mean of trials		0.07%	0.16%	0.08%	0.25%	*Totals*	4	10	6124	9	32	12133
	SEM		0.04%	0.03%	0.03%	0.08%							

Table S6 (continued)

Relevant genotype	Strain	Trial No.	Sectoring Frequencies					Actual Colony Counts					
			Before induction		After Induction			Before Induction			After Induction		
			Red/White	Red/Pink	Red/White	Red/Pink		Red/White	Red/Pink	All colonies	Red/White	Red/Pink	All colonies
ARS317 at CEN5, Δrad52	10171	1	0.05%	0.15%	0.96%	1.26%		1	3	1995	19	25	1978
	10171	2	0.06%	0.22%	0.52%	1.13%		1	4	1810	10	22	1939
	10172	3	0.00%	0.14%	0.54%	0.98%		0	3	2145	11	20	2049
	10171	4	0.11%	0.26%	0.98%	1.09%		2	5	1901	18	20	1833
	10172	5	0.00%	0.50%	0.47%	1.25%		0	10	1995	9	24	1913
	Mean of trials		0.04%	0.26%	0.69%	1.14%	*Totals*	4	25	9846	67	111	9712
	SEM		0.02%	0.07%	0.11%	0.05%							
ARS317 at CEN5, Δdnl4	10176	1	0.00%	0.48%	1.15%	7.05%		0	0	2097	27	165	2339
	10176	2	0.05%	0.29%	1.19%	8.77%		1	6	2068	13	96	1095
	10177	3	0.10%	0.29%	1.17%	7.40%		2	6	2070	12	76	1027
	10177	4	0.00%	0.31%	0.87%	6.40%		0	7	2267	9	66	1031
	Mean of trials		0.04%	0.34%	1.10%	7.41%	*Totals*	3	19	8502	61	403	5492
	SEM		0.02%	0.05%	0.07%	0.50%							
No ARS317, Δrad52	10164	1	0.05%	0.38%	0.06%	0.79%		1	8	2120	1	14	1772
	10165	2	0.00%	0.56%	0.05%	1.03%		0	11	1981	1	21	2040
	10164	3	0.14%	0.42%	0.00%	0.94%		3	9	2133	0	22	2346
	Mean of trials		0.06%	0.45%	0.04%	0.92%	*Totals*	4	28	6234	2	57	6158
	SEM		0.04%	0.05%	0.02%	0.07%							
No ARS317, Δdnl4	10168	1	0.00%	0.19%	0.05%	0.66%		0	4	2104	1	12	1832
	10169	2	0.00%	0.00%	0.09%	0.37%		0	0	2212	2	8	2138
	10168	3	0.00%	0.14%	0.05%	0.25%		0	3	2135	1	5	2026
	Mean of trials		0.00%	0.11%	0.07%	0.43%	*Totals*	0	7	6451	4	25	5996
	SEM		0.00%	0.06%	0.01%	0.12%							
ARS317 at CEN5, Δrad52Δdnl4	10238	1	0.05%	0.24%	0.56%	1.02%		1	5	2115	10	18	1771
	10238	2	0.00%	0.33%	0.64%	0.85%		0	6	1838	12	16	1883
	10240	3	0.05%	0.33%	0.61%	1.21%		1	7	2096	14	28	2312
	Mean of trials		0.03%	0.30%	0.60%	1.03%	*Totals*	2	18	6049	36	62	5966
	SEM		0.02%	0.03%	0.02%	0.10%							

Table S6 (continued)

Relevant genotype	Strain	Trial No.	Sectoring Frequencies					Actual Colony Counts					
			Before induction		After Induction			Before Induction			After Induction		
			Red/White	Red/Pink	Red/White	Red/Pink		Red/White	Red/Pink	All colonies	Red/White	Red/Pink	All colonies
No ARS317, Δrad52Δdnl4	10235	1	0.05%	0.14%	0.10%	0.72%		1	3	2115	2	15	2080
	10235	2	0.00%	0.26%	0.00%	0.46%		0	5	1939	0	10	2167
	10236	3	0.00%	0.26%	0.14%	0.72%		0	4	1526	3	15	2096
	Mean of trials		0.02%	0.22%	0.08%	0.63%	*Totals*	1	12	5580	5	40	6343
	SEM		0.02%	0.04%	0.04%	0.09%							
ARS317 at CEN5 (no arrest)	9637	1	0.00%	0.00%	0.17%	1.96%		0	0	1938	6	70	3563
	9637	2	0.00%	0.05%	0.26%	2.60%		0	1	2193	5	50	1920
	9637	3	0.00%	0.00%	0.35%	2.86%		0	0	2076	8	64	2273
	9639	4	0.00%	0.00%	0.42%	2.23%		0	0	2100	10	51	2381
	Mean of trials		0.00%	0.01%	0.30%	2.41%	*Totals*	0	1	8307	29	235	10137
	SEM		0.00%	0.01%	0.05%	0.20%							
No ARS317 (no arrest)	9627	1	0.00%	0.00%	0.00%	0.23%		0	0	1931	0	9	3887
	9627	2	0.00%	0.05%	0.10%	0.31%		0	1	1965	2	6	1966
	9627	3	0.00%	0.00%	0.00%	0.13%		0	0	2178	0	3	2228
	9629	4	0.00%	0.05%	0.05%	0.37%		0	1	2160	1	8	2156
	Mean of trials		0.00%	0.03%	0.04%	0.26%	*Totals*	0	2	8234	3	26	10237
	SEM		0.00%	0.01%	0.02%	0.05%							

Table S7: Conversion of sectoring frequency to segregation. Sectoring frequencies were converted to segregation frequencies by multiplying the mean sectoring frequency of the re-replication trials ($n \geq 3$) by the fraction of colonies that had the expected distribution of Chr5 copy number for the relevant segregation event (see Materials and Methods).

Red/white sectoring frequency conversion to 2:0 segregation events			
Genotype	**Mean sectoring frequency (see Table S6)**	**Fraction of colonies showing 2:0 distribution of Chr5**	**Estimated frequency of 2:0 segregation events**
ARS317 at CEN5	0.78%	9/11 (82%) *see Table S2*	0.64%
No ARS317	0.07%	3/4 (75%) *see Table S2*	0.05%
ARS317 at CEN5 (no arrest)	0.30%	8/10 (80%) *see Table S4*	0.24%
No ARS317 (no arrest)	0.04%	1/1 (100%) *see Table S4*	0.04%

Red/pink sectoring frequency conversion to 2:1 segregation events			
Genotype	**Mean sectoring frequency (see Table S6)**	**Fraction of colonies showing 2:1 distribution of Chr5**	**Estimated frequency of 2:1 segregation events**
ARS317 at CEN5	2.42%	9/11 (82%) *see Table S3*	1.98%
No ARS317	0.23%	4/10 (10%) *see Table S3*	0.09%
ARS317 at CEN5, *rad52*Δ	1.14%	9/10 (90%) *see Table S3*	1.03%
ARS317 at CEN5, *dnl4*Δ	7.41%	9/10 (90%) *see Table S3*	6.67%
ARS317 at CEN5, *rad52*Δ*dnl4*Δ	1.03%	9/10 (90%) *see Table S3*	0.92%
ARS317 at CEN5 (no arrest)	2.41%	10/10 (100%) *see Table S5*	2.41%
No ARS317 (no arrest)	0.26%	7/10 (70%) *see Table S5*	0.18%

Table S8: Strains used in this study. For each locus, the allele of the MATa parent is listed first. Key features of each strain are in bold.

Strain number	Genotype
YJL8590	*ORC2-(NotI, SgrAI)/ORC2-(NotI, SgrAI) orc6(S116A)/orc6(S116A) leu2/leu2 ura3::{ACT1term-pGAL1/10-CDC6term}/ura3::{ACT1term-pGAL1/10-CDC6term} trp1-289/trp1-289 ade2/ade2 ade3/ade3 MCM7-2NLS/MCM7-2NLS bar1::LEU2/bar1::LEU2 HMRa::HPHMX/HMRa::HPHMX* ***ChrXVI_550kb::{ade3-2p, ARS317, kanMX}/ChromXVI*** *MATa/MATα*
YJL9627	*ORC2-(NotI, SgrAI)/ORC2-(NotI, SgrAI) orc6(S116A)/orc6(S116A) leu2/leu2 ura3::{ACT1term-pGAL1/10-delntCDC6,cdk2A-CDC6term}/ura3::{ACT1term-pGAL1/10-delntCDC6,cdk2A-CDC6term} trp1-289/trp1-289 ade2/ade2 ade3/ade3 MCM7-2NLS/MCM7-2NLS bar1/bar1 HMRa::HPHMX/HMRa::HPHMX* ***ChrV_160::{KanMX, ade3-2p}/ChrV_160::URA3 ChrV_548::{NatMX, ade3-2w}/ChrV_548*** *MATa/MATα*
YJL9629	*ORC2-(NotI, SgrAI)/ORC2-(NotI, SgrAI) orc6(S116A)/orc6(S116A) leu2/leu2 ura3::{ACT1term-pGAL1/10-delntCDC6,cdk2A-CDC6term}/ura3::{ACT1term-pGAL1/10-delntCDC6,cdk2A-CDC6term} trp1-289/trp1-289 ade2/ade2 ade3/ade3 MCM7-2NLS/MCM7-2NLS bar1/bar1 HMRa::HPHMX/HMRa::HPHMX* ***ChrV_160::{KanMX, ade3-2p}/ChrV_160::URA3 ChrV_548::{NatMX, ade3-2w}/ChrV_548*** *MATa/MATα*
YJL9631	*ORC2-(NotI, SgrAI)/ORC2-(NotI, SgrAI) orc6(S116A)/orc6(S116A) leu2/leu2 ura3::{ACT1term-pGAL1/10-delntCDC6,cdk2A-CDC6term}/ura3::{ACT1term-pGAL1/10-delntCDC6,cdk2A-CDC6term} trp1-289/trp1-289 ade2/ade2 ade3/ade3 MCM7-2NLS/MCM7-2NLS bar1/bar1 HMRa::HPHMX/HMRa::HPHMX* ***ChrV_160::{KanMX, ade3-2p}/ChrV_160::URA3 ChrV_548::{NatMX, ade3-2w, ARS317}/ChrV_548*** *MATa/MATα*
YJL9633	*ORC2-(NotI, SgrAI)/ORC2-(NotI, SgrAI) orc6(S116A)/orc6(S116A) leu2/leu2 ura3::{ACT1term-pGAL1/10-delntCDC6,cdk2A-CDC6term}/ura3::{ACT1term-pGAL1/10-delntCDC6,cdk2A-CDC6term} trp1-289/trp1-289 ade2/ade2 ade3/ade3 MCM7-2NLS/MCM7-2NLS bar1/bar1 HMRa::HPHMX/HMRa::HPHMX* ***ChrV_160::{KanMX, ade3-2p}/ChrV_160::URA3 ChrV_548::{NatMX, ade3-2w, ARS317}/ChrV_548*** *MATa/MATα*
YJL9637	*ORC2-(NotI, SgrAI)/ORC2-(NotI, SgrAI) orc6(S116A)/orc6(S116A) leu2/leu2 ura3::{ACT1term-pGAL1/10-delntCDC6,cdk2A-CDC6term}/ura3::{ACT1term-pGAL1/10-delntCDC6,cdk2A-CDC6term} trp1-289/trp1-289 ade2/ade2 ade3/ade3 MCM7-2NLS/MCM7-2NLS bar1/bar1 HMRa::HPHMX/HMRa::HPHMX* ***ChrV_160::{KanMX, ade3-2p, ARS317}/ChrV_160::URA3 ChrV_548::{NatMX, ade3-2w}/ChrV_548*** *MATa/MATα*
YJL9639	*ORC2-(NotI, SgrAI)/ORC2-(NotI, SgrAI) orc6(S116A)/orc6(S116A) leu2/leu2 ura3::{ACT1term-pGAL1/10-delntCDC6,cdk2A-CDC6term}/ura3::{ACT1term-pGAL1/10-delntCDC6,cdk2A-CDC6term} trp1-289/trp1-289 ade2/ade2 ade3/ade3 MCM7-2NLS/MCM7-2NLS bar1/bar1 HMRa::HPHMX/HMRa::HPHMX* ***ChrV_160::{KanMX, ade3-2p, ARS317}/ChrV_160::URA3 ChrV_548::{NatMX, ade3-2w}/ChrV_548*** *MATa/MATα*
YJL10164	*ORC2-(NotI, SgrAI)/ORC2-(NotI, SgrAI) orc6(S116A)/orc6(S116A) leu2/leu2 ura3::{ACT1term-pGAL1/10-delntCDC6,cdk2A-CDC6term}/ura3::{ACT1term-pGAL1/10-delntCDC6,cdk2A-CDC6term} trp1-289/trp1-289 ade2/ade2 ade3/ade3 MCM7-2NLS/MCM7-2NLS bar1/bar1 HMRa::HPHMX/HMRa::HPHMX* ***ChrV_160::{KanMX, ade3-2p}/ChrV_160::URA3 ChrV_548::{NatMX, ade3-2w}/ChrV_548 Δrad52::LEU2/Δrad52::LEU2*** *MATa/MATα*
YJL10165	*ORC2-(NotI, SgrAI)/ORC2-(NotI, SgrAI) orc6(S116A)/orc6(S116A) leu2/leu2 ura3::{ACT1term-pGAL1/10-delntCDC6,cdk2A-CDC6term}/ura3::{ACT1term-pGAL1/10-delntCDC6,cdk2A-CDC6term} trp1-289/trp1-289 ade2/ade2 ade3/ade3 MCM7-2NLS/MCM7-2NLS bar1/bar1 HMRa::HPHMX/HMRa::HPHMX* ***ChrV_160::{KanMX, ade3-2p}/ChrV_160::URA3 ChrV_548::{NatMX, ade3-2w}/ChrV_548 Δrad52::LEU2/Δrad52::LEU2*** *MATa/MATα*

Table S8 (continued)

Strain number	Genotype
YJL10168	*ORC2-(NotI, SgrAI)/ORC2-(NotI, SgrAI) orc6(S116A)/orc6(S116A) leu2/leu2 ura3::{ACT1term-pGAL1/10-delntCDC6,cdk2A-CDC6term}/ura3::{ACT1term-pGAL1/10-delntCDC6,cdk2A-CDC6term} trp1-289/trp1-289 ade2/ade2 ade3/ade3 MCM7-2NLS/MCM7-2NLS bar1/bar1 HMRa::HPHMX/HMRa::HPHMX* ***ChrV_160::{KanMX, ade3-2p}/ChrV_160::URA3 ChrV_548::{NatMX, ade3-2w}/ChrV_548 Δdnl4::LEU2/Δdnl4::LEU2*** *MATa/MATα*
YJL10169	*ORC2-(NotI, SgrAI)/ORC2-(NotI, SgrAI) orc6(S116A)/orc6(S116A) leu2/leu2 ura3::{ACT1term-pGAL1/10-delntCDC6,cdk2A-CDC6term}/ura3::{ACT1term-pGAL1/10-delntCDC6,cdk2A-CDC6term} trp1-289/trp1-289 ade2/ade2 ade3/ade3 MCM7-2NLS/MCM7-2NLS bar1/bar1 HMRa::HPHMX/HMRa::HPHMX* ***ChrV_160::{KanMX, ade3-2p}/ChrV_160::URA3 ChrV_548::{NatMX, ade3-2w}/ChrV_548 Δdnl4::LEU2/Δdnl4::LEU2*** *MATa/MATα*
YJL10171	*ORC2-(NotI, SgrAI)/ORC2-(NotI, SgrAI) orc6(S116A)/orc6(S116A) leu2/leu2 ura3::{ACT1term-pGAL1/10-delntCDC6,cdk2A-CDC6term}/ura3::{ACT1term-pGAL1/10-delntCDC6,cdk2A-CDC6term} trp1-289/trp1-289 ade2/ade2 ade3/ade3 MCM7-2NLS/MCM7-2NLS bar1/bar1 HMRa::HPHMX/HMRa::HPHMX* ***ChrV_160::{KanMX, ade3-2p, ARS317}/ChrV_160::URA3 ChrV_548::{NatMX, ade3-2w}/ChrV_548 Δrad52::LEU2/Δrad52::LEU2*** *MATa/MATα*
YJL10172	*ORC2-(NotI, SgrAI)/ORC2-(NotI, SgrAI) orc6(S116A)/orc6(S116A) leu2/leu2 ura3::{ACT1term-pGAL1/10-delntCDC6,cdk2A-CDC6term}/ura3::{ACT1term-pGAL1/10-delntCDC6,cdk2A-CDC6term} trp1-289/trp1-289 ade2/ade2 ade3/ade3 MCM7-2NLS/MCM7-2NLS bar1/bar1 HMRa::HPHMX/HMRa::HPHMX* ***ChrV_160::{KanMX, ade3-2p, ARS317}/ChrV_160::URA3 ChrV_548::{NatMX, ade3-2w}/ChrV_548 Δrad52::LEU2/Δrad52::LEU2*** *MATa/MATα*
YJL10176	*ORC2-(NotI, SgrAI)/ORC2-(NotI, SgrAI) orc6(S116A)/orc6(S116A) leu2/leu2 ura3::{ACT1term-pGAL1/10-delntCDC6,cdk2A-CDC6term}/ura3::{ACT1term-pGAL1/10-delntCDC6,cdk2A-CDC6term} trp1-289/trp1-289 ade2/ade2 ade3/ade3 MCM7-2NLS/MCM7-2NLS bar1/bar1 HMRa::HPHMX/HMRa::HPHMX* ***ChrV_160::{KanMX, ade3-2p, ARS317}/ChrV_160::URA3 ChrV_548::{NatMX, ade3-2w}/ChrV_548 Δdnl4::LEU2/Δdnl4::LEU2*** *MATa/MATα*
YJL10177	*ORC2-(NotI, SgrAI)/ORC2-(NotI, SgrAI) orc6(S116A)/orc6(S116A) leu2/leu2 ura3::{ACT1term-pGAL1/10-delntCDC6,cdk2A-CDC6term}/ura3::{ACT1term-pGAL1/10-delntCDC6,cdk2A-CDC6term} trp1-289/trp1-289 ade2/ade2 ade3/ade3 MCM7-2NLS/MCM7-2NLS bar1/bar1 HMRa::HPHMX/HMRa::HPHMX* ***ChrV_160::{KanMX, ade3-2p, ARS317}/ChrV_160::URA3 ChrV_548::{NatMX, ade3-2w}/ChrV_548 Δdnl4::LEU2/Δdnl4::LEU2*** *MATa/MATα*
YJL10235	*ORC2-(NotI, SgrAI)/ORC2-(NotI, SgrAI) orc6(S116A)/orc6(S116A) leu2/leu2 ura3::{ACT1term-pGAL1/10-delntCDC6,cdk2A-CDC6term}/ura3::{ACT1term-pGAL1/10-delntCDC6,cdk2A-CDC6term} trp1-289/trp1-289 ade2/ade2 ade3/ade3 MCM7-2NLS/MCM7-2NLS bar1/bar1 HMRa::HPHMX/HMRa::HPHMX* ***ChrV_160::{KanMX, ade3-2p}/ChrV_160::URA3 ChrV_548::{NatMX, ade3-2w}/ChrV_548 Δdnl4::LEU2/Δdnl4::LEU2 Δrad52::URA3/Δrad52::NatMX*** *MATa/MATα*
YJL10236	*ORC2-(NotI, SgrAI)/ORC2-(NotI, SgrAI) orc6(S116A)/orc6(S116A) leu2/leu2 ura3::{ACT1term-pGAL1/10-delntCDC6,cdk2A-CDC6term}/ura3::{ACT1term-pGAL1/10-delntCDC6,cdk2A-CDC6term} trp1-289/trp1-289 ade2/ade2 ade3/ade3 MCM7-2NLS/MCM7-2NLS bar1/bar1 HMRa::HPHMX/HMRa::HPHMX* ***ChrV_160::{KanMX, ade3-2p}/ChrV_160::URA3 ChrV_548::{NatMX, ade3-2w}/ChrV_548 Δdnl4::LEU2/Δdnl4::LEU2 Δrad52::URA3/Δrad52::NatMX*** *MATa/MATα*
YJL10238	*ORC2-(NotI, SgrAI)/ORC2-(NotI, SgrAI) orc6(S116A)/orc6(S116A) leu2/leu2 ura3::{ACT1term-pGAL1/10-delntCDC6,cdk2A-CDC6term}/ura3::{ACT1term-pGAL1/10-delntCDC6,cdk2A-CDC6term} trp1-289/trp1-289 ade2/ade2 ade3/ade3 MCM7-2NLS/MCM7-2NLS bar1/bar1 HMRa::HPHMX/HMRa::HPHMX* ***ChrV_160::{KanMX, ade3-2p, ARS317}/ChrV_160::URA3 ChrV_548::{NatMX, ade3-2w}/ChrV_548 Δdnl4::LEU2/Δdnl4::LEU2 Δrad52::URA3/Δrad52::NatMX*** *MATa/MATα*

Table S8 (continued)

Strain number	Genotype
YJL10240	*ORC2-(NotI, SgrAI)/ORC2-(NotI, SgrAI) orc6(S116A)/orc6(S116A) leu2/leu2 ura3::{ACT1term-pGAL1/10-delntCDC6,cdk2A-CDC6term}/ura3::{ACT1term-pGAL1/10-delntCDC6,cdk2A-CDC6term} trp1-289/trp1-289 ade2/ade2 ade3/ade3 MCM7-2NLS/MCM7-2NLS bar1/bar1 HMRa::HPHMX/HMRa::HPHMX* ***ChrV_160::{KanMX, ade3-2p, ARS317}/ChrV_160::URA3 ChrV_548::{NatMX, ade3-2w}/ChrV_548 Δdnl4::LEU2/Δdnl4::LEU2 Δrad52::URA3/Δrad52::NatMX*** *MATa/MATα*
YJL10665	*ORC2-(NotI, SgrAI) orc6(S116A) leu2 ura3::{ACT1term-pGAL1/10-delntCDC6,cdk2A-CDC6term} trp1-289::{GFP-TUB1, TRP1} ade2::{pCUP1-tetR-tdTomato, URA3, ADE2} ade3 MCM7-2NLS bar1 his7? sap3? HMRa::HPHMX* ***ChrV_160::{KanMX, ade3-2p} ChrV_548::{NatMX, ade3-2w} Chr5_151::{LEU2, tetOx128}*** *MATa*
YJL10666	*ORC2-(NotI, SgrAI) orc6(S116A) leu2 ura3::{ACT1term-pGAL1/10-delntCDC6,cdk2A-CDC6term} trp1-289::{GFP-TUB1, TRP1} ade2::{pCUP1-tetR-tdTomato, URA3, ADE2} ade3 MCM7-2NLS bar1 his7? sap3? HMRa::HPHMX* ***ChrV_160::{KanMX, ade3-2p} ChrV_548::{NatMX, ade3-2w} Chr5_151::{LEU2, tetOx128}*** *MATa*
YJL10671	*ORC2-(NotI, SgrAI) orc6(S116A) leu2 ura3::{ACT1term-pGAL1/10-delntCDC6,cdk2A-CDC6term} trp1-289::{GFP-TUB1, TRP1} ade2::{pCUP1-tetR-tdTomato, URA3, ADE2} ade3 MCM7-2NLS bar1 his7? sap3? HMRa::HPHMX* ***ChrV_160::{KanMX, ade3-2p, ARS317} ChrV_548::{NatMX, ade3-2w} Chr5_151::{LEU2, tetOx128}*** *MATa*
YJL10672	*ORC2-(NotI, SgrAI) orc6(S116A) leu2 ura3::{ACT1term-pGAL1/10-delntCDC6,cdk2A-CDC6term} trp1-289::{GFP-TUB1, TRP1} ade2::{pCUP1-tetR-tdTomato, URA3, ADE2} ade3 MCM7-2NLS bar1 his7? sap3? HMRa::HPHMX* ***ChrV_160::{KanMX, ade3-2p, ARS317} ChrV_548::{NatMX, ade3-2w} Chr5_151::{LEU2, tetOx128}*** *MATa*

Table S9: Flanking homologies for re-replication cassettes. Re-replication cassettes were inserted into the genome using the targeting homologies (5' to 3' on the Watson strand as per the latest S288C reference sequence R64-1-1 on the Saccharomyces Genome Database) shown below.

Homology for ChrV_160	
Upstream homology	*Downstream homology*
AGATTCCAGAGGTTGCTAGGCTATCCAGTTTATGGCGATGAG GTAGGAAAAGTTGGTGTTCATTTGGCGTTGAATACTTCTGGG AAAGACAAGGTTCAGTTTGTCTCCAGCAAGGACATTCTTGAC ATCTCAGCTTCTCTGGAGAAGATTGCTACCTAAA	CAACCAACGGCTTCTTCTCGCAGCTACAGTTGTATTTTACTGTGACGTACTTTTGCGCGC GTACGGGTTCAATGAATTACGGATTTTCAACAACTTCACACAATCATAGCTTTTTTTACT TTTTCGCCTCATTATTTTCTTTAAAGAAACGATGATAAACAGAGATTTATCGTCATGTTA TTTCGTTCGTATATATCGTATTTGCGTTTTAGCTGTATAAAGTAAAATACTATATCTAAC GTGGCTTTTTTTATTTCCCCGTCTGCCCTCTTATGCTCATAGAAAACACTAATGATCGGTT TGGTATCGTCATAGATGCAGGGTCTTCGGGTTCGAGAATCCATGTGTTTAAGTGGCAGG ACACGGAATCGCTTCTTCATGCAACAAACCAGGACTCACAGTCCATATTACAATCAGTA CCTCATATTCATCAAGAAAAAGACTGGACTTTTAAGCTGAATCCAGGCTTGTCGAGTTTT GAAAAAAAACCTCAAGATGCGTACAAATCTC
Homology for ChrV_548	
Upstream homology	*Downstream homology*
GCCATTCTATGTCTGATCCCGGTACTACCTACAGAACTAGAG ACGAGATTCAGCATATGAGATCCAAGAACGATCCAATTGCT GGTCTTAAGATGCATTTGATTGATCTAGGTATTGCCACTGAA GCTGAAGTCAAAGCTTACGACAAGTCCGCTAGAAAATACGT TGACGAACAAGTTGAATTAGCTGATGCTGCTCCTCCTCCAGA AGCCAAATTATCCATCTTGTTTGAAGACGTCTACGTGAAAGG TACAGAAACTCCAACCCTAAGAGGTAGGATCCCTGAAGATA CTTGGGACTTCAAAAAGCAAGGTTTTGCCTCTAGGGATTAAT TAAATCGTAAGGAAAAATAAAATAATAGTGCTGTGATCGCA TGATATTCTTCC	CTGGAAGCGCCATTTTATAGCAAGAAATGTAAGTCAAGTATATTTTAACTGTATATCAA CAATATAGCTCTTTTTTATGCCTTGTTGTTTTTCTTCGGGTTTTCCCCACACATTGTGTGG AGAGATAGTTATTAACAGACCGGAAAATAGCCGCCCAAGGATAAACTTTTATATAAAG GGAAGGGTAGTTGACCCAAAAAATTTGGATTCTACTTTTCCAGATTTACTTTCACCCTTT TATATTTGCTGTAGTCTGTTATGCCAATCAGGAAAGCATTTGAACAAATATGTCTGTTAC AGGAACTGAGATCGATAGTGATACAGCAAAAAATATTCTTAGTGTAGATGAATTACAGA ACTATGGTATTAATGCCTCAGATCTTCAAAAATTGAAGTCTGGTGGGATATACACAGTC AATGTATGTTATAATAACATTTTTAAAACCTCTGCTGTAGAGGTTCTTTCCCCCTTTCTTT TACTAACTAATAATTTGGAAAGGAACTTTTATAGACCGTTTTGTCAACAACAAGAAGAC ATCTATGTAAAATTAAAGGGTTAAGTGAGGTGAAAGT
Homology for *rad52*Δ	
Upstream homology	*Downstream homology*
AACTAGAGGATTTTGGAGTAATAAATAATGATGCAAATTTTT TATTTGTTTCGGCCAGGAAGCGTT	CCAACAACACACCAAAGCCACCAGAACCTTCAGCAGTTCTTGGCAACCTCCTTGTTTGC AT
Homology for *dnl4*Δ	
Upstream homology	*Downstream homology*
TACATATGTAGGATAGTATTAAATAAACTTCAAAAAATTAAG CCTCCGCAAAACGCACCA	ACCTAAATAATCCGTTACTATTTCCTTCAGTTCTAGATTTTTATTTTAGTATTTATTTTCC AC
Homology for *HMRa*Δ	
Upstream homology	*Downstream homology*
TTGTTTACTTTTTCTATCAGTGTTTTCAATTTTTTATTAAACAA TGTTTGATTTTTTAAATCGCAATTTAATACC	TTAATACCTTTAAATGTTGAGGTAAATAGCTATTTTCTCTCTTCTTTTCCTTTAGTTGGAA TTTGCACAAGAAAA
Homology for *TRP1* insertion at ChrV_151 (target for pSR14 integration)	
Upstream homology	*Downstream homology*
TCTTCATTAACAGGGGAACGCTTGCCTACCATCAAGCCCATT CAATGCAGATGTGATTAA	TTGGTAAACAAAGGGCCAAGCAAAAATACATCTCTCCTACATGCTACATAAGTCCGAGA

Table S10: List of all oligonucleotides used for construction of strains. Uppercase indicates where oligo hybridizes to the PCR template; lowercase corresponds to the chromosomal sequences flanking the deletion. See Materials and Methods for details of their use.

Oligo number	Sequence (*all are 5' to 3'*)	Disruption
OJL1639	attaaacaatgtttgatttttaaatcgcaatttaataccCGGATCCCCGGGTTAATTAA	*HMRa*Δ
OJL1642	agagaaaatagctatttacctcaacatttaaaggtattaaCATCGATGAATTCGAGCTCG	*HMRa*Δ
OJL2200	ttgtttacttttctatcagtgttttcaatttttattaaacaatgtttgatttttaaa	*HMRa*Δ
OJL2201	ttttcttgtgcaaattccaactaaaggaaaagaagagagaaaatagctatttacctcaac	*HMRa*Δ
OJL2821	gcttctctggagaagattgctacctaaaGAGCAGATTGTACTGAGAGTG	*URA3* at *CEN5*
OJL2822	ctgtagctgcgagaagaagccgttggttgaGCATCTGTGCGGTATTTCAC	*URA3* at *CEN5*
OJL2823	tctccagcaaggacattcttgacatctcagcttctctggagaagattgct	*URA3* at *CEN5*
OJL2824	cgcgcaaaagtacgtcacagtaaaatacaactgtagctgcgagaagaagc	*URA3* at *CEN5*
OJL2117	gaaggttctggtggctttggtgtgttgttgGAGCAGATTGTACTGAGAGTG	*rad52*Δ (with *LEU2* or *URA3*)
OJL2118	aatgatgcaaatttttttatttgtttcggccaggaagcgttGCATCTGTGCGGTATTTCAC	*rad52*Δ (with *LEU2* or *URA3*)
OJL1753	aagaactgctgaaggttctggtggctttggtgtgttgttgCGGATCCCCGGGTTAATTAA	*rad52*Δ (with *NatMX*)
OJL1754	aatgatgcaaatttttttatttgtttcggccaggaagcgttCATCGATGAATTCGAGCTCG	*rad52*Δ (with *NatMX*)
OJL2119	atgcaaacaaggaggttgccaagaactgctgaaggttctggtggctttgg	*rad52*Δ
OJL2120	aactagaggatttttggagtaataaataatgatgcaaatttttttatttgtttcggc	*rad52*Δ
OJL2097	gaactgaaggaaatagtaacggattatttaggtGAGCAGATTGTACTGAGAGTG	*dnl4*Δ
OJL2098	caaaaaattaagcctccgcaaaacgcaccaGCATCTGTGCGGTATTTCAC	*dnl4*Δ
OJL2099	gtggaaaataaatactaaaataaaaatctagaactgaaggaaatagtaacgg	*dnl4*Δ
OJL2100	tacatatgtaggatagtattaaataaacttcaaaaaattaagcctccgc	*dnl4*Δ
OJL3113	atcaagcccattcaatgcagatgtgattaaAGCGGATGCCGGGAGCAGAC	*TRP1* amplification for pSR14 targeting
OJL3114	tgtatttttgcttggccctttgtttaccaaGTGAGCTGATACCGCTCGCC	*TRP1* amplification for pSR14 targeting
OJL3115	tcttcattaacaggggaacgcttgcctaccATCAAGCCCATTCAATGCAG	*TRP1* amplification for pSR14 targeting
OJL3116	tctcggacttatgtagcatgtaggagagaTGTATTTTTGCTTGGCCCTTT	*TRP1* amplification for pSR14 targeting

Table S11: Cell scoring for Figure 5. Percentages are based on the total number of cells scored for the indicated initial spot number. See Materials and Methods for details of how cells were scored before and after nocodazole treatment.

	No *ARS317* (Trial 1: 111 cells, Trial 2:100 cells)						***ARS317* at *CEN5*** (Trial 1: 109 cells, Trial 2:110 cells)					
	Initially 2 spots		Initially 3 spots		Initially 4 spots		Initially 2 spots		Initially 3 spots		Initially 4 spots	
	Trial 1	*Trial 2*	*Trial 1*	*Trial 2*	*Trial 1*	*Trial 2*	*Trial 1*	*Trial 2*	*Trial 1*	*Trial 2*	*Trial 1*	*Trial 2*
1 spot after nocodazole	**92** (83%)	**87** (87%)	0	0	0	0	**36** (77%)	**31** (72%)	**29** (56%)	**36** (69%)	**3** (30%)	**4** (21%)
2 spots after nocodazole	**19** (17%)	**13** (13%)	0	0	0	0	**11** (23%)	**12** (28%)	**19** (37%)	**11** (21%)	**4** (40%)	**6** (32%)
3 spots after nocodazole	0	0	0	0	0	0	0	0	**4** (8%)	**5** (10%)	**2** (20%)	**6** (32%)
4 spots after nocodazole	0	0	0	0	0	0	0	0	0	0	**1** (10%)	**3** (16%)
Totals	111	100	0	0	0	0	47	43	52	52	10	19

Chapter Three: Conclusions and Future Directions

The results in CHAPTER TWO represent the majority of the research I conducted during my pre-doctoral training. The story is clear-cut: centromeric re-replication disrupts the proper segregation of a chromosome. What is less clear is the mechanism of how centromeric re-replication produces aberrant chromosomal segregation, as well as if this disturbance can affect the stability of other chromosomes. In this chapter, I will address these questions raised by my research to provide future directions that will expand our understanding of how centromeric re-replication can promote W-CIN.

HOW DOES RE-REPLICATION AFFECT CENTROMERIC CONTEXT?

In budding yeast, sister chromatid centromeres under tension are pulled so far apart that marking them with a fluorescent protein produces two resolvable spots (Goshima and Yanagida 2000). They are prevented from being completely pulled apart because of the cohesin that holds them together (Tanaka *et al*. 2000). This pericentromeric cohesin is quite different from arm cohesin: it holds intermolecular as well as intramolecular strands together (Yeh *et al*. 2008), promotes the biorientation of sister chromatids (Eckert *et al*. 2007; Ng *et al*. 2009; Sakuno *et al*. 2009), and has its own protective spirit Shugoshin, or Sgo1, which prevents pericentromeric cohesin destruction during meiosis and mitosis (Wantanabe 2005).

If a re-replication fork was to pass through the region of pericentromeric cohesin, how may this affect the centromeric context? Based on our knowledge of cohesin establishment, three possible models can be proposed: the re-replication fork will break/displace the existing cohesin and more will be established behind the fork (much like S phase) around the newly re-replicated strands; the fork will displace the pericentromeric cohesin, but mechanisms that re-establish cohesin will place more around the centromeres after they are under tension; or the

fork will displace all the pericentromeric cohesin to effectively remove it from the centromere. The first possibility is not likely as Eco1, a protein essential for cohesin loading during S phase, is destroyed to prevent post-replicative cohesin establishment (Lyons and Morgan 2011). However, there is evidence that two pools of cohesin exist: the cohesin that is placed around DNA during replication, and the cohesin that can be replaced around the centromere after stretching (Ocampo-Hafalla *et al* 2007). Additionally, cohesin loading is necessary during DNA damage repair, indicating the cell has the potential to re-establish cohesin outside of S phase that is independent of the establishment during S phase (Ström *et al*. 2004). This means the third possibility is unlikely since there are post-S phase mitotic mechanisms to re-establish cohesin at centromeres, however, the pathway's existence doesn't necessitate its functionality. Examination of the experiments presented in Figure 5A and 5B of CHAPTER TWO indicate that the centromeres of re-replicated chromosomes are able to collapse into a single unresolvable spot after spindle tension was removed. This indicates the centromeres are bound together, which is dependent upon pericentromeric cohesin. Thus, I hypothesize that the effect of centromeric re-replication on pericentromeric cohesin is minimal, and is not the primary stimulant of improper chromosome segregation.

To examine pericentromeric cohesin after centromeric re-replication, I would perform a chromatin immunoprecipitation followed by sequencing or quantitative PCR to observe the amount of cohesin present at a centromere before re-replication, during re-replication, and after re-replication has been terminated. I predict that the levels of cohesin may change, but after re-replication has ceased, levels will return to normal.

I would also perform genetic and microscopy tests to determine if the disturbance of cohesin loading factors has an effect on the number of centromeric spots observed post-re-

replication. If after centromeric re-replication, the loading of pericentromeric cohesin was important to biorient the re-replicated centromeres, one would expect less 3-spot cells in a microscopy assay: if the re-replicated chromosome does not biorient and both centromeres are pulled to one pole, then the spots would be unresolveable and the cell would appear to only have two. Of course, one could always plate the cells to see if the frequency of missegregation changes as well, but colony assays are tedious and cannot obtain the mechanistic resolution of microscopy.

When the cell re-replicates, the fork passes through the centromere to knock off kinetochore proteins. I believe both the kinetochore and the centromeric histone Cse4 are not affected by this re-replication since a functional kinetochore can reassemble after S phase (Collins *et al* 2005), and the Cse4 histone is well-targeted to centromeric DNA via sequence identity (Bloom and Carbon 1982; Verdaasdonk and Bloom 2011). Additionally, the resolution of centromeric spots observed in Figure 5 of CHAPTER TWO indicate tension is being placed on the re-replicated centromeres, which would be completely reliant upon functional centromeres and kinetochore complexes post-re-replication. Taken together, I believe the centromeric context of the re-replicated chromosome is not intrinsically disrupted.

CAN CENTROMERIC RE-REPLICATION AFFECT THE SEGREGATION OF OTHER CHROMOSOMES?

The context of a centromere extends beyond the elements that bind to it: in yeast, centromeres are clustered together in the nucleus (Duan *et al*. 2010). Could the re-replication of one centromere affect the segregation of another? Comparison of the frequency of non-Chr V missegregation in sectored colonies examined via aCGH (roughly 20-30% of Chr V aneuploid colonies; see Tables S2-S5 in CHAPTER TWO) between strains with and without the

re-replicating origin indicates that centromeric re-replication may not stimulate missegregation of other chromosomes. This data, however, cannot predict if the sources of the non-Chr V missegregation are the same. If the re-replication conditions imposed on cells without *ARS317* made them genomically unstable, then cells that were identified to have missegregated Chr V would have an increased chance of missegregating another chromosome as well. Due to the potent effect of centromeric re-replication and aneuploidy generation, this background instability that is not *ARS317*-dependent re-replication would be masked. Just as likely, the residual Chr V missegregation events in the strain lacking *ARS317* may be due to undetectable cryptic re-replication involving *CEN5*. Though its Chr V missegregation frequency may be much lower than the strain with *ARS317*, the same perturbation is occurring in both instances, and therefore the same frequency of non-Chr V missegregation events would be expected.

Another reason the current aCGH data cannot predict how *CEN5* re-replication will affect the segregation of other chromosomes is that the sectored colonies were identified by their alleged Chr V aneuploidy. If *CEN5* re-replication stimulates specific chromosomes to co-missegregate (perhaps, due to their proximity in the nucleus or connection via *trans* factors), and the resulting aneuploidy is incompatible with a Chr V aneuploidy, the cells would perish before forming a colony (or greatly impact the fitness of the progeny so that the final colony would not be scored).

In order to test if this kind of co-missegregation is occurring, a system needs to be built where events that are dependent on both the re-replicated chromosome AND another chromosome missegregating can be screened instead of scored. For example, if the *CAN1* marker (presence confers canavanine sensitivity) is on the re-replicating chromosome, and the *URA3* marker (presence confers 5'FOA sensitivity) is on different chromosome, colonies lacking

both of these markers can be identified by replica-plating to plates containing one or both drugs to determine the frequency of independent missegregation and co-missegregation events after centromeric re-replication.

Though the potential of co-missegregation is applicable to all the chromosomes, it may be especially relevant to the non-re-replicating homolog of Chr V. It is clear that re-replication from *ARS317* produces breaks (Finn and Li 2013), and though sister chromatids are the preferred substrate for repair over the homolog, the homolog can still be used (Kadyk and Hartwell 2002). Therefore, if centromeric re-replication destabilizes and breaks one homolog, and it uses the other homolog to recombine with and repair from, both homologs are now physically entwined. If both missegregate (a 4:0 distribution), then only one of the two daughter cells will survive, thus prohibiting the formation of a sectored colony. It would be interesting to determine if the 4:0 frequency is increased after centromeric re-replication as I did not observe reciprocal-missegregation events. If centromeric re-replication was affecting the segregation of its non-re-replicating homolog, then it may be expected that some events result in two, 2:0 segregation events (a reciprocal missegregation) to yield an overall 2:2 chromosome distribution. In my assay, I used color to identify the copy number of the re-replicating chromosome, so a reciprocal missegregation would result in a red-white colony (which would be scored). Genotypic aCGH analysis would show two copies of Chr V in each sector, and out of all the red-white colonies I examined, I did not observe any of these events. Discovering that centromeric re-replication can promote co-missegregation of the homolog but not reciprocal-missegregation would be highly interesting. If each homolog was labeled with a different fluorescent marker (tetO::tetR-tdTom for the re-replicating homolog, lacO::lacI-GFP for the homolog), then once again microscopy could be used to determine how these chromosomes interact and segregate.

Why are the chromosome aneuploidy frequencies so much lower than the frequency of centromeric re-replication?

Array CGH demonstrates that roughly half of the *ARS317* origins in a population reinitiate after three hours of induction (see Figure 1 in Chapter Two). This measurement is supported by microscopy data that looks directly at the number of *CEN5* molecules in a single cell (see Figure 5 in Chapter Two). With ~60% of the cells undergoing centromeric re-replication, why do only 3% result in aneuploidy? Observation of re-replicated cells in real-time shows that they are arrested in a violent metaphase: the spindle yanks and drags the chromosomes from one end of the cell to the other. This rough spindle tension may ultimately result in the missegregation and/or breakage of chromosomes, especially the re-replicated chromosome if the spindle is connected to each of the centromeres and is applying harsh force to a fragile re-replication bubble. Again, a specific colony phenotype was scored in these experiments, leaving open the possibility that centromeric re-replication can cause a plethora of rearrangements and instabilities that were not scored.

To determine how many missegregation events are occurring after centromeric re-replication, one must look at cells immediately following re-replication induction to observe how many missegregate or break the re-replicated chromatid. This process may take time, especially because the cells are arresting in metaphase after re-replication and may not come out of the arrest until they adapt to the checkpoint or correct the problem. Cells that end up missegregating the re-replicated chromosome should be followed through a few generations to observe the chromatid's fate; it is possible the discrepancy in re-replication induction and aneuploidy frequency resides in the generations after the missegregation.

Appendices A through E

Appendix A: Whole-chromosomal instability of Chromosome XVI

When I joined the Li Lab, I decided to continue my rotation project: examine the effect of centromeric re-replication on the segregation of a chromosome. I used a haploid strain a previous graduate student had made where the re-replicating origin *ARS317* and the color marker *ade3-2p* were near the centromere on Chromosome XVI. The principle of the experiment was to induce re-replication, plate single cells, then identify red colonies: if the color marker (and, by extension, Chr XVI) properly segregated, each of the daughter cells would survive and be pink, growing into a pink colony. If Chr XVI was to missegregate, then two copies would move to one daughter and the other would have none. The daughter without Chr XVI would perish while the daughter with both chromatids would have two copies of *ade3-2p* and turn red.

Great labor was taken to screen the colonies that resulted from the re-replication experiment. Ultimately, I picked up on a particular colony phenotype that was enriched in the strain that underwent centromeric re-replication. This phenotype was not so much red as it was brown, and there were little white sectors that were on the fringe of the colony, so I called this phenotype "sector red" to distinguish it from other shades of red I identified in my screenings (Figure 1B).

When these colonies were expanded and harvested for chromosome copy number analysis via aCGH, the results were disappointing: every chromosome was euploid, including Chr XVI (Figure 1A and 1B). Under closer inspection, the profile for Chr XVI was ever so slightly higher than the others, which made me think that, if this was a disomy to begin with, it is rather unstable and I must try to enrich for a population of these special "sector red" colonies. Going to the freezer stock I had made, I struck out cells to see how many still present the "sector red" phenotype. In general, ~5% of the streak colonies had the phenotype, indicating it is very

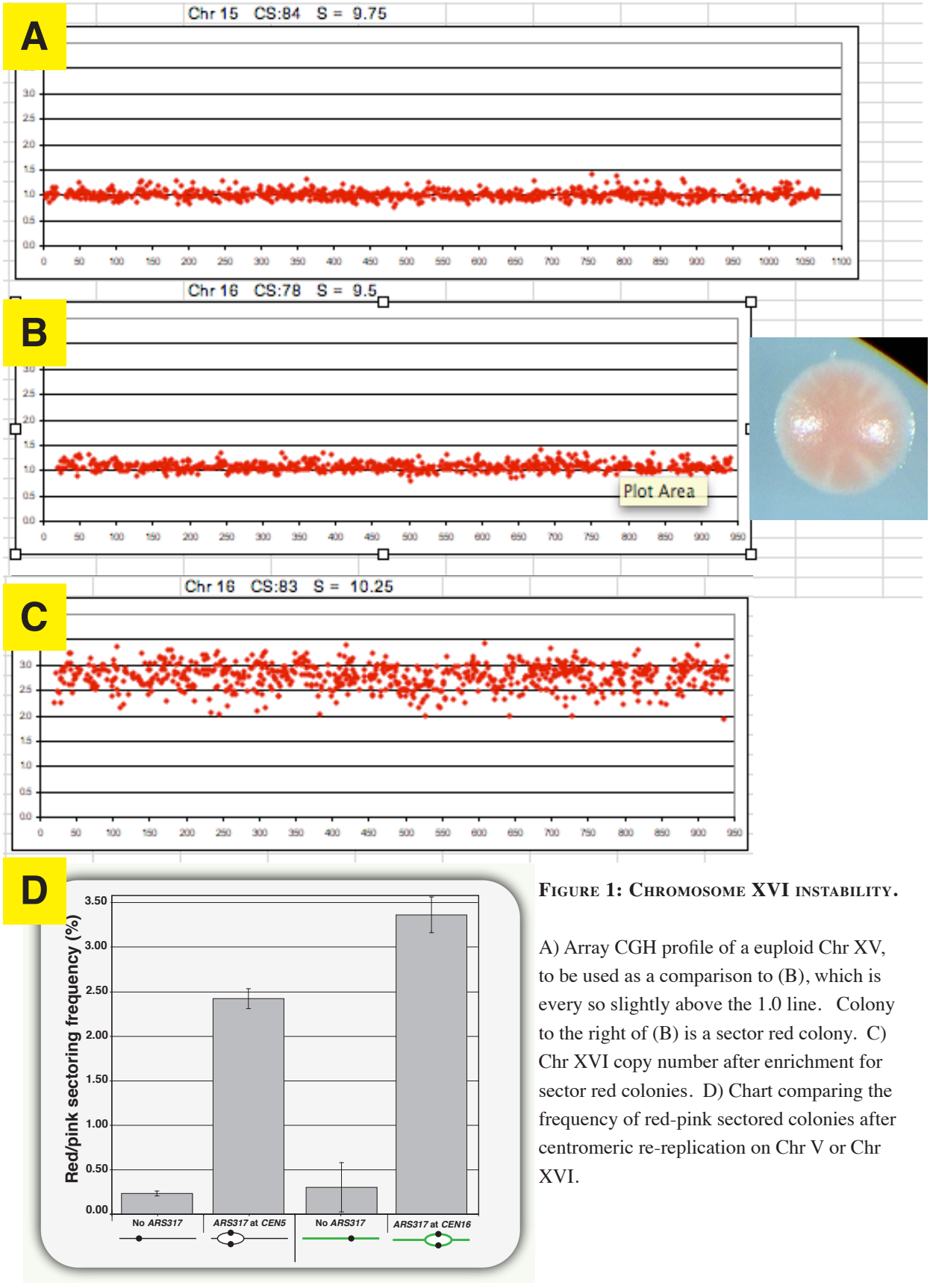

Figure 1: Chromosome XVI instability.

A) Array CGH profile of a euploid Chr XV, to be used as a comparison to (B), which is every so slightly above the 1.0 line. Colony to the right of (B) is a sector red colony. C) Chr XVI copy number after enrichment for sector red colonies. D) Chart comparing the frequency of red-pink sectored colonies after centromeric re-replication on Chr V or Chr XVI.

unstable. I then struck out many more, gathered them up, harvested the DNA and checked their genotype. To my pleasure, these colonies were in fact aneuploid for Chr XVI (Figure 1C).

After the promising results with the haploid strain, I constructed a diploid strain where one of the two homologs of Chr XVI was marked with *ade3-2p* and had *ARS317* near the centromere (*CEN16*). With this diploid strain, I hoped I would be able to see the progeny from a missegregation event involving Chr XVI: if the re-replicated copy of Chr XVI missegregated, the non-re-replicating homolog should presumably segregate properly to produce red-white sectored colonies with a 3:1 Chr XVI segregation pattern. After *CEN16* re-replication in a diploid, I saw no red-white colonies, however, I did see a stimulation of red-pink colonies. The color reporter indicates these colonies should have two copies of Chr XVI in the pink sector and three copies of Chr XVI in the red sector, and aCGH verifies this 3:2 distribution. But how did this extra chromosome come to be, and why did I not see any red-white colonies?

We began to suspect cells that were monosomic for Chr XVI were either very sick or dead (Chr XVI is a large chromosome—948 kb), so our efforts moved on to find a chromosome that would be tolerated as a monosome. We found that Chr V monosomies had little to no growth defect as compared to euploid cells (see Appendix B), so we decided to construct the re-replication setup around *CEN5*. Red-pink colonies were also observed with *CEN5* re-replication, and it turns out they are likely the product of a breakage event that was repaired to reconstitute an entire, whole chromosome. Though there is more work necessary to determine the exact origin of these chromosomes (see Appendix C), we believe the red-pink colonies observed with Chr XVI are products of the same breakage and repair process. As compared to Chr V, the frequency of Chr XVI 3:1 segregation events is very similar, despite being nearly twice the size (Figure 1D). Thus, centromeric re-replication can produce whole-chromosomal instability.

Appendix B: Hemizygous-tolerating chromosomes

Since the goal of centromeric re-replication in a diploid was to be able to see *both* daughter cell progeny after a missegregation event, I needed to find a chromosome that could be tolerated as a hemizygote. My work with Chr XVI hinted that I would be unable to use it, but I wanted to formally test it as well as other chromosomes to determine which, if any, could exist as a monosome when all other chromosomes were disomic, i.e., exist as a hemizygote.

To test if a chromosome can exist as a hemizygote, I needed to selectively get rid of a single homolog in a diploid background. Using the strategy from the Rothstein lab (Alvaro *et al*. 2006), I placed an inducible galactose promoter next to the centromere on one of two homologs for several chromosomes. When induction is off, the centromere is functional, however when induction is on, the active transcription drives through the centromere to prevent kinetochore assembly and render it nonfunctional. A chromosome that cannot segregate properly will soon be lost, leaving only cells that have a single copy of the chromosome.

I employed this strategy to test several chromosomes (Figure 2). After the centromeric inactivation, I picked colonies and performed aCGH to determine their ploidy. As chromosomes got larger, the bimodal distribution of colony size became evident, distinguishing cells that were likely monosomic from those that were not. Chr I, the smallest chromosome, has no problem being monosomic. Chr XV (a little over 1 Mb) was not able to tolerate monosomy. From this screening I was able to obtain viable cells that were monosomic for Chr V and for Chr IX, giving me two chromosomes to work with for upcoming re-replication assays. I decided to use Chr V first to better safeguard against re-replication through to entire chromosome (it is larger than Chr IX).

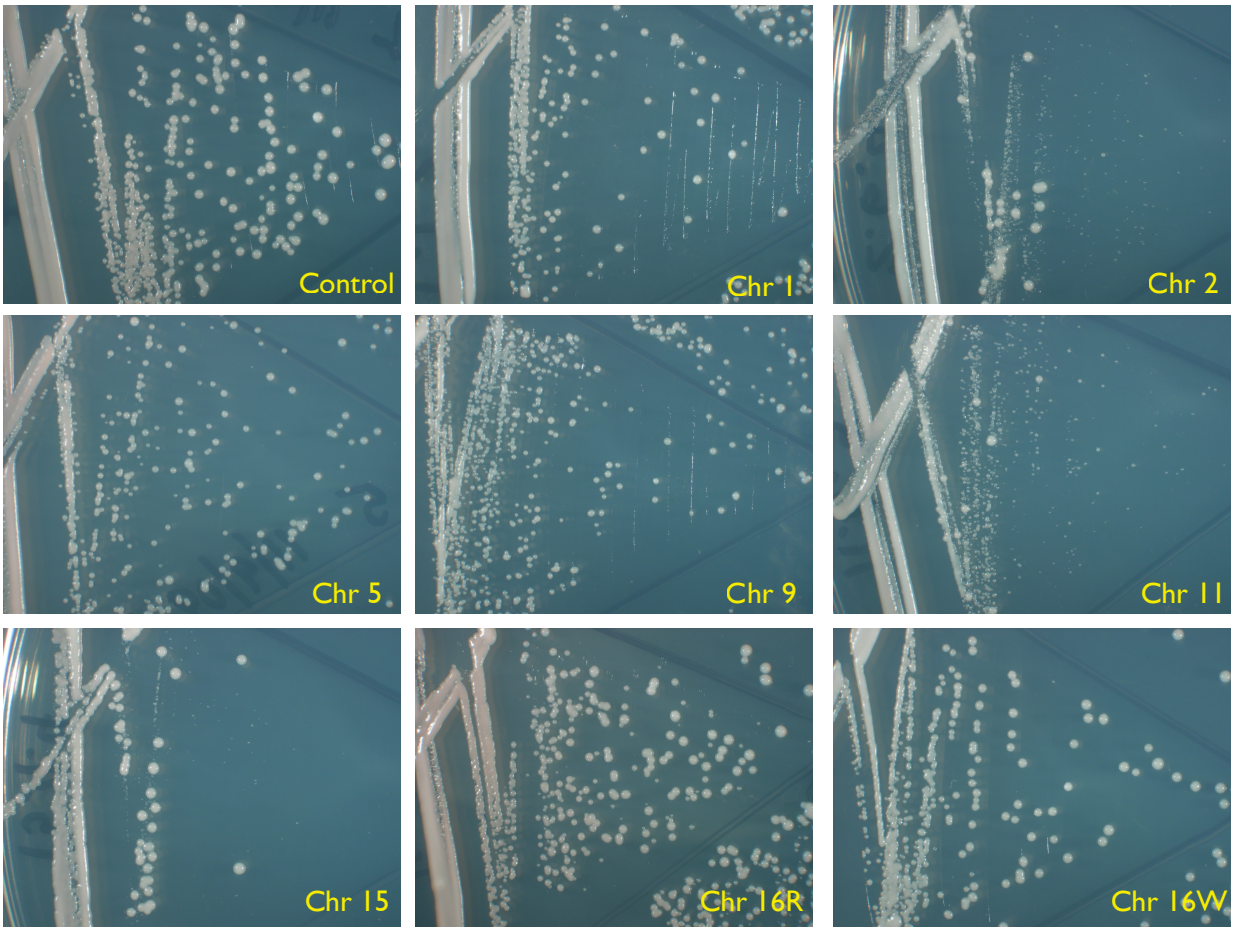

Figure 2: Finding a chromosome that will tolerate hemizygocity.

The galactose promoter was placed adjacent to the centromere on the chromosome as indicated above, then induced to force the loss of that chromosome. As shown, smaller chromosomes (like Chr I, ~230 kb) don't have a bimodal colony phenotype, whereas larger chromosomes (like Chr XI, ~666 kb)) have large colonies and very small colonies. The large and small colonies (or, subjectively the largest and smallest colonies on the plate for chromosomes without clear growth differences) were tested for ploidy via aCGH. Large colonies were typically euploid, and small colonoes were monosomic for the indicated chromosome. The "R" and "W" for Chr XVI indicates the color of the isolate after forced chromosome loss. Thus, "16R" is red because the non *ade3-2p* marked chromosome was lost, and "16W" is white because the galactose promoter was positioned on the *ade3-2p* marked homolog.

Appendix C: Insights into red-pink colony formation through DNA repair

After inducing centromeric re-replication on Chr V or on Chr XVI, there was a stimulation of red-pink colonies. Array CGH analysis of the sectors of these colonies revealed the color reporter was accurate: the red portion contained an extra copy of the re-replicated homolog, and the pink portion was euploid. Somehow, centromeric re-replication was able to induce the generation of a complete chromosome.

The initial thought was that a select few re-replication forks had made it to the ends and re-replicated the entire chromatid. This phenotype was not observed after arm re-replication on Chr IV (Green *et al*. 2010), but Chr XVI is ~500 kb shorter, which may put it inside the maximal range of a re-replication fork. As a simple test, I moved *ARS317* down onto the arm of the Chr V but kept the color reporter *ade3-2p* near the centromere. When re-replication was initiated here, there was no stimulation of red-pink colonies, indicating they were not due to whole-chromosomal re-replication. The argument could be made that the forks are fatigued when they arrive at the centromere-kinetochore complex and are unable to re-replicate through it. If the centromere is a burden to re-replicate, then if they start near the centromere they can power through it more easily and then transverse the remainder of the chromosome.

To definitively test the dependence of centromeric re-replication on the generation of red-pink colonies, a replication fork barrier is essential. This block would prevent forks from moving through the centromere and demonstrate that its re-replication is required for red-pink colony formation. Unfortunately, the replication fork barrier that exists in yeast (Labib and Hodgson 2007) does not work in our hands (May Szeto, unpublished data). Therefore, I tried two genetic approaches to determine the origin of the red-pink colonies.

The first approach I took was a classic one: using selectable markers, I tagged the re-replicating homolog and the non-re-replicating homolog so that I would be able to deduce the chromosomal composition of a sector by its growth properties. For example, one copy of each homolog would allow for growth on six different types of medias, whereas the loss of one of the homologs would only allow for growth on three medias (since the remaining three markers were lost). If the red-pink colony was forming due to whole-chromosomal re-replication, then all six markers should be present in both sectors. However, if the red-pink colonies were forming because of something else, such as a breakage and repair event, then I would expect the pink portions of the colony to be missing markers. During re-replication, if the bubble breaks and two centric fragments are segregated to each daughter, the fragments could repair from either the sister or the homolog (in what will become the red portion) or only the homolog (in what will become the pink portion). Repair using the homolog will restore a full-length chromosome, but the marker will forever be lost. I expected to see this marker loss in nearly all of my pink sectors, but only 8% of pink sectors had lost a marker—the remainder had all six present. I began to wonder if it was in fact whole-chromosomal re-replication until I found a paper from the Hartwell lab that describes how broken chromatids prefer to use their sisters for repair templates instead of their homologs (Kadyk and Hartwell 2002). If this is what is happening, then that means there is still repair going on, and that repair is taking place before anaphase.

This line of reasoning led me to my second approach to test whether either of the two major repair pathways were necessary for red-pink colony formation (described in detail in CHAPTER TWO). In summation, red-pink colony formation largely depends on *RAD52*, an essential component of the homologous recombination repair pathway. Oddly enough, *DNL4* antagonizes red-pink colony formation; when it is removed, the frequency of red-pink colonies

nearly quadruples.

My interpretation of the repair pathway data is simple: the broken double-stranded breaks that result from re-replication are either carefully repaired through homologous recombination, or they are jammed together through non-homologous end joining. If the latter occurs, the end result is a dicentric chromatid, which can have major problems (Gascoigne and Cheeseman 2013). If the former occurs, the repair could go through to the end of the chromosome to produce the extra copy observed in the red sectors.

The precedence for such repair exists: break-induced replication is mostly dependent upon *RAD52*, and can repair kilobases of DNA. It is also entirely dependent on *POL32*, a component of the replisome that is totally dispensible under normal replication but is essential for break-induced replication. I peformed a re-replication assay (Figure 3) where I removed *POL32* or *RAD51*, and after adjusting for the decrease in re-replication efficiency (*POL32* re-replication is not robust for reasons we do not understand), the frequency of red-pink colonies dropped two-fold, around the same frequency as seen with *Δrad52* strains. This data is promising, but will need to be repeated at least two more times.

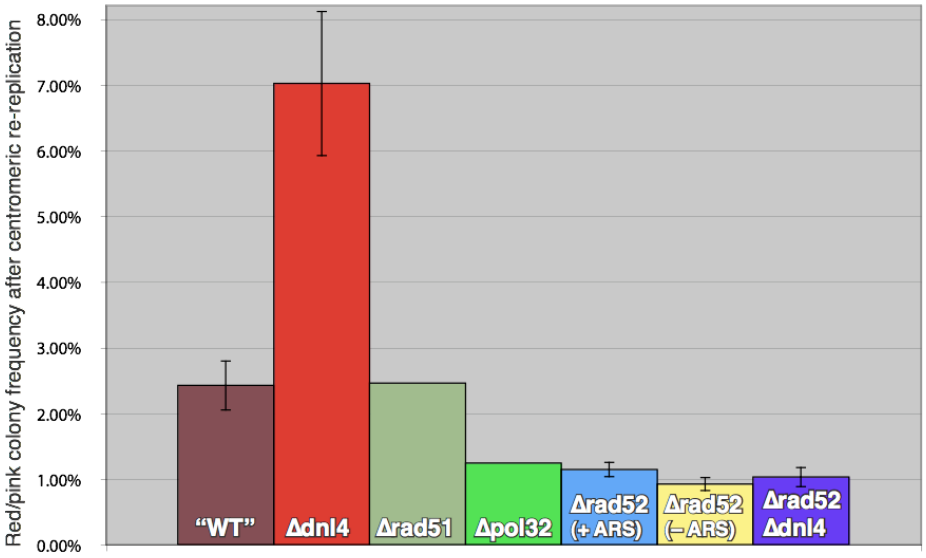

Figure 3: Red-pink colony frequency in DNA repair mutants.

As shown, *RAD52* plays an important part in the formation of red-pink colonies. Due to *POL32*'s similar frequency, it is possible the *RAD52*-dependent events are also *POL32*-dependent, indicating they may be formed via BIR.

In addition to the genetic frequency data, I have also observed products of unrestricted homologous recombination, especially in cells lacking *DNL4*. I isolated these products from red-pink colonies, and aCGH of the red portion shows a segmental duplication encompassing the centromere (Figure 4). In one example, there is also a segmental triplication, with all junctions being regions of homology. I interpret this to mean there are actually no segmental amplifications, but that all three extra pieces make up a whole chromosome. In another example, there is no additional duplication, but the boundaries of the centromeric duplication are regions of homology. I believe this isolate has a large, circular extra-chromosomal element that was able to form by connecting the regions of homology on its ends. Together, I believe the red-pink colonies arise from breakage and repair and are not due to of whole-chromosomal re-replication.

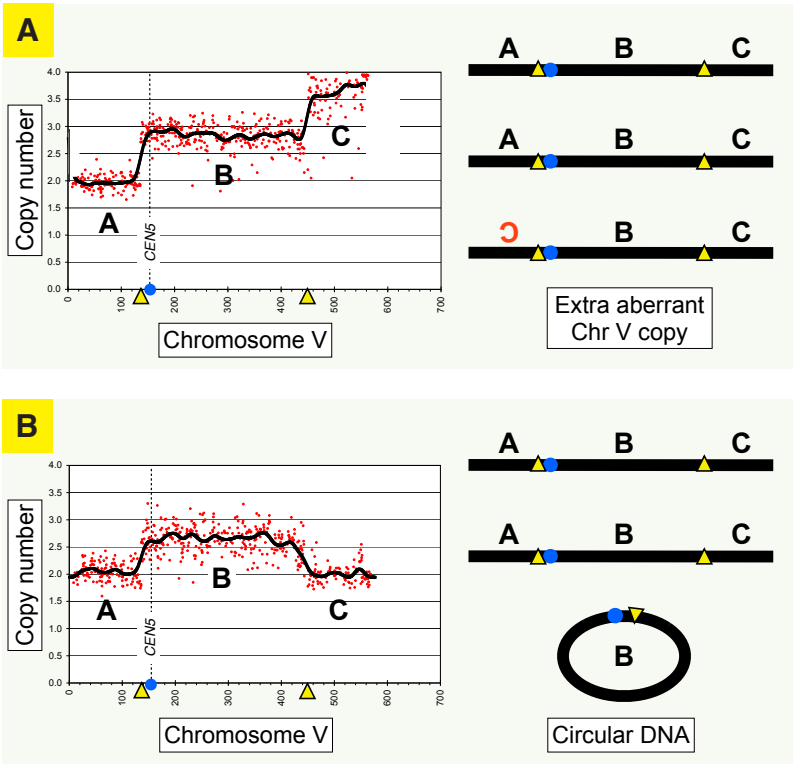

Figure 4: Chromosomal structures that likely formed via homologous recombination.

A) Array CGH profile of a red sector isolate that has a segmental duplication and triplication, but due to the ratios of the amplifications, the locations of the junctions, as well as the duplication encompassing the centromere, this is likely the signature of an aberrant copy of Chr V.
B) Array CGH of a red sector isolate that has a segmental duplication. Due to the duplication encompassing the centromere, it is likely not intrachromosomal, but due to the lack of telomere amplifications (on Chr V or elsewhere in the genome, data not shown), this is likely the signature of a circular piece of DNA.

Appendix D: Arresting the cell cycle genetically with a Mad2-Mad3 fusion construct

In all of my re-replication experiments, it was useful to be able to control when re-replication was initiated. I used nocodazole to arrest the cells in G2/M and induce re-replication, but unfortunately it has effects of its own. It enhances the rate of missegregation (Taylor-Mayer *et al*. 1988), meaning the frequencies I observe may be partially dependent upon it. Therefore, I wanted a way to genetically arrest my cells to make sure the aneuploidy I observe is dependent on centromeric re-replication and not nocodazole.

The most widely-used genetic G2/M-arrest tool is the pMET3-Cdc20 construct. Cdc20 is the activator of the anaphase promoting complex (APC); having it around enables anaphase to proceed, whereas its removal arrests cells in metaphase. Methionine will shut off the pMET3 promoter driving Cdc20 production, so cells can be arrested by adding methionine to the media. This means to keep cells growing, the media must lack methionine. Unfortunately, the red pigment that colorizes our cells negatively affects growth and color development on media lacking methionine, making the pMET3-Cdc20 construct unusable.

In order to circumvent this problem, I took the opposite approach: instead of controlling the activator for the APC, I decided to control its inhibitor. During checkpoint activation, the mitotic checkpoint complex (MCC) forms (Chao *et al*. 2012). This complex consists of Bub3, Mad2, Mad3, and Cdc20, and when it forms, it sit in the active site of the APC to prevent its function. Seeing that overexpression of a linked Mad2-Mad3 can arrest cells just as well as Cdc20 depletion can (Lau and Murray 2011), I placed a linked Mad2-Mad3 under the control of the methionine promoter. This way, I can grow my cells normally on media containing

methionine (which will keep the construct off), and to arrest my cells, I will remove the methionine so the Mad2-Mad3 MCC mimic is produced.

This construct was very functional in my hands, but it had two major flaws. First, re-replication induction during this genetic G2/M arrest enabled other re-replication origins to fire (Figure 5). If I cannot control the re-replication, then I cannot be sure whether an induction of aneuploidy is due to *ARS317* re-replication or other genomic re-replication. Second, when I quickly examined my colored colonies by eye, I did not see evidence of aneuploidy. Normally, I am able to pick out red-pink colonies without using the stereoscope, but with colonies that had undergone re-replication during this pMET3-Mad2-Mad3 (pM3) arrest, I could see nothing. Though I do not know if this result is repeatable, I think it would be interesting to determine if this arrest has an affect on the chromosome segregation during centromeric re-replication. I can imagine a scenario where the mimic of the mitotic checkpoint complex somehow helps to promote biorientation, so that any aberrant connections that would have been made after centromeric re-replication are corrected before the cell leaves metaphase.

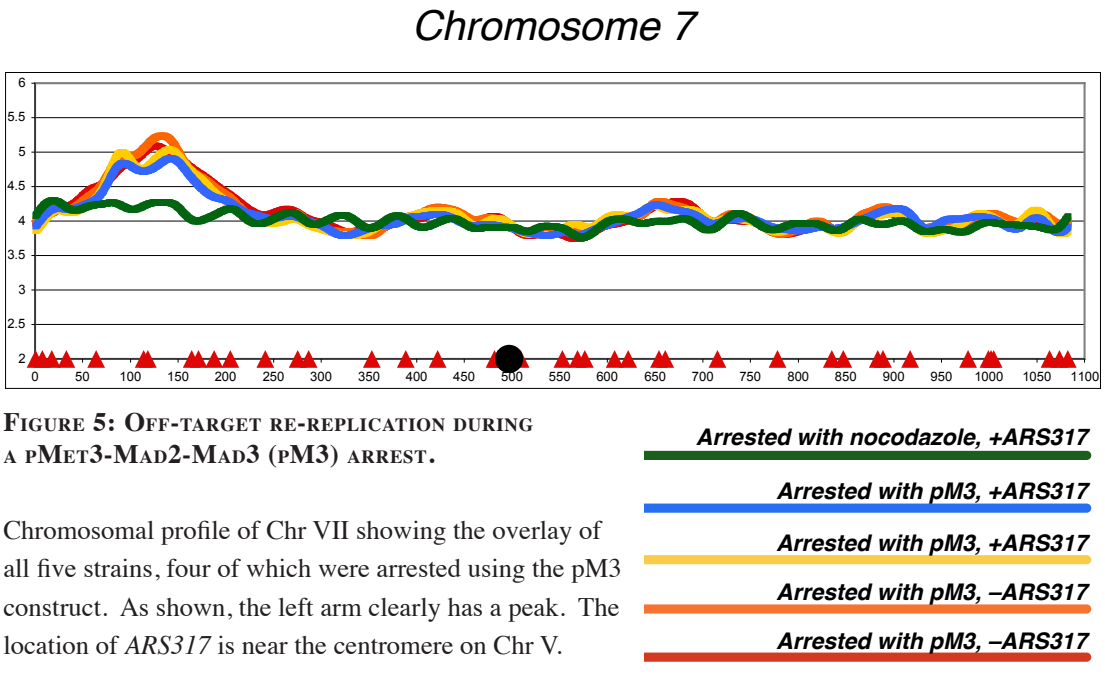

Figure 5: Off-target re-replication during a pMet3-Mad2-Mad3 (pM3) arrest.

Chromosomal profile of Chr VII showing the overlay of all five strains, four of which were arrested using the pM3 construct. As shown, the left arm clearly has a peak. The location of *ARS317* is near the centromere on Chr V.

Appendix E: Freeze-thawing imposes a stress on genomically unstable cells

When I was obtaining aCGH data to determine the ploidy of various sector isolates, several of my white isolates were not at a Chr V copy number of ~1, but were closer to 1.9 instead. Though by eye it appeared the copy number may be a bit lower than the other chromosomes, nothing was as striking as the copy numbers I had previously generated. Thinking back, I realized I had not frozen the white isolates before I performed aCGH. In order to get a better idea of what the original colony sector ploidy was, I removed half of the freezer stock and performed aCGH on it: using a little stick, I scooped out some of the cell pellet that was in the 96-well plate I kept my isolates it. This sample went into a tube and was immediately entered into the Hanlon DNA prep, followed by aCGH.

For nearly all of my white sector samples, the copy number of Chr V plummeted to around 1.3 (Figure 6). This indicates that the stress of freeze-thawing is detrimental to these monosomic cells; the red portions were all thawed and tested, and had maintained their extra chromosome. It is unclear if the freeze-thaw itself is stressing the cell, or if there is a gene that is beneficial during the freeze-thaw that is located on Chr V, so cells that are disomic have a greater fitness than the monosomes.

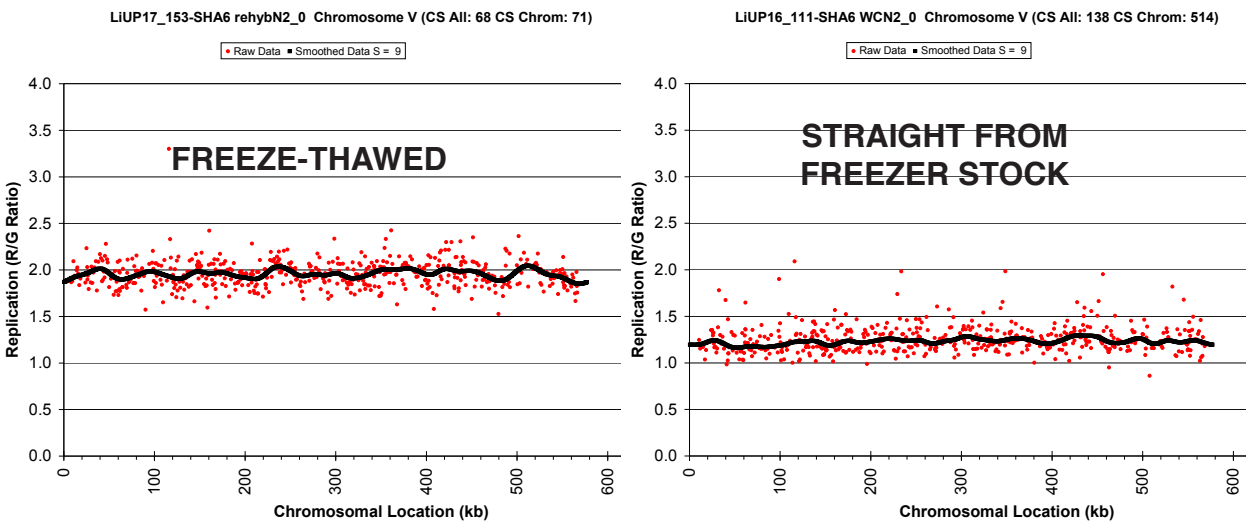

Figure 6: Freeze-thawing of once-monosomic cells leads to restored euploidy

These are Chr V aCGH profiles from the same isolate (SHA6), with the only difference being whether or not the cells were freeze-thawed prior to DNA extraction.

References for Chapter Three and Appendices

Alvaro D., Sunjevaric I., Reid R. J. D., Lisby M., Stillman D. J., Rothstein R., 2006 Systematic hybrid LOH: a new method to reduce false positives and negatives during screening of yeast gene deletion libraries. Yeast 23: 1097–1106.

Bloom K. S., Carbon J., 1982 Yeast centromere DNA is in a unique and highly ordered structure in chromosomes and small circular minichromosomes. Cell 29: 305–317.

Chao W. C. H., Kulkarni K., Zhang Z., Kong E. H., Barford D., 2012 Structure of the mitotic checkpoint complex. Nature: 1–7.

Collins K., Castillo A., Tatsutani S., Biggins S., 2005 De novo kinetochore assembly requires the centromeric histone H3 variant. Mol Biol Cell 16: 5649–5660.

Duan Z., Andronescu M., Schutz K., McIlwain S., Kim Y. J., Lee C., Shendure J., Fields S., Blau C. A., Noble W. S., 2010 A three-dimensional model of the yeast genome. Nature 465: 363–367.

Eckert C. A., Gravdahl D. J., Megee P. C., 2007 The enhancement of pericentromeric cohesin association by conserved kinetochore components promotes high-fidelity chromosome segregation and is sensitive to microtubule-based tension. Genes & Development 21: 278–291.

Finn K. J., Li J. J., 2013 Single-Stranded Annealing Induced by Re-Initiation of Replication Origins Provides a Novel and Efficient Mechanism for Generating Copy Number Expansion via Non-Allelic Homologous Recombination. PLoS Genet 9: e1003192.

Gascoigne K. E., Cheeseman I. M., 2013 Induced dicentric chromosome formation promotes genomic rearrangements and tumorigenesis. Chromosome Res 21: 407–418.

Goshima G., Yanagida M., 2000 Establishing biorientation occurs with precocious separation of the sister kinetochores, but not the arms, in the early spindle of budding yeast. Cell 100: 619–633.

Green B. M., Finn K. J., Li J. J., 2010 Loss of DNA replication control is a potent inducer of gene amplification. Science 329: 943–946.

Kadyk L. C., Hartwell L. H., 2002 Sister chromatids are preferred over homologs as substrates for recombinational repair in Saccharomyces cerevisiae. Genetics 132: 387–402.

Labib K., Hodgson B., 2007 Replication fork barriers: pausing for a break or stalling for time? EMBO Rep 8: 346–353.

Lau D. T. C., Murray A. W., 2011 Mad2 and Mad3 Cooperate to Arrest Budding Yeast in Mitosis. Current Biology: 1–11.

Lyons N. A., Morgan D. O., 2011 Cdk1-Dependent Destruction of Eco1 Prevents Cohesion Establishment after S Phase. Molecular Cell 42: 378–389.

Ng T. M., Waples W. G., Lavoie B. D., Biggins S., 2009 Pericentromeric sister chromatid cohesion promotes kinetochore biorientation. Mol Biol Cell 20: 3818–3827.

Ocampo-Hafalla M. T., Katou Y., Shirahige K., Uhlmann F., 2007 Displacement and re-accumulation of centromeric cohesin during transient pre-anaphase centromere splitting. Chromosoma 116: 531–544.

Sakuno T., Tada K., Watanabe Y., 2009 Kinetochore geometry defined by cohesion within the centromere. Nature 458: 852–858.

Ström L., Lindroos H. B., Shirahige K., Sjögren C., 2004 Postreplicative recruitment of cohesin to double-strand breaks is required for DNA repair. Molecular Cell 16: 1003–1015.

Tanaka T., Fuchs J., Loidl J., Nasmyth K., 2000 Cohesin ensures bipolar attachment of microtubules to sister centromeres and resists their precocious separation. Nat Cell Biol 2: 492–499.

Taylor-Mayer R. E., Mayer V. W., Goin C. J., 1988 Effect of treatment medium on induction of aneuploidy by nocodazole in Saccharomyces cerevisiae. Environ Mol Mutagen 11: 323–331.

Verdaasdonk J. S., Bloom K., 2011 Centromeres: unique chromatin structures that drive chromosome segregation. Nature Publishing Group 12: 320–332.

Watanabe Y., 2005 Shugoshin: guardian spirit at the centromere. Curr Opin Cell Biol 17: 590–595.

It is the policy of the University to encourage the distribution of all theses, dissertations, and manuscripts. Copies of all UCSF theses, dissertations, and manuscripts will be routed to the library via the Graduate Division. The library will make all theses, dissertations, and manuscripts accessible to the public and will preserve these to the best of their abilities, in perpetuity.

I hereby grant permission to the Graduate Division of the University of California, San Francisco to release copies of my thesis, dissertation, or manuscript to the Campus Library to provide access and preservation, in whole or in part, in perpetuity.

Stacey L. Hanlon, Author

September 16th, 2014

Date